THE EFFECT OF GROUNDWATER PUMPING ON BASEFLOW IN THE DESCHUTES RIVER OF WASHINGTON STATE

by

Eunbi Lee

A Thesis

Submitted in partial fulfillment

of the requirements for the degree

Masters of Environmental Studies

The Evergreen State College

June 2020

This Thesis for the Master of Environmental Studies Degree

by Eunbi Lee

has been approved for

The Evergreen State College

by

_____

Dr. EJ Zita

Member of the Faculty

_____

Date

ABSTRACT

The Effect of Groundwater Pumping on Baseflow in the Deschutes River of Washington State

Eunbi Lee

Groundwater pumping via wells has been identified as a critical element in groundwater depletion and consequent hydrologic alterations on numerous streams across the globe. The deficit in groundwater reduces baseflow, which originates from the groundwater and contributes to the surface flow, potentially putting the low streamflow at risk during a low flow period. In Deschutes River in Washington, U.S., the capacity of baseflow has decreased during the dry season in summer.

This research project utilized two baseflow analyses. First, the 'natural' baseflow without the impact of the withdrawals (W=0), and the 'impacted' baseflow including existing groundwater pumping (W≠0) were compared using two-sample Student's t-test. Second, a low flow frequency analysis estimated the times when the currently impacted baseflow within the stream exceeded and fell below an ecological threshold, or "environmentally critical baseflow." Both analyses used baseflow data extracted from streamflow discharge data measured at the lower Deschutes River (river mile 2.4) near Tumwater. The total study period is 75 years (1945-2019) with 110 recession periods in the dry season between June to October.

There was a significant difference between the 'natural' and 'impacted' minimum baseflow, signifying that baseflow contribution would have been substantially higher without the pumping effect. I project that the future baseflow within the stream will decrease and reach the environmentally critical baseflow (ECB) in 2061. The work presented here describes anthropogenic impact on the interactive regime between the groundwater and surface water (quantity) and the ecological function (quality) of the streams in the Pacific Northwest.

Table of Contents

List of Figures

List of Tables

Acknowledgements

There are several groups and individuals whom I acknowledge for their help in completing this thesis. First and foremost, I would like to thank my husband, Sean Wood, for his unwavering trust and support that helped me to put this educational pursuit forth and accomplish it. Thank you for being with me in rain and sunshine all the way through this program.

This thesis project would not have been possible without the direction and guidance of my faculty advisor, EJ Zita. Also, I want to thank all the MES faculty for their support. Especially, I received a great amount of help from the program director, Kevin Francis, who openly communicated with me in regard to difficulties and successes.

There are several agencies and professionals that I would like to thank. Erica Marbet from the Squaxin Island Tribe has given me valuable support and guidance from the early stage of my research and interest in hydrology. Kevin Hansen from Thurston County Water Planning offered instructive details and data regarding the groundwater withdrawals that were essential for this project. Scott Malone from the Department of Ecology provided expert advice on hydrogeologic knowledges. Numerous people were willing to answer my questions, provided data, and invited me to meetings to broaden my understanding on the subject matter and I thank them: Brian McTeague from Squaxin Island Tribe, Kenneth Tabbutt from the Evergreen State College, Jim Pacheco, Lisa Kean, Joe Witczak from the Department of Ecology, and Nathaniel Kale and Mark Biever from Thurston County Water Planning.

Finally, I thank my parents for their unchanging support in all the paths I chose in my life.

Chapter 1: Introduction

Over the past 100 years, human water demand increased almost 8-fold due to the quadrupling of the global population and continues to rise (Wada et al., 2016). Socioeconomic developments increasingly put pressure on our freshwater resources with rising per-capita demands and standards of living (Veldkamp et al., 2017). Pressure on available freshwater resources has occurred in both water systems: groundwater within underground aquifers and surface water flowing over the surficial levels. The two water systems—groundwater and surface water—are hydraulically interconnected, such that exploitation of one system (e.g., groundwater) inevitably depletes the other system (e.g., surface water).

Groundwater is a primary source of freshwater in many parts of the world and supplies more than one-third of the U.S. population with drinking water[1] (Konikow, 2013). Though seemingly infinite, groundwater is a finite resource that is vulnerable to depletion due to perpetuated withdrawals (Famiglietti, 2014). Some regions that are increasingly dependent on groundwater consume groundwater faster than it is naturally replenished and cause water tables to decline (Rodell et al., 2009). Lowered water tables disconnect the interaction between groundwater and surface water, deplete the surface water, and put risk on the ecology of the flowing stream systems (de Graaf et al., 2014).

Recent studies assessed the impact of human activities (e.g., groundwater pumping) on hydrologic processes between groundwater and surface water[2]. The interaction between groundwater and surface water is a critical element to sustain the

[1] Globally, groundwater accounts for 30% of available freshwater (Gleick, 1996)
[2] Wang & Cai (2009); Thomas et al. (2013); Gleeson & Richter (2018); de Graaf et al. (2019).

ecological functions of a river, wetland, lake, and terrestrial ecosystem (Gleeson & Richter, 2018). Yet, current groundwater management in some regions has not explicitly included the potential impacts of groundwater pumping on depleted groundwater storage and degraded surface water ecology. The lack of management of the impacts of groundwater pumping on the interactive water systems is relatively riskier in regions with prolonged droughts and extended low streamflow.

The impact of groundwater pumping on lowering water tables and reducing surface water leads to detrimentally low streamflow during the dry summertime in the Pacific Northwest (PNW). Traditionally, summer streamflow in PNW maintained a 'low flow' status from prolonged droughts with little to no precipitation to recharge the surface flow (Konikow, 2013). The low flow results in degraded water quality with heightened stream temperature, low dissolved oxygen level, unbalanced pH level, and spreading diseases (DoE, 2015). With increased groundwater exploitation, the quantity of stored groundwater and the amount of groundwater contributing to the surface flow ('baseflow') are expected to decrease in urbanized regions (Georgiadis et al., 2018).

The decreasing trend of baseflow in PNW due to perpetuated groundwater pumping relates to exacerbated low flow and consequent water quality issues. The Deschutes River in Washington State is faced with a continuous rise in stream temperature and water quality degradation, most of which have been the focus of studies on the quality of the stream[3]. In contrast, there have been relatively fewer studies regarding the impacts of groundwater withdrawals on reduced baseflow contribution on

[3] Deschutes River does not meet water quality standards and is on the Clean Water Act Section 303(d) list for one or more Total Maximum Daily Load (TMDL) parameters: fecal coliform bacteria, temperature, dissolved oxygen (DO), pH, or fine sediments (Wagner & Bilhimer, 2015).

the surface flow, even though the baseflow is a major source of streamflow during the low flow period[4]. The lack of quantitative studies on baseflow may be attributed to the common perception of ample precipitation in wet seasons (Fall, Winter, and Spring) recharging low streamflow. However, PNW under rapid urbanization is no longer exempt from being a naturally sustainable low flow region. Groundwater storage and baseflow contribution here may be at risk of decreasing below the level that they cannot sustain minimally required streamflow for the riverine ecosystem[5]. Thus, the decreasing trend of baseflow ('baseflow recession') of the Deschutes River should be carefully monitored and analyzed because the aquifer, which is hydraulically related to the river, has been exploited. Such groundwater pumping and appropriation have met the fast-growing demands of burgeoning Thurston County populations and development[6].

A quantitative baseflow recession analysis delineates the impact of groundwater withdrawals on surface streamflow. The baseflow recession analysis explains the fluctuating baseflow, which links the effect of groundwater depletion on the surface flow. Streams in PNW already are faced with both quantity and quality degradation due to climate change and recurring ocean-atmosphere patterns, such as Pacific Decadal Oscillation and El Niño-Southern Oscillation (Georgiadis et al., 2018). Coupled with climatic elements, the unsustainable groundwater withdrawal practices without considering the baseflow recession will exacerbate the low flow and ecological functions on riverine ecosystems. Additionally, analyzing the low flow period, maintained by

[4] Baseflow consisted of the surface flow on average 83% of the streamflow between 1945 and 2019 (see section 2.3.3).
[5] Hamlet et al. (2010); Luce & Holden (2009).
[6] Thurston County was ranked as the third-fastest growing region in Western Washington (USGS, 2015).

mostly baseflow contribution during dry seasons, explains the impact of the baseflow recession. A frequency analysis explains how the future low flow status will change in relation to the sustainable level of baseflow contribution to the stream.

The two research questions this study intends to answer are 1) To what extent has groundwater demand impacted baseflow recession in the lower Deschutes River in Washington State? and 2) At what point of time in the future will critically low groundwater supply to the Deschutes River occur? The quantitative baseflow recession analysis on the Deschutes groundwater system estimates numeric values to describe the baseflow pattern between 1945 and 2019. The estimated values are categorized into two scenarios; the "natural" groundwater system is a hypothetical scenario of the baseflow without groundwater pumping; the "impacted" groundwater system represents the current baseflow status with groundwater pumping accounted. The "natural" and "impacted" baseflow are compared to understand the effect of groundwater pumping on the baseflow contribution to the surface flow. This study hypothesized that the effect of groundwater withdrawal is significant when the baseflow recession under the "natural" versus "impacted" scenarios are statistically compared. Finally, the withdrawal impact on baseflow recession is assessed in a view from whether the baseflow in the future will sustain a minimum baseflow threshold, or environmentally critical baseflow (ECB, adopted from Gleeson & Richter, 2013; de Graaf, 2019). Through this study, baseflow recession elucidates a quantitative effect of groundwater pumping and whether current withdrawal practice is environmentally sustainable for future streams.

1.1: Description of the Study Area

Deschutes River is a 50-mile-long (80 km) river in Washington, United States. From the Gifford Pinchot National Forest in Lewis County, it flows from southeast to the northwestern part of Thurston County and empties into Budd Inlet at the southernmost arm of Puget Sound. The capitol city of Washington, Olympia, is located on the southern Deschutes River, and the greater-Olympia area, where fast-growing cities, such as Tumwater, Lacey, and Yelm, rely on the Deschutes River for their development.

The study area includes parts of Thurston County where unconsolidated sediments are at land surface (510 square miles; figure 1). The unconsolidated layers of the Puget Sound aquifer represent the geologic units where groundwater interacts with the surface water of the Deschutes River. The selected study area covers most of the river's watershed (162 square miles), except for some areas in the southeast where there are consolidated sediment layers at the land surface. The range of selected geologic map layers included Quaternary alluvium (Qa), Pleistocene continental glacial drift (Qgd), and Pleistocene alpine glacial drift (Qad). The excluded areas include consolidated geologic layers of Tertiary volcanic rocks (Tv(c)), Tertiary marine sedimentary rocks (Tm), and Tertiary nearshore sedimentary rocks (Tn) [7]. The range of the included geologic layers are the selected study area (blue area in Fig. 1).

U.S. Geologic Survey (USGS) collected the streamflow data for the lower Deschutes River, gauged at the station in Tumwater, Washington, 2.4 miles away from the river mouth (river mile 2.4). I used the collected streamflow data to extract the

[7] Geologic map layer source: City of Tacoma, 2019.

baseflow contribution from the groundwater aquifer to the stream. This study demonstrates the impact of groundwater withdrawals on the baseflow, which is a part of the surface flow. The lower (northern) Deschutes River, toward which the water flows due to hydraulic gradients, was chosen for this study because it incorporates the groundwater deficit from its upper stream.

Figure 1

Study Area

ESRI online map layer sources: City of Tacoma, 2019 (geologic unit layers); WSDOT, 2012 (county boundary); Bilhimer, 2014 (Deschutes River).

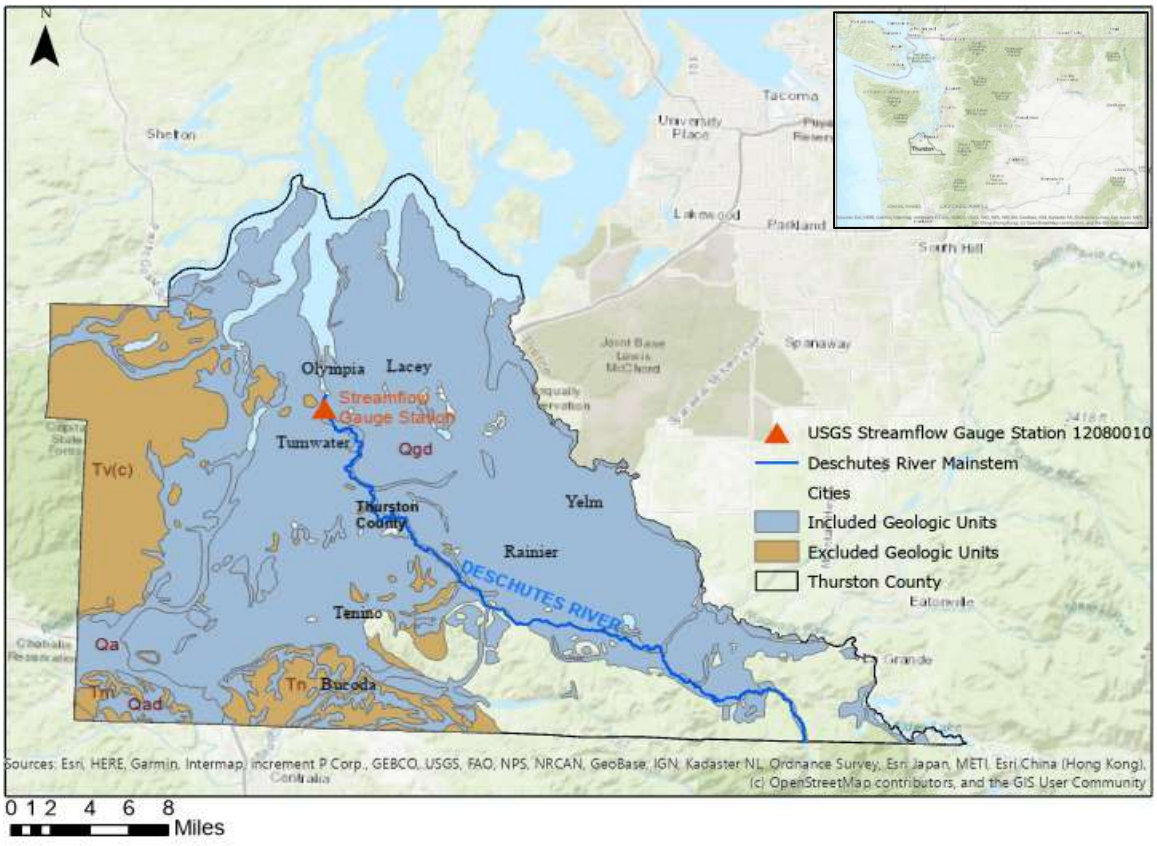

Note. Light blue: included geologic units (Qa, Qgd, Qad). This area represents the whole study area. Brown: excluded geologic units (Tv(c), Tm, Tn). The streamflow gauge station is located on E street, Tumwater, WA.

Chapter 2: Literature Review

2.1: Roadmap

This literature review is organized into 8 sections: an introduction, Sections 1-6, and a concluding summary. The introduction describes the concept of baseflow and its importance during low flow periods. Section 1 provides a conceptual understanding of interconnected groundwater and surface water as a single source. Section 2 addresses low flow trends in the Pacific Northwest region and possible causes of the low flow phenomenon. Section 3 describes the concept of baseflow recession, and how groundwater demand and withdrawals can affect the baseflow recession and water qualities in streams. Section 4 describes the water wells' pumping mechanism. Section 5 explains a baseflow recession analysis in a quantitative way. Section 6 provides a frequency analysis, for a different perspective to interpret the streamflow depletion in a low flow period. Finally, the conclusion summarizes why the quantitative analysis of streamflow is imperative for preserving groundwater and surface water resources.

2.2: Introduction

Streamflow in the Pacific Northwest (PNW) region has been depleted during dry summertime in recent decades (Georgiadis et al., 2018). While many people may think that rivers in the PNW sustain significant flow rates due to ample precipitation events in wet seasons, this is not true in the dry season when surface streamflow is lowered significantly. Low streamflow ("low flow") is detrimental to the ecological functions of rivers to sustain aquatic species and natural values of flowing streams (DoE, n.d.). Low

flow is a natural phenomenon that occurs in dry seasons, which maintains streamflow from groundwater contribution during the non-precipitated period. During low flow periods, groundwater inflow into the surface water system can alleviate low streamflow and cool streams; the groundwater inflow is referred to as "baseflow" (Fig. 2).

Figure 2

Baseflow: Groundwater Contribution to the Stream. Winter et al., 1999.

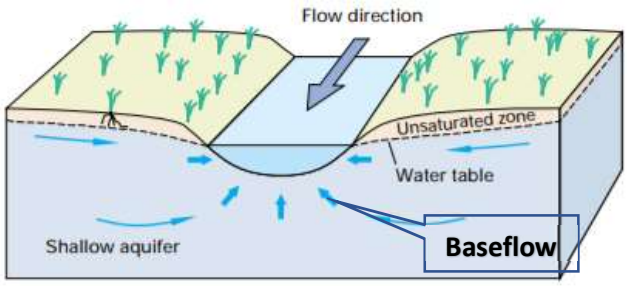

Note. Baseflow is denoted with blue arrows (upward) from groundwater to the surface flow.

Baseflow is a natural regime of hydraulic movement between groundwater–surface water systems. Baseflow is associated with both quantity and quality of water in streams. When there is less groundwater available, baseflow decreases within the surface stream. The reduced baseflow contributes to severely low flow and degraded water quality in a surface stream. This relationship is important to understand streamflow from a holistic perspective. Baseflow is a connective system between groundwater and surface water, where an effect on one system (i.e., groundwater) will have an impact on the other.

Water quality in the Deschutes River in Washington State has brought attention to environmental and societal issues in the South Puget Sound area. Many studies explored degraded water qualities (e.g., warm stream temperature, low oxygen retention, and

unbalanced pH level). However, there have not been significant studies related to the trend of changing quantity of baseflow and its effect on the surface water. The effect of baseflow on the water quality enhancement signifies why we should pay attention to the fluctuating baseflow trends. Furthermore, the human interception of groundwater via well pumping has altered the quantity of groundwater and surface water, which entails possible degradation of the stream quality.

2.3: Interconnectivity between Groundwater and Surface Water

2.3.1: Single Water System

A paradigm shift in the late 20th century increased attention on the interconnectedness of groundwater and surface water as an integrated body (Winter et al., 1998). Surface water is the most recognizable source of water in the form of streams, rivers, lakes, reservoirs, and oceans (Winter et al., 1999). Groundwater, though unseen at the landscape level, exists underground in saturated zones, filling pores and fractures between sediment beneath the land surface and forming aquifers (Fig. 3, Barlow & Leake, 2012). Surface water percolates down through sediment fractures to recharge groundwater, while groundwater moves upward to contribute to the surface water above riverbeds (Fig. 3). "Baseflow" constitutes a part of streamflow, contributed from the groundwater system, and connects the two water systems (Hall, 1968; Tallaksen, 1995).

Figure 3

Groundwater and surface water system. Winter et al., 1999.

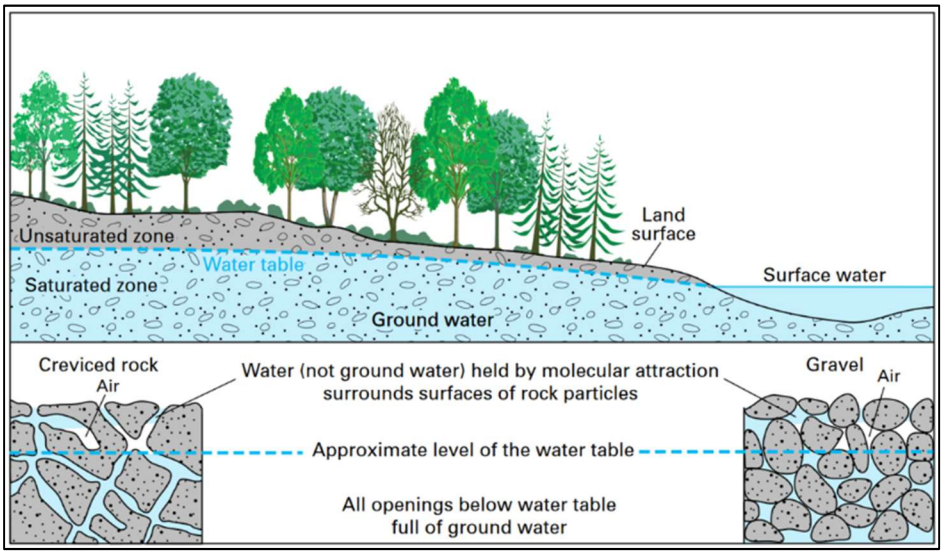

2.3.2: What is Baseflow?

The surface water system is composed of "baseflow" and "direct runoff". Baseflow flows up into surface streams, originating from groundwater below. Direct runoff flows within streams, primarily from rainfall or artificial recharge which "runs off" the land surface (Nolan & Hill, 1990). After a precipitation event (e.g., rainfall, snow, or flood), direct runoff can overwhelm the surface water system (Fig. 4). But the opposite occurs during low flow periods and drought when there is little to no precipitation; the surface water we see is mostly baseflow, which seeps from the underground water into the stream (USGS, n.d.). Below, surface water recharges groundwater through "infiltration" and "percolation", which describes the process of surface water moving vertically down through sedimentary pores of an aquifer and

adding to the groundwater. Baseflow flows into the surface flow where it is combined with direct runoff (or, "surface runoff" below[8]) to form the total surface water system.

Figure 4

Schematic groundwater flow and baseflow. Smith, 2010.

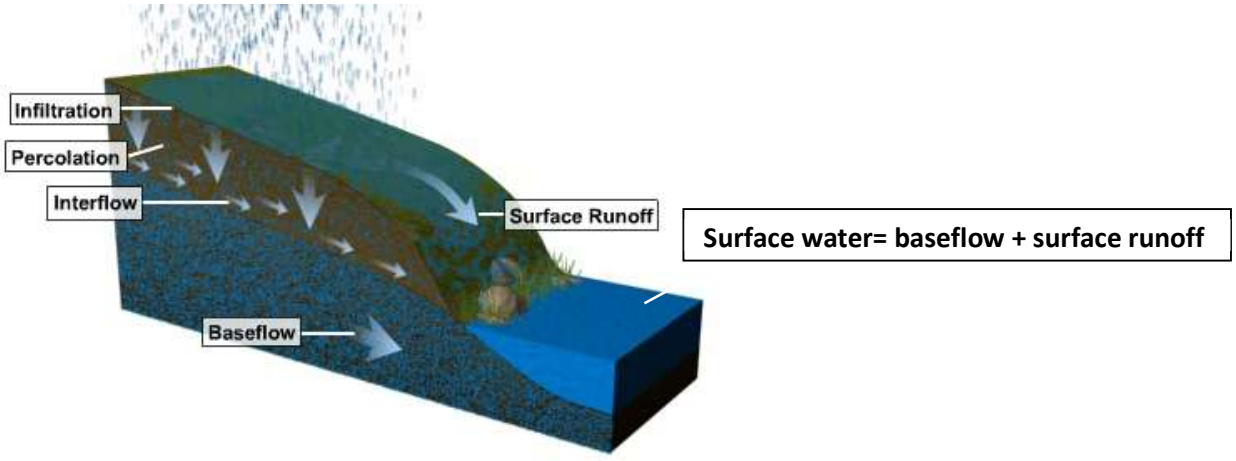

Baseflow maintains surface water when there is no precipitation recharging the direct runoff on a stream. For example, the Deschutes River in Washington maintained streamflow above zero even during a severe drought in 2005 with the inflow from the groundwater (OWSC, 2009; Anderson et al., 2016). Without the baseflow contribution, the surface water would not have maintained the flow without consistent inflow from precipitation. In detail, the low flow is exacerbated when high air temperature yields increased evaporation. Alike many glacier/snowmelt-dominated Washington Cascade rivers, the glacier retreat due to global warming results in an increasing number of days with substantially low flow (Pelto, 2011). However, the low flow without precipitation inflow did not completely dry in the summer of 2005 of the Deschutes River. Most days

[8] In this study, "surface runoff" is equivalent to the "direct runoff".

in July showed almost no precipitation (0 inches), but the surface streamflow remained at least 24 feet high (Fig. 5). The baseflow from the groundwater sustained the low flow.

Figure 5

Streamflow height and precipitation.

Streamflow data retrieved from USGS National Water Information System: Web Interface (NWIS), gauge station 12080010 near Tumwater. Precipitation data from NOAA.

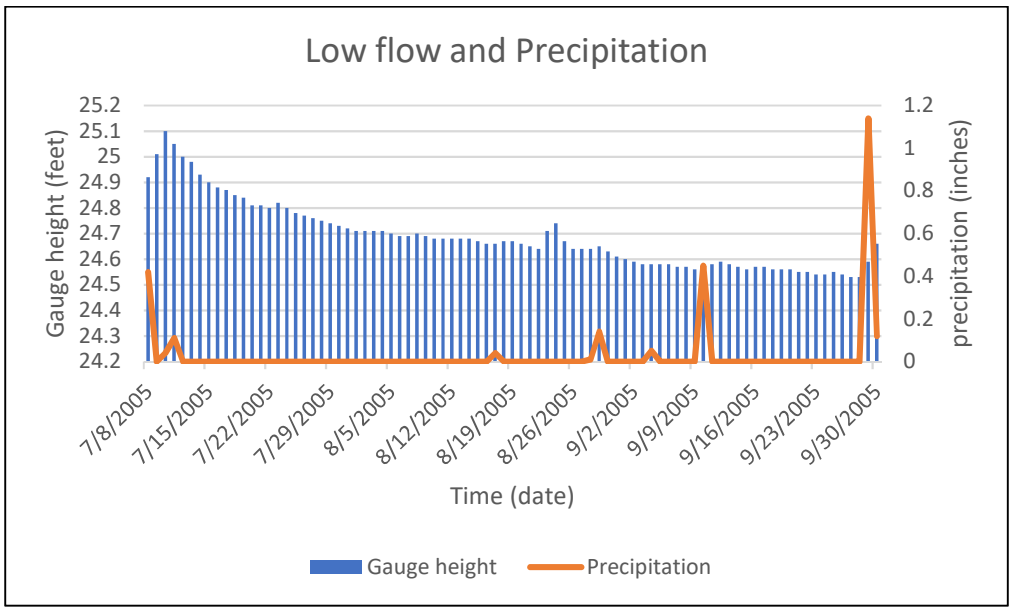

Note. Blue columns denote daily average gauge height, or the level of the surface flow reaching in height at the gauging station (USGS 12080010 near Tumwater). The orange line denotes the amount of rainfall.

2.3.3: Baseflow as a Major Inflow

Baseflow can maintain the minimum surface flows that are required for ecological functions of a river during "low flow" or prolonged drought period (Hall, 1968; Tallaksen, 1995; Stuckey, 2006; Gustard & Demuth, 2008). Low flow refers to the phase when surface streamflow is primarily sustained by baseflow (the groundwater contribution to the surface flow) during prolonged, but non-drought, dry weather (Stuckey, 2006; Gleeson & Richter, 2016). Low flow is an important parameter to

determine whether the surface flow without precipitation input sustains aquatic species and intrinsic values (Gleeson & Richter, 2018).

Baseflow is a major inflow to the surface flow during low flow periods assuming the river maintains streamflow during the absence of precipitation input. Rivers located in areas with extremely variant precipitation between seasons rely heavily on baseflow contribution during dry seasons to maintain minimum flows. A hydrograph, describing the variance in the amount of flow component, of the Lower Deschutes River below (Fig. 6) shows the baseflow component within surface streamflow in dry and wet seasons[9]. Using the web-based hydrograph analysis tool (WHAT), the baseflow component within the surface flow represents how much groundwater contribution occurs of a water year, typically between October to next year September. Between 2014 and 2015, the baseflow (orange) dominates the surface flow (blue) during the dry season. Also, the direct runoff, which is the other component of the streamflow contributed from mainly precipitation, decreased in the same dry period.

[9] Typically, the dry season is from June to October and the wet season is November to May in Pacific Northwest (Kormos et al., 2016).

Figure 6

Hydrograph of surface flow and baseflow of the Deschutes River.

Streamflow data from NWIS, gauge station 12080010 near Tumwater; baseflow data separated using a web-based hydrograph analysis tool (WHAT).

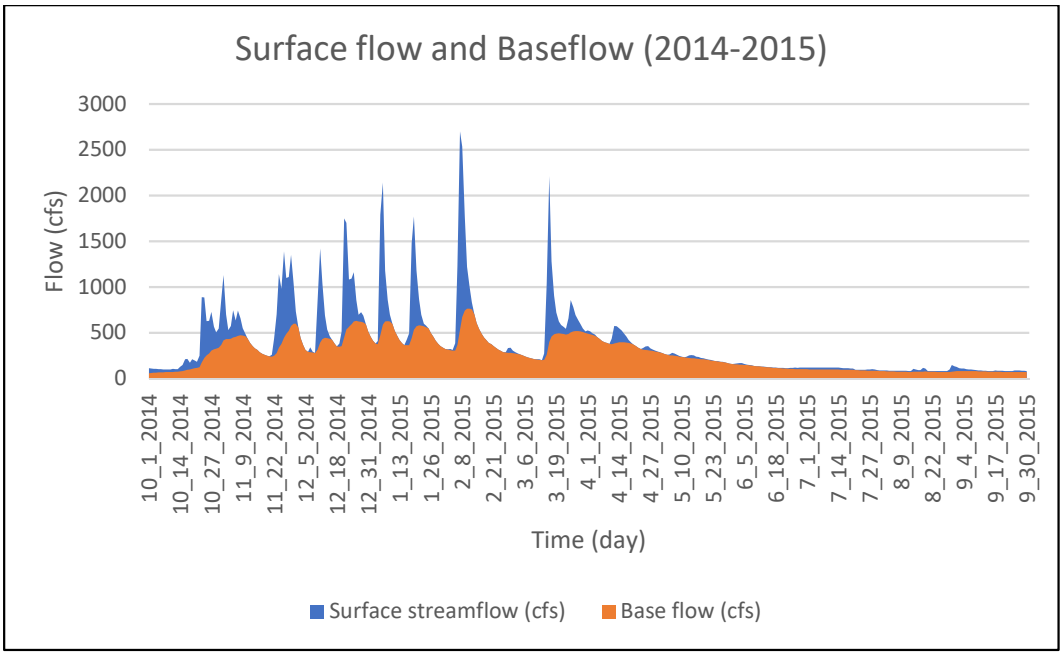

Note. The surface streamflow (blue) includes both the baseflow (orange) and direct runoff (blue area without orange area). Data selected for the water year between October 2014 and September 2015.

The portion of baseflow within the surface flow is dominant during low flow periods in Pacific Northwest streams. In summer, streams experience peak evaporation rates from flowing water as well as evapotranspiration from plants due to heightened air temperature and transpiration process[10]. The lack of rainfall and heightened evapotranspiration reduce the surface flow volume; thus, streams in PNW depend on baseflow to prevent complete depletion (Miller et al., 2016). The Deschutes River showed a large dependency on baseflow contribution during low flow periods of summer

[10] Evapotranspiration is the combined process of water loss through the leaves of plants (transpiration) and water changes to vapor in the atmosphere (evaporation) (Yang et al., 2016).

compared to the average dependency of other streams in Washington State (Fig. 7) (Sinclair & Pitz, 1999). Sinclair and Pitz (1999) separated the baseflow from the streamflow component and determined that the average baseflow comprised 69%-86% of 582 Washington State summer stream gauge stations in 1991 (gray bar in Fig. 7). For the Lower Deschutes River, the baseflow composition within the stream ranged from 74% to 97% in the same period (blue bar in Fig. 7) (Sinclair & Pitz, 1999).

Figure 7

Baseflow composition of total annual streamflow. Data from Sinclair & Pitz, 1999.

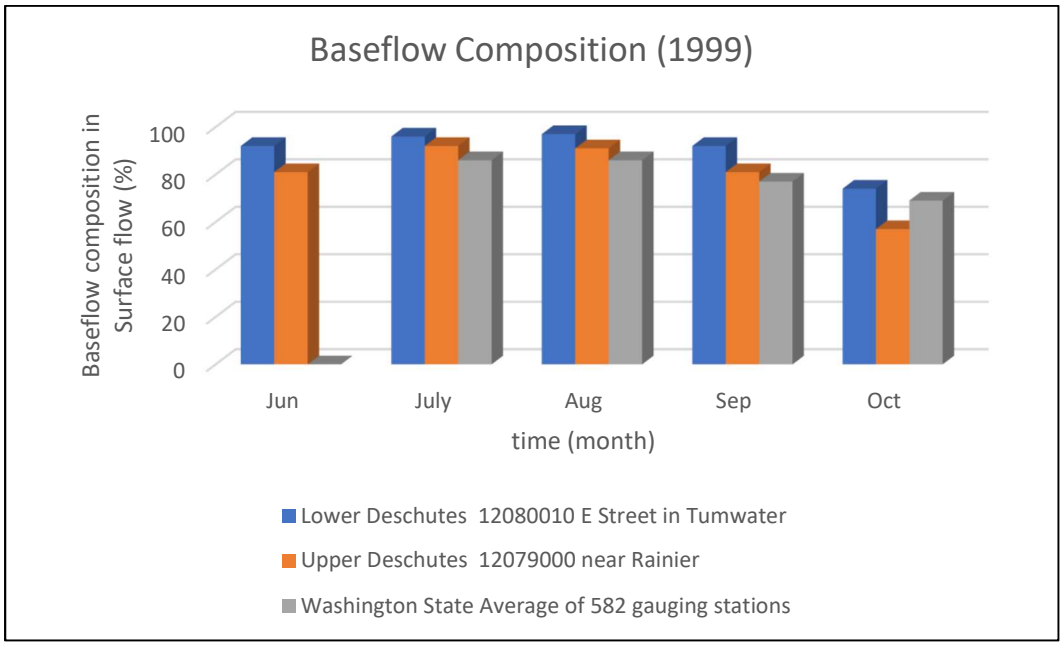

Note. Baseflow composition in the Lower Deschutes River is consistently higher than the Upper Deschutes River or the average of 582 gauge stations in Washington State. A unit for flow is cubic feet per second (cfs).

The baseflow has consistently been high during summer in the lower Deschutes River. On the other hand, direct runoff has been highly variable; the blue column (surface flow) without the baseflow portion (orange column) fluctuates to a larger degree (Fig. 8). Baseflow consistently accounts for a large portion of the surface flow; 83% of

the streamflow has been baseflow component over 65% of the time between 1945 to 2019[11]. This shows how the groundwater inflow (i.e., baseflow) dominated the surface water system (i.e., low flow) during the dry season in the Deschutes River. Therefore, we should understand that the baseflow is a major surface water component during low flow periods and how it affects the surface water quantity of the Deschutes River.

Figure 8

Historic and Present Baseflow Composition of the lower Deschutes River.

Streamflow data from NWIS gauge station 12080010 near Tumwater; baseflow data separated using a web-based hydrograph analysis tool (WHAT).

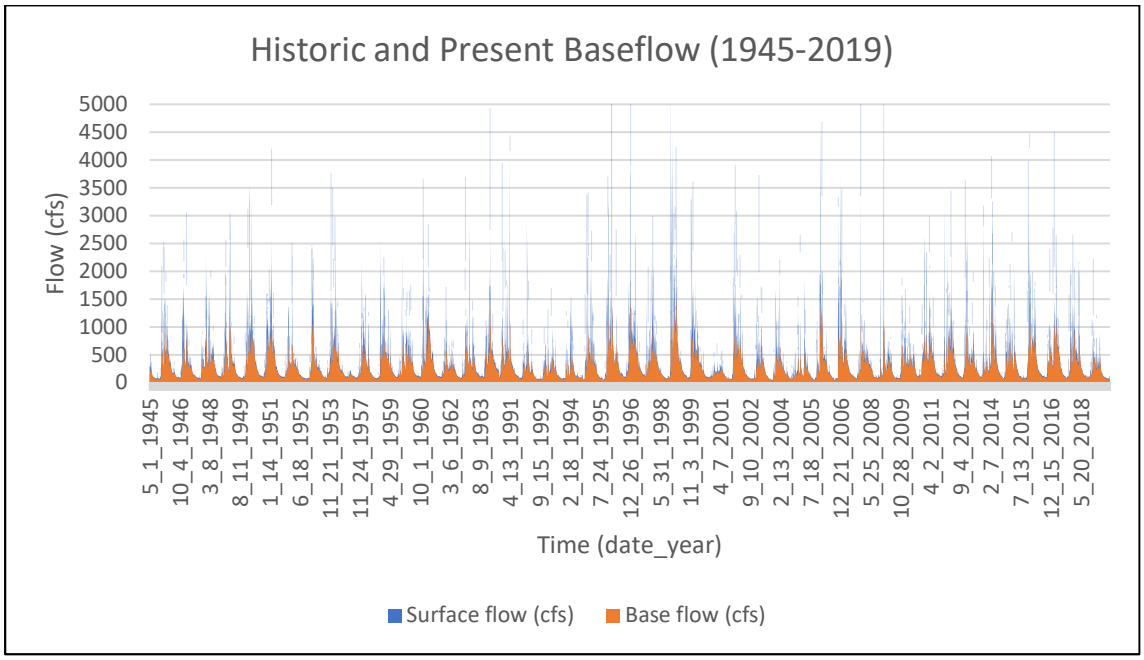

Note. Baseflow (orange) from groundwater has consistently been a major component of the Deschutes surface flow (blue). Units for flows are in cubic feet per second (cfs).

[11] Appendix A. Baseflow composition analysis in Lower Deschutes River. Data includes the entire water year of the Lower Deschutes River.

2.4: Low flow Trends and Attributions

2.4.1: Low flow in Pacific Northwest

Low flow phenomena occur in streams in 'wet' regions of the Pacific Northwest (PNW). As noted, low flow is the "flow of water in a stream during prolonged dry weather" (EPA, 2018). The low flow represents a certain flow rate to regulate minimum streamflow that should be kept for instream values (EPA, 2018). Typically, the PNW region is perceived to be free of risks of stream depletion because of ample rainfall throughout Fall, Winter, and Spring seasons. In other words, even though Summer flow remains low, the deficit streamflow is expected to be recovered or compensated by the following precipitation during wet winter (Konikow, 2013).

The perception that ample precipitation during wet winter alleviating the low streamflow during dry season may be an incomplete analysis on the low flow in PNW (Konikow, 2013). Summertime flows in PNW streams have deteriorated in recent years in both Eastern and Western Washington (Georgiadis, 2018). The reasons for streamflow deterioration can be climatic and anthropogenic; in this study, the attributing factors are divided into "precipitation", "climate change", and "groundwater exploitation".

2.4.1.1: Attribution 1. Precipitation

An empirical assessment of low flow in Puget Sound streams showed that most stream flows have deteriorated over the past 63 years on average[12] (Georgiadis et al.,

[12] 11 out of 13 streams of interest showed moderate to significant deterioration of low flow (Grorgiadis et al., 2018). 9 streams that showed significant deterioration include NE Stillaguamish near Arlington, Issaquah Creek near mouth, Deschutes River near Rainier, Deschutes River near Tumwater, South Fork Snoqualmie, Snoqualmie River near Carnation, Cedar River above Chester Morse Dam, Soos Creek, and Newaukum Creek. 2 streams with moderate deterioration include North Fork Snoqualmie and Snohomish near Monrow.

2018). Georgiadis, et al. showed that streamflow is positively associated with precipitation in wet seasons (winter, spring, and some summer wet periods). This means the low flow is enhanced as the surface water is recharged from the rainfall. On the other hand, the streamflow in low flow periods is negatively associated with the number of years (Table 1). The two findings combined indicated that the streams in PNW have experienced reduced flow in low flow periods, even with the precipitation recharging the flow (Hamlet, 2010; Luce et al., 2014; Georgiadis et al., 2018).

Table 1

Elements associated with low flow in streams of the PNW. Georgiadis et al., 2018.

Gauge Name	N (years)	Mean Low Flow (cfs)	R^2	Probability	Model Coefficients			
					Summer Rain	Spring Rain	Winter+ Fall Rain	Years of records
Nisqually River	72	8.98	0.17	1.37E-02	0.027	0.071	0.032	0.005
					4.58E-01	7.37E-03	2.60E-02	7.06E-01
Puyallup River near Orting	84	6.89	0.22	4.42E-02	0.171	0.162	0.095	0.021
					1.71E-02	2.72E-03	1.43E-03	2.71E-02
NF Stillaguamish near Arlington	87	7.61	0.42	3.17E-09	1.006	0.228	0.110	-0.025
					4.54E-08	4.47E-02	1.62E-02	4.79E-02
Issaquah Creek near the mouth	52	0.61	0.70	1.11E-11	0.030	0.022	0.008	-0.008
					2.19E-04	4.52E-06	1.23E-04	3.02E-08
Deschutes River near Rainier	53	0.90	0.67	5.12E-11	0.047	0.038	0.006	-0.004
					3.51E-04	2.33E-08	2.90E-03	3.26E-05
Deschutes River near Tumwater	40	2.40	0.60	4.05E-06	0.137	0.038	0.006	-0.004
					5.83E-03	3.75E-05	5.92E-04	1.71E-02
North Fork Snoqualmie	71	2.40	0.55	1.01E-10	0.348	0.034	0.022	-0.005
					1.59E-11	2.64E-01	834E-02	2.27E-01
South Fork Snoqualmie	53	1.28	0.68	3.14E-11	0.148	0.032	0.008	-0.010
					3.18E-10	1.03E-02	1.47E-01	2.99E-03
	85	22	0.42	6.17E-09	1.462	0.045	0.158	-0.110

Snoqualmie River near Carnation					2.86E-09	7.08E-01	1.31E-03	5.86E-03
Snohomish near Monroe	47	44.92	0.60	5.09E-08	7.914	2.319	0.717	-0.268
					5.81E-15	4.59E-03	3.52E-02	8.72E-02
Cedar River above Chester Morse Dam	70	1.12	0.70	2.26E-16	0.084	0.012	0.005	-0.004
					5.82E-15	6.49E-03	2.26E-02	4.45E-03
Soos Creek	49	29.40	0.52	1.40E-06	1.533	1.193	0.119	-0.119
					2.46E-03	5.53E-07	2.23E-01	1.10E-02
Newaukum Creek	62	16.30	0.52	8.19E-09	0.722	0.722	0.171	-0.080
					1.08E-03	7.21E-07	5.36E-04	6.45E-05

Note. Green denotes a positive effect on low flows and red a negative effect. Darker shades denote significance at alpha=0.05.

The result of a multi-year reduction in streamflow indicates that winter precipitation has not been a 'solution' to summer low flow, regardless of the precipitation input. The effect of precipitation recharging streamflow happens in a short-term period; instead, the long-term low flow has not been resolved by precipitation. This suggests that other elements are more likely to affect the deteriorated flow in PNW streams.

2.4.1.2: Attribution 2. Climate Change

Diverse elements of climate change due to anthropogenic effects are associated with the declining surface flow and increased low flow periods in the PNW. The elements of climate change include 1) greenhouse effect and increased air temperature, 2) modified ocean-atmospheric patterns in the Pacific Ocean, and 3) frequent extreme precipitation events.

First, Luce et al (2013) found that streamflow declines in the rivers of PNW are more associated with anthropogenic climate change elements, such as the greenhouse effect, land-use alteration, or groundwater pumping activities, than they are with a trend

of precipitation (Luce et al., 2013). They concluded that annual streamflow in the PNW has shown marked declines while annual precipitation has not changed significantly. This highlights climate change as a stressor on hydrology in the PNW (Luce et al., 2013).

Second, modified ocean-atmospheric patterns in the Pacific Ocean due to climate change are associated with declining streamflow in the PNW. The Pacific Decadal Oscillation, the El Nino Southern Oscillation, and the Pacific North American patterns (Hamlet & Lettenmaier 2007; Luce & Holden, 2009) increase the seasonal disparity in streamflow between dry and wet periods, mostly exacerbating low flow phenomena[13].

Lastly, a low flow period prolongs as streamflow decreases via frequent extreme precipitation events, which result from a combined effect of heightened air temperature and drier weather patterns from climate change. Historically, a substantially reliable amount of precipitation and snowpack has replenished low flows in streams of the PNW; many streams are glacier/snowmelt dependent in PNW (Pelto, 2011). Climate change has threatened the natural recharge and storage regimes by changing the timing of snowmelt and the amount of water available to streams (Fig. 9) (EPA, 2016). The warmer climate contributes to earlier and more concentrated precipitation and snowmelt, which can cause higher streamflow in wet seasons and lower flows in summer (Hamlet, 2010). In sum, the climate change and its effect on oceanic currents are highly associated

[13] The oceanic climate change attributions explain the streamflow disparity in the PNW. The interannual variability is linearly correlated with climate change variabilities realized through the Pacific Decadal Oscillation ($r^2 = 0.33, p < 0.001$), the Pacific North American pattern ($r^2 = 0.3, p < 0.001$), and the El Nino-Southern Oscillation ($r^2 = 0.28, p < 0.001$). Together they explain some ($r^2 = 0.37, p < 0.001$) interannual variability in streamflow.

with extreme precipitation patterns and increased streamflow disparities: higher flows during the wet season versus lower flows during the dry season.

Figure 9

Climate change effect on precipitation and low flow. Tohver & Hamlet, 2010; EPA, 2016.

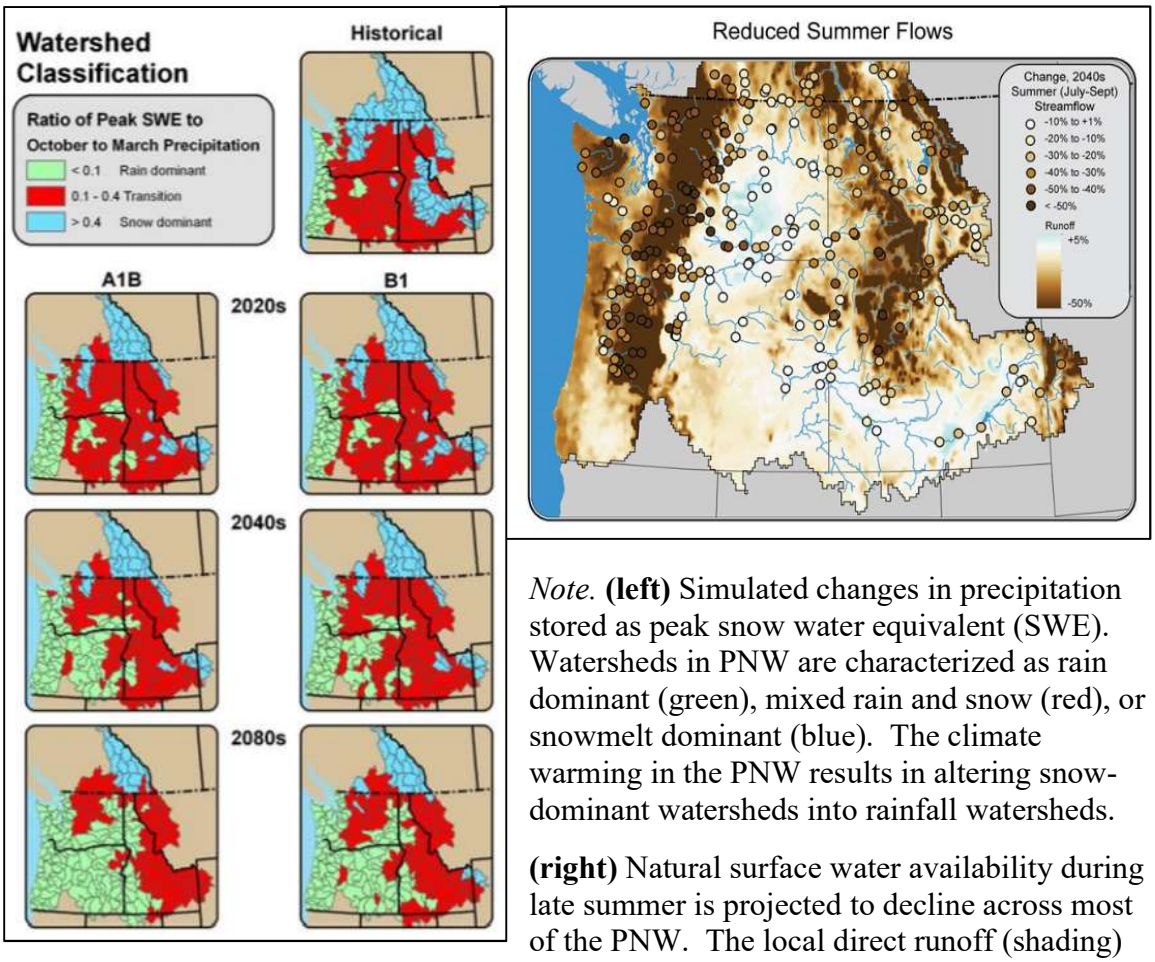

Note. **(left)** Simulated changes in precipitation stored as peak snow water equivalent (SWE). Watersheds in PNW are characterized as rain dominant (green), mixed rain and snow (red), or snowmelt dominant (blue). The climate warming in the PNW results in altering snow-dominant watersheds into rainfall watersheds.

(right) Natural surface water availability during late summer is projected to decline across most of the PNW. The local direct runoff (shading) and surface streamflow (colored circles) for the 2040s (compared to the period 1915 to 2006) are expected to decline, associated with the climate change effect.

2.4.1.3: Attribution 3. Groundwater exploitation

Groundwater pumping can explain much of the groundwater storage reduction and consequent deterioration of low flow during dry periods. Excessive pumping consumes, intercepts, and depletes groundwater and natural waterways, compromising

surface water ecosystems (Lambert, 2019). De Graaf et al. studied the deleterious impact of groundwater withdrawals on reducing surface flow in agricultural regions of the globe (Fig. 10; de Graaf et al., 2019). For example, about 15 to 21 percent of surface water in the globe has already reached the ecological tipping point, such that the streamflow cannot serve the usual ecological functions due to heavy groundwater pumping (de Graaf et al., 2019). By 2050, the authors estimate that 42 to 79 percent of pumped watersheds of major rivers in the globe will have crossed this tipping point (Graaf et al, 2019), leaving the streams too dry to provide ecological functions, such as healthy habitats for aquatic-dependent species.

In Pacific Northwest, the increased pumping and reduced surface flow have caused harm to the anadromous fish populations (Hebert, 2016). In Eastern Washington, groundwater extraction has already led to large reductions in groundwater storage over more than 10,000 square miles (Pitz, 2016). Groundwater levels in Eastern Washington have declined by more than 300 feet in some areas with deeper basalt aquifers (Burns et al., 2019). Reduced groundwater storage and discharge (i.e., baseflow) greatly affects the ecological function of a river system.

Figure 10

Modeled timing when an environmental flow limit has been or will be reached for the first time in streams of the globe. Graaf et al., 2019

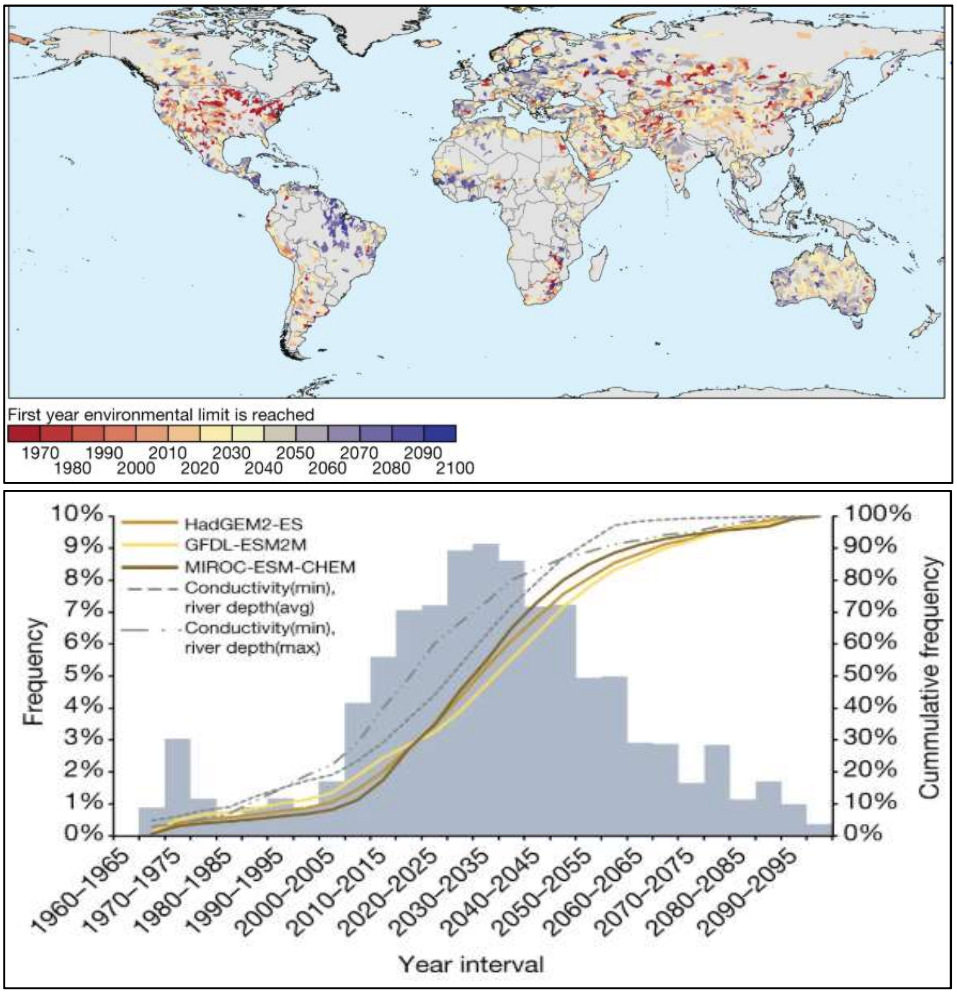

Note. **(top)** The first time at which environmental flow limits have been, or will be, reached, by year, averaged per sub-watershed[14]. Red denotes streams that have already reached the flow limits; blue denotes the streams that are projected to reach the limits by 2010. **(bottom)** Global distribution of estimated first times at which environmental flow limits have been, or will be, reached, under different projection models. Over half of the studied streams are projected to reach flow limits around 2030-2045.

Groundwater pumping and its effect on reducing streamflow during a low flow period are not limited to agricultural regions, such as the Eastern Washington region. In

[14] Environmental flow limits refer to the streamflow at a level to sustain the ecological functions of a stream.

Western Washington, increased groundwater pumping from population growth has stressed the groundwater storage and surface flow, especially during low flow in the summertime. Here, the increased groundwater pumping is assumed to directly reduce the baseflow during dry seasons. Pitz (2016) argued that groundwater pumping may deteriorate the summertime low flow and baseflow more than consequences due to climate change (Pitz, 2016). Already, Western Washington groundwater dynamics (i.e., storage and discharges, baseflow) faces reduced annual recharge due to climate change effects[15]. More extreme precipitation and drier low flow period imply that the amount of groundwater recharge in dry season decreases. Streams under existing stressors will experience an exacerbated low flow with increasing groundwater extraction.

2.5: Baseflow Recession in the Deschutes

2.5.1: What is Baseflow Recession?

The role of baseflow connecting the two water systems—surface water and groundwater system—is especially vital during low flow periods due to prolonged dry spell. The deterioration of baseflow, "baseflow recession", is detrimental in a low flow period when a surface stream is most dependent on baseflow from groundwater.

Groundwater pumping is an anthropogenic impact that converts the river from a balanced flow to a predominantly losing stream (Fleckenstein et al. 2004). "Losing stream" occurs when the uppermost level of groundwater, or "water table", is lowered to a level that groundwater no longer reaches to the surface streamflow (Fig. 11). When

[15] Skagit River basin (Johnson & Savoca, 2011) and Chambers-Clover Creek watershed (Johnson et al., 2011) show a 20% reduction in annual groundwater recharge to climate change effects.

groundwater is overly consumed by excessive pumping, the water table drops, and groundwater is likely to disconnect from the surface flow system (Panza et al., 2015). In that case, baseflow is no longer hydraulically connected nor contributing to the surface flow, resulting in streamflow depletion (Barlow & Leake, 2012).

Figure 11

Schematic effects of pumping on a water movement. Barlow & Leake, 2012.

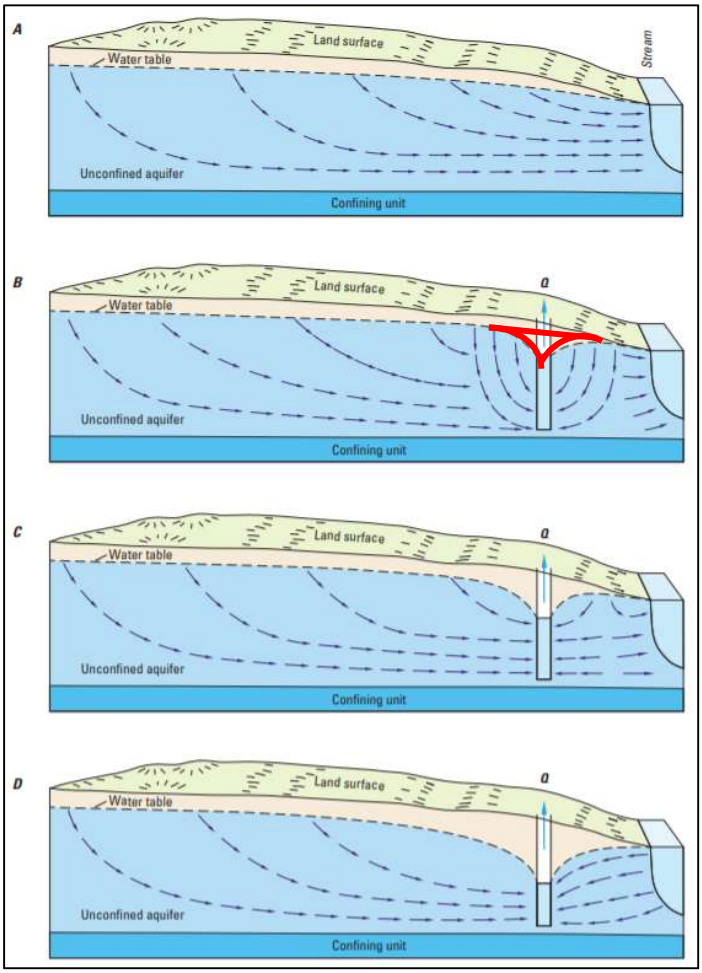

Note. (10-A) Under natural conditions, recharge at the water table is equal to discharge (i.e., baseflow) at the stream. (10-B) Soon after pumping begins, all the water pumped by the well is derived from groundwater storage. (10-C) As the cone of depression (red) expands, the well begins to capture groundwater that would otherwise have discharged to the stream. (10-D) The pumping rate of the well may be large enough to cause water to flow from the stream to the aquifer, a process called "induced infiltration" of streamflow. The stream then transforms into a "losing stream" (Barlow & Leake, 2012).

2.5.2: Baseflow Recession in the Deschutes River

Baseflow is a proxy for groundwater discharge (Q). Depending on the destination of groundwater outflow, the groundwater discharge (Q) may take a form of "baseflow" when discharged to surface stream or of "submarine groundwater discharge" when discharged to sea water (Stieglitz, 2011). In this study, groundwater discharge (Q) is used interchangeably with baseflow. The "baseflow recession period" refers to the period of baseflow reduction. The highest point of recession (Q_0) is when the baseflow starts to decline; the lowest point of recession (Q_t) is the baseflow right before when the it starts to increase after continuous recession. The time of each recession event (t) varies with the length of each recession on the baseflow hydrograph (Fig. 12).

Figure 12

Components of baseflow. Streamflow data from NWIS; Precipitation data from NOAA.

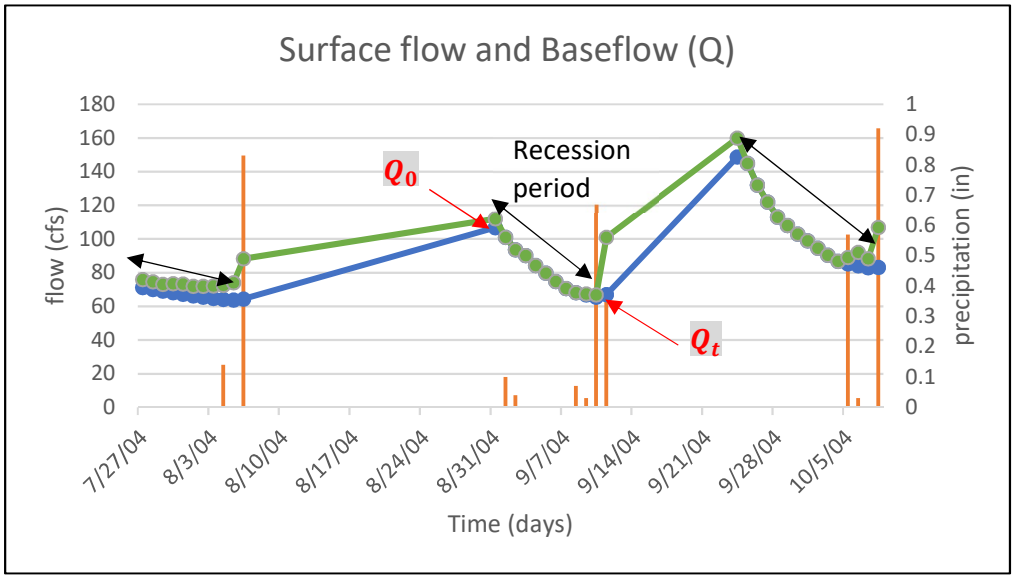

Note. Surface flow (green) is restored by base flow (blue) while there is no precipitation (orange). The lowest point (Q_t) refers to the least amount of baseflow contribution, indicating depletion in the groundwater storage or dry year.

Thurston County (2002: Thurston County, 2012) and Department of Ecology (2007: Sinclair & Bilhimer, 2017) monitored the baseflow recession of streams in Washington. The baseflow recession period (t) varies each year, depending on the amount of precipitation and groundwater storage. The lowest point of baseflow (Q_t), the least amount of baseflow contribution, in the Deschutes River showed a decline from 1945 to 2019 (Fig. 13). The declining trend of the Q_t during the recession period indicates that the capacity of groundwater contribution has weakened or decreased.

Figure 13

Lowest Baseflow in the Deschutes. Streamflow data from NWIS. Baseflow separated using WHAT.

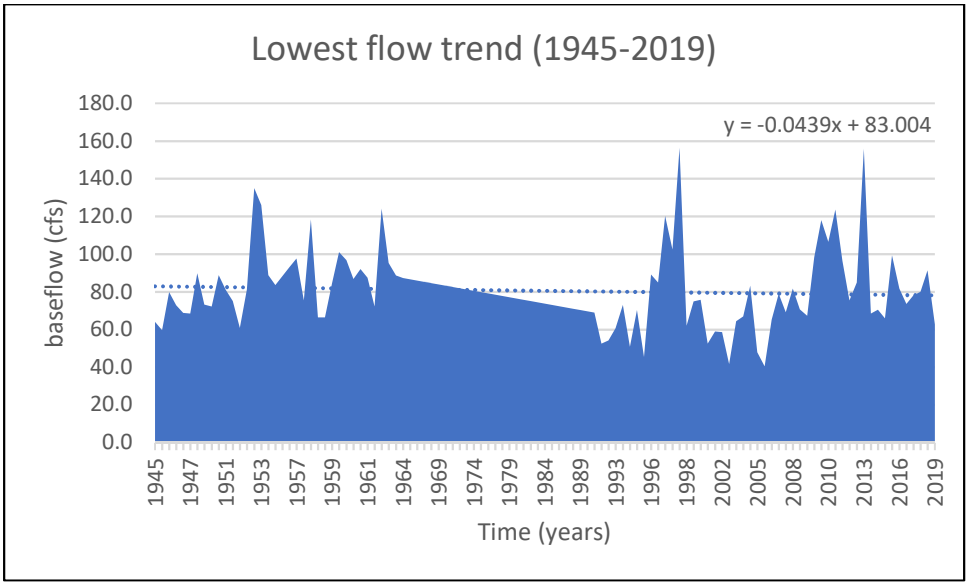

Note. The linear regression (dotted line) of the decline has a gradual negative coefficient of -0.0439. This implies the future points of lowest baseflow (Q_t) are likely to show declining trend.

The mean baseflow of this set of streams declined from 293 cubic feet per second (cfs) of the earlier period (1949-1963) to 258 cfs of the later period (1991-1997) (Sinclair & Pitz, 1999). Between 1956 and 1994 there was a decrease in baseflow of 35cfs or 450

gallons per minute (gpm). The decreased baseflow represents the "lost" flow rate that would have been available as baseflow discharge from the underground aquifer to the surface flow. Such a baseflow recession trend explains groundwater storage depletion, which may be attributed to climate change and human groundwater withdrawals. Groundwater pumping is detrimental in stream ecology during low flow as it intercepts the groundwater storage and causes baseflow recession (Barlow & Leake, 2012).

2.5.3: Groundwater demand

2.5.3.1: Reliance on Groundwater in the US

Groundwater is used for various purposes (Table 2). Among the different purposes for groundwater withdrawals, public water supply and general domestic uses in metropolitan and greater city areas have soared due to population growth (Konikow & Kendy, 2005; Jakeman et al., 2016). In 2015, one-third of the US population (about 115 million people) relied on publicly or privately supplied groundwater (USGS, 2015). Some major cities such as San Antonio, Texas, rely solely on groundwater for all their public and privately supplied water consumption (USGS, n.d.). The interdependence of groundwater and population has grown as the groundwater supplies both public wells inside city water limits and outside in suburban or rural areas (Fienen & Arshad, 2016).

Table 2

Purposes of wells. Dieter et al., 2018.

Category	Purposes
Public Supply Group A (Chapter 246-290 WAC)	Water withdrawn by public and private water suppliers that provide water to at least 25 people or minimum of 15 connections. Supplied for domestic, commercial, industrial, thermoelectric-power, and public water use (firefighting, street washing, flushing of water lines, and maintaining municipal parks and swimming pools).

Irrigation	Water to assist crop and pasture growth, or to maintain vegetation on recreational lands such as parks and golf courses.
Commercial	Water for motels, hotels, restaurants, office buildings, other commercial facilities, and military and nonmilitary institutions.
Industrial	Water for fabrication, processing, and cooling in industries, such as chemical and allied products, food, mining, paper, petroleum refining, and steel.
Livestock	Water used for livestock watering, feedlot, dairy operations, and other on-farm needs.
Domestic General	Water used for indoor household purposes such as drinking, food, preparation, bathing, washing clothes and dishes, flushing toilets, and outdoor purposes such as watering lawns and gardens. Domestic water use includes public supply water (A and B) and self-supplied water.
Public Supply Group B (Chapter 246-291 WAC)	Water serving fewer than 15 connections or 25 people per day. Most Group B water systems use the groundwater permit exemption (RCW 90.44.050) (DoH, 2018).

Population growth has become the second-largest factor reducing groundwater, after the agricultural purpose (Groundwater Facts, n.d.). The groundwater withdrawal rate for agriculture has comparably slowed down while the withdrawal rate for the urbanization and population growth has grown faster in recent years (Rosegrant & Cai, 2009). "Domestic use" categorizes the groundwater demand to meet growing population and urbanization, and it comprises about 87% of the groundwater withdrawals for the public supply (public supply A and public supply B, from Table 2; Dieter et al., 2018). Self-supplied domestic water use is typically withdrawn from private sources, such as a well, or captured as rainwater in a cistern (Dieter et al., 2018). Public and domestic water use has comprised much of the total groundwater withdrawals in the past 20 years (between 58% to 73%; Dieter et al., 2018). This may threaten the depleting groundwater

resources with projected increases in withdrawals or freshwater delivery from other watersheds[16].

2.5.3.2: Groundwater demand in Thurston County

With the third-fastest growing population in the nation (US Census Bureau, 2019), Washington State's reliance on groundwater for domestic use through public supply water and self-supplied wells increased between 1985 to 2010 (Lane & Welch, 2015). The domestic water use via public supply in Thurston County has increased at a fast pace compared to other 19 Western Washington counties[17].

Groundwater is the major source of freshwater use in the Thurston County (85%)[18]. Most groundwater withdrawal is associated with domestic water use through public supply and self-supplied wells. The public supply (blue) and general domestic water use (orange) has consistently accounted for most of withdrawals (Fig. 14): 69% in 1985, 71% in 1990, 72% in 1995, 65% in 2000, 60% in 2005, 58% in 2010, and 73% in 2015. The groundwater withdrawal data below collected by USGS includes uncertainties for wells exempted from recording withdrawal amounts (see section 2.5.4.2).

[16] E.g., City of Bellevue purchases water from Seattle, delivering it for public supply from Cedar River and Tolt River watersheds through water pipes (City of Bellevue Utilities, n.d.).
[17] The rate of groundwater appropriation for Thurston County in 2010 was ranked as the 5th highest in the nation (Lane & Welch, 2015).
[18] Thurston County's total water withdrawals is estimated for 52.3 Mgal/day; the water source composites groundwater with 44.2 Mgal/day (84.51%) and surface water with 8.16 Mgal/day (15.60%).

Figure 14

Groundwater withdrawal purposes in Thurston County (1985-2015). Withdrawal data from USGS, 2018.

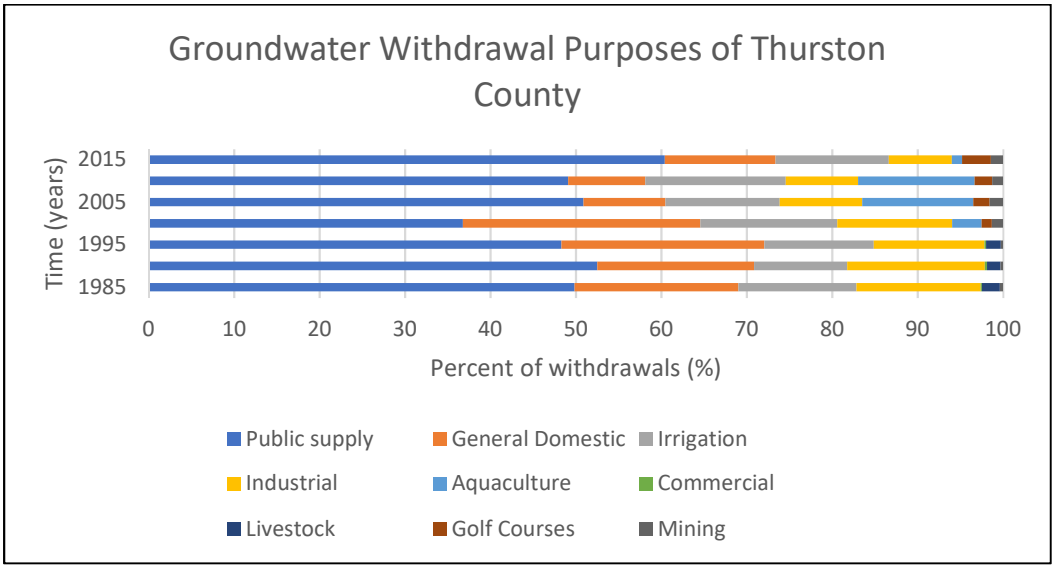

2.5.3.3: Growing demands in Thurston County

Population increase positively associates with the amount of groundwater demand (Dieter, 2018). Thurston Regional Planning Council projected that the total population in Thurston County will grow by over 25% by 2045 compared to the population in 2012 (TRPC, 2019)[19] while some major cities, such as Olympia-Tumwater-Lacey urban areas, are projected to have almost double the population of 1995 in 2045 (Fig. 15).

[19] Population projection information in Appendix B.

Figure 15

Population trend and projection in Olympia-Tumwater-Lacey urban area. TRPC, 2019.

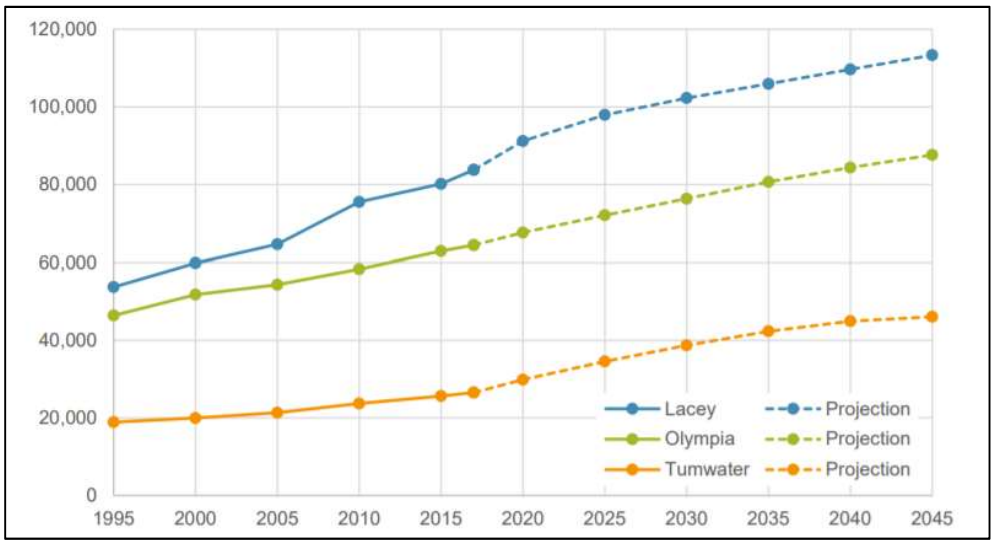

Olympia and Yelm have greater growth rates for their urban growth area (UGA) of 1.2% and 4.0% when projected from 2017 to 2045, respectively, than within their city limits (TRPC, 2019). This suggests the possibility that: 1) the groundwater pumping rate will increase to supply water to the expanding cities; 2) individual wells for domestic uses may increase in urban growth areas (UGAs), intercepting more groundwater via pumping. UGAs are outside urban centers and designated to be "annexed into city limits over 20 years" to accommodate urban growth (TRPC, 2019). As City limits expand to meet projected population increases, resultant freshwater demands may depend proportionally more on self-supplied domestic wells than public supply water. This is concerning as self-supplied domestic wells are mostly exempted wells that are not regulated for their withdrawals.

Lacey, Tenino, and Tumwater city project greater population growth in UGA of 1.8%, 3.5%, and 3.8%, respectively (Appendix B) that the population growth will mostly

occur within UGAs (TRPC, 2019). The number of dwelling units (Appendix C) projects an increase in all parts of Thurston County that new development relying on self-supplied domestic wells in rural areas is expected[20]. This may result in more frequent interception of groundwater through pumping in rural areas, which are not regulated for the withdrawals under groundwater permit exemption (Chapter 90.44.050 RCW, 1945). The unregulated wells' withdrawals are not monitored or reported so that their hydrological impact on lowering groundwater and surface water is difficult to identify. The issue of sprawling unregulated wells and their effect of lowered streamflow elicited Hirst Decision (2016), which enforced permit-exempt wells and monitoring rural development (see 2.5.4.3).

2.5.4: Hydrological Impact of Wells in Deschutes River

2.5.4.1: Instream Flow

Baseflow input to the surface water system has hydrological and ecological impacts on low flow during dry seasons. The Department of Ecology established minimum water flows or levels for streams required to protect the resource[21] or preserve water quality, referred to as "instream flows" (RCW 90.22.010) [22]. The instream flows intend to protect the river flows and limit new development or withdrawals that could harm ecological streamflow. Also, the instream flows protect senior water rights that were established prior to the instream flow (1980 for WRIA 13 Deschutes River Basin).

[20] The number of dwelling units is in Appendix C

[21] Instream values or merits for a healthy riverine ecosystem include fish, wildlife, recreation, aesthetics, water quality, and navigation.

[22] Instream flows for 26 watersheds in the Washington State differ from individual watersheds (or Watershed Resource Inventory Areas, WRIA) and were established at different times. The instream flow of the Deschutes River Basin (WRIA 13) was established in 1980 under the authority of Chapter 90.54 RCW (Water Resources Act of 1971), Chapter 90.22 RCW (Minimum Water Flows and Levels), and Chapter 173-500 WAC (later Resources Management Program) (Washington, 1980)

According to the "prior appropriation doctrine", the senior water rights (i.e., pre-existing water rights) are guaranteed before junior water rights do ("first-in-time, first-in-right"). The instream flow protects senior water rights, such as Native Tribes' sovereign water rights, for their priority, as it restricts excessive groundwater pumping (Osborn, 2013).

The instream flows during low flow periods in the Deschutes River show the need to protect water quantity. The instream flow is "closed" for additional uses from April 15th to October 31st (Fig. 16) to restrict further consumptive appropriations that would harmfully impact instream values (Chapter 173-513 WAC, 1988), based on the basin hydrology and surveys of fish production capabilities (Kavanaugh, 1980).

Figure 16

Instream flow of the Deschutes River Basin[23]*. Chapter 173-513 WAC, 1988.*

INSTREAM FLOWS IN THE DESCHUTES RIVER BASIN
(in Cubic Feet per Second)

Month	Day	USGS Gage 212-0800-00 Deschutes River
Jan.	1	400
	15	400
Feb.	1	400
	15	400
Mar.	1	400
	15	400
Apr.	1	350
	15	(Closed)
May	1	(Closed)
	15	(Closed)
June	1	(Closed)
	15	(Closed)
July	1	(Closed)
	15	(Closed)
Aug.	1	(Closed)
	15	(Closed)
Sept.	1	(Closed)
	15	(Closed)
Oct.	1	(Closed)
	15	(Closed)
Nov.	1	150
	15	200
Dec.	1	300
	15	400

Note. "Closed" denotes the period when all consumptive uses are restricted[24].

[23] Chapter 90.22 and 90.54 RCW. 80-08-019 (Order DE 80-11), § 173-513-030, filed 6/24/1980.
[24] "Water use" can take two forms, consumptive or withdrawal. Withdrawal water use refers to "water diverted or withdrawn from a surface water or groundwater source". Consumptive water use refers to

The low flow trend of the Deschutes has shown that the flow during the closed period violates and falls below the instream flow levels (Fig. 17). The minimum required instream flows during closed periods was set around 100 cubic feet per second (cfs) (Kavanaugh, 1980). The surface flow shows that the lowest flows were near or lower than 100 cfs, reaching as low as 40 cfs (for example, around 2003 and 2006 in Fig. 17). This denotes that the low flow status during a closed period is questionable whether it can sustain ecological streamflow and can preserve the instream values.

Figure 17

Trend of surface flow of the lower Deschutes River (1991-2019). Modified from streamflow data from NWIS.

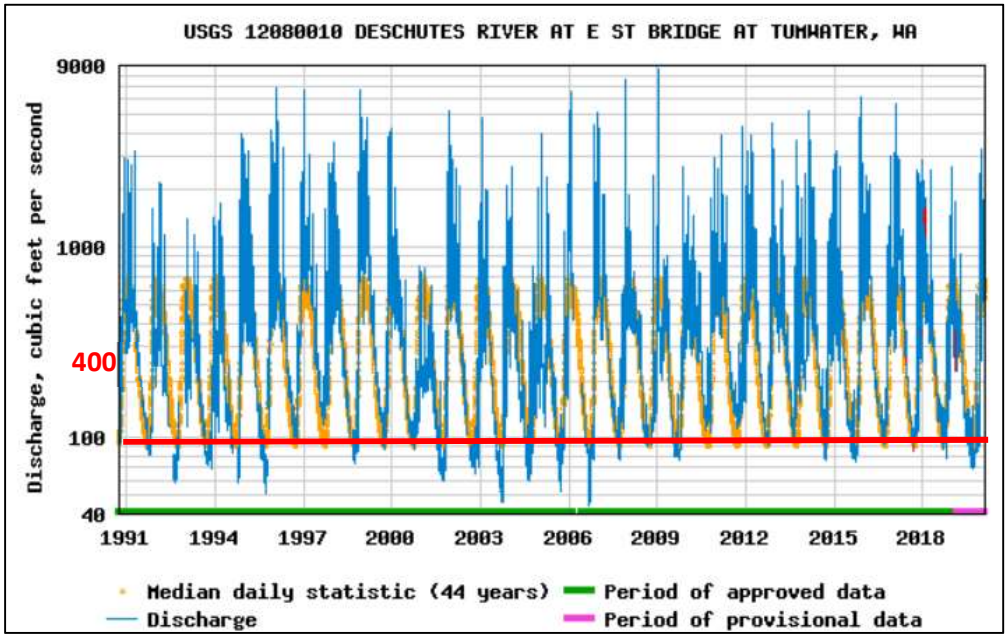

Note. The daily surface flow, or discharge, shows the average daily streamflow (blue line). The median daily surface flow in the past 44 years shows a historical trend of surface flow change (yellow line). The approved surface flow data (green line) and provisional data (purple line) indicate an official period of surface flow record. Daily surface flow (blue line) has exceeded and violated the wet and dry period instream flow (denoted in red) since 1999.

"water use that permanently withdraws water from its source that water is no longer available and removed from the immediate water environment (Water footprint calculator, 2018).

2.5.4.2: Permit-exempt Wells and Instream Flows

To protect the minimum instream flow in the Deschutes, consumptive water use has been restricted. However, there are some exemptions to the instream flow rule. The effect of additional consumptive water uses through exempted withdrawals has not been clarified; however, they are still in use. Types of withdrawals that are exempt from surface stream closure include domestic use wells for single residence and stock watering, except for feedlot (Chapter 173-513 WAC, 1988). These domestic wells are typically "permit-exempt" wells that do not require a procedural obligation to obtain water use permits; however, they are still subject to the prior appropriation rule that their use cannot hypothetically interrupt senior water rights. Most importantly, new permit-exempt wells have been allowed in rural areas even though their groundwater extraction has not been analyzed for a potential effect of reducing groundwater and surface water to an unsustainable level (AGO, 1997). The continued withdrawal via permit-exempt wells is a regulatory and ecological interruption of the senior instream flow, which has often been violated (Fig. 17). Therefore, the potential impact of permit-exempt wells on the low flow hydrology should be analyzed from a more precautionary respective.

2.5.4.3: Permit-exempt Wells' Effects on Baseflow

While permit-exempt wells are intended for "small withdrawals", the hydrological impact of permit-exempt wells on the extent of groundwater reduction and baseflow decrease has not been analyzed in the Deschutes River. Therefore, we should pay close attention to some uncertainties regarding permit-exempt withdrawals as their impact is not identified. Three considerations include 1) the possible increase in permit-exempt wells in rural areas, 2) disparity of allowed withdrawals through permit-exempt wells and

public water use permit-exempt wells, and 3) the importance to understand the impact of withdrawals—rather than consumptive uses—on the groundwater storage and baseflow.

First, permit-exempt uses may increase with projected population growth; their withdrawals are not monitored and may reduce groundwater storage. As discussed, the population increase in urban growth areas (UGA) in Thurston County (see section 2.5.3.3) may result in increased permit-exempt well constructions. Increasing permit-exempt wells will result in uncertainties in groundwater management because of permit-exempt wells not being monitored or restricted for their uses. Because the actual withdrawals from individual permit-exempt wells are unknown, municipalities rely on averaged withdrawal rates estimated from septic system use (Hansen, 2018). The withdrawals via unregulated permit-exempt wells remain uncertain to estimate the precise impact on the groundwater storage.

Second, recently established regulations on withdrawal allowances may not help to solve groundwater depletion and baseflow recession during low flow. The Hirst Decision[25] directed counties to develop watershed plans that offset impacts from new domestic permit-exempt wells. This includes setting a new withdrawable groundwater amount depending on the individual watershed situation. Before the Hirst Decision, the groundwater withdrawal per well was limited to a maximum annual average of 5,000 gallons per day (gpd). After the Hirst Decision, this maximum withdrawal amount changed to 950 gpd, which may be curtailed to 350 gpd under declaration of a drought (TCCP, 2018). The 950 gpd withdrawal applies to the small withdrawals for domestic,

[25] Whatcom Cty. v. Hirst, 186 Wash, 2016.

industrial, and commercial uses; stock water is allowed for unlimited withdrawals. As permit-exempt wells are generally not monitored, their future withdrawals remain as uncertain as their current withdrawals.

The newly established withdrawal amount after the Hirst Decision, however, may still overestimate the practical domestic water use and set the bar higher than our typical consumption. Daily water consumption in the US estimated in 2010 was on average 79 gpd per person (Bracken, 2010). Equivalently, the withdrawal per dwelling was estimated with 205 gpd with an assumption that 2.95 people live in a dwelling (Golder Associates, 2015), sharing one permit-exempt well. Another study conducted in 2014 showed that the daily average was 111 gpd per person (The Associated Press, 2014), or 327 gpd from the same assumption of 2.95 people sharing a well. These daily average water consumption per well (205 or 327 gpd) is much lower than the regulated maximum withdrawals of 950 gpd (or 350 gpd under a drought scenario). Other uses, such as irrigations or stock-water, may require extractions near 950 gpd or even 5,000 gpd, which was the previous limitations on permit-exempt well withdrawals prior to the Hirst Decision. On top of this, the stock-watering is allowed for an unlimited amount; these curtails of 950 gpd (or 350 gpd) are not quite restrictive to permit-exempt well uses, which was originally purposed for "small withdrawals" (RCW 90.44.050).

Third, the permit-exempt wells' impact on the baseflow recession accounts for their total withdrawal amount, rather than their consumptive use. Typically, when quantifying the impact of withdrawals on the surface flow, consumptive use represents

the "impact" or the "lost" flow[26]. The consumptive use[27] refers to the amount that is completely used or lost from the surface system:

$$Consumptive\ use = (Withdrawal\ amount) - (Return\ to\ groundwater)$$

Consumptive use does not fully describe the impact of pumping on groundwater loss; instead, total withdrawal amount associates with a direct reduction of baseflow and affects baseflow recession. This is because the baseflow is a proxy of groundwater storage that discharges to the surface water system (EPA, 2018). Therefore, the total withdrawal amount of groundwater pumping wells will be a better index than consumptive use to estimate the impact of groundwater withdrawals on the streamflow.

2.5.5: Consequences of Baseflow Recession

Baseflow recession refers to the phenomenon when the amount of baseflow contributing to the surface flow reduces or recedes (see section 2.6.1). The baseflow recession impacts the water quality as it associates with some water quality indices, such as water temperature, dissolved oxygen, pH, and pathogen. Such an impact on surface water quality affects the surface water—groundwater interaction within the hyporheic zone, which serves as a desirable habitat environment for salmon and other anadromous species.

2.5.5.1: Baseflow Function on Water Quality

Summer low flows affect rivers' ecological functions on biotic and abiotic conditions and aquatic species dependent on the flow. Potential negative impacts of low

[26] Technical reports aiming to discern the impact of groundwater withdrawals on the surface flow utilize the consumptive use instead of withdrawal amount as their subject (e.g., Golder Associates, 2015).
[27] Return to groundwater can come from septic systems or irrigation through land or surface flow.

summer flows include higher water temperatures, low dissolved oxygen, and more frequent diseases (Essington et al., 2010). Ecological functions during low flow largely rely on baseflow contributions. Baseflow adds refreshing cold groundwater to summer low streamflow (DoE, 2012). In reverse, baseflow recession can have devastating ramifications on the river's ecological functions including degraded water quality or undesirable habitat environments.

A longitudinal survey on total maximum daily load (TMDL) shows the surface water quality in the Deschutes River since 2003 (DoE, 2015). TMDL refers to the "highest pollutant loads a surface water body can receive and still meet water quality standard" (DoE, 2015). The mainstem Deschutes River is impaired by high water temperature and low dissolved oxygen (DO), which affects the physiology and behavior of fish and other aquatic life (DoE, 2015). The warmer stream provides less capacity to hold oxygen within water molecules, entailing deficient oxygen and unbalanced organic matters (e.g., high phosphorous or nitrogen[28]) within the stream. High temperature generates to degraded pH, which can impair the ecological function of the river. In the following sections, we will discuss the reduced baseflow function on water quality.

2.5.5.1.1: Function 1. Lowering Stream Temperature

Low stream temperature is essential for aquatic species, especially anadromous fish, such as salmon. Warm streams result in deteriorated water quality as it reduces the stream's capacity for dissolved oxygen level and other water quality standards, such as

[28] Walczyńska & Sobczyk, 2017

pH or pathogen. During low flow in the summertime, the temperature in the stream increases, and the baseflow contribution can positively lower the stream temperature.

Stream temperatures in the upper and lower Deschutes River are at a threatening level to sustain healthy salmon habitats (Fig. 18). The mean stream temperature at the upstream Deschutes River (near Rainier) was 10.56 °C (wet season 7.92 °C; dry season 15.83 °C). At the downstream Deschutes River (near Tumwater), the mean stream temperature was significantly higher, at 11.71 °C (wet season 9.00 °C; dry season 17.14 °C). Compared to the standard stream temperature desirable to protect fish and their habitats[29], the stream temperatures during dry seasons in the lower Deschutes River exceed the core summer salmon habitat standards (16 °C); if not, the maximum temperature for salmonid spawning, rearing, and migrating (17.5 °C). However, the difference between the lower stream temperature in the dry season, and the standard is 0.36 °C, which is a marginal gap that can be exceeded by increasing dry season stream temperature.

[29] The standards were estimated with 7-DADMax; a 7-day average of daily maximum temperatures should not be exceeded more than once every 10 years on average.

Figure 18

Stream Temperatures and salmon habitat standard temperatures. Data from DoE, 2015.

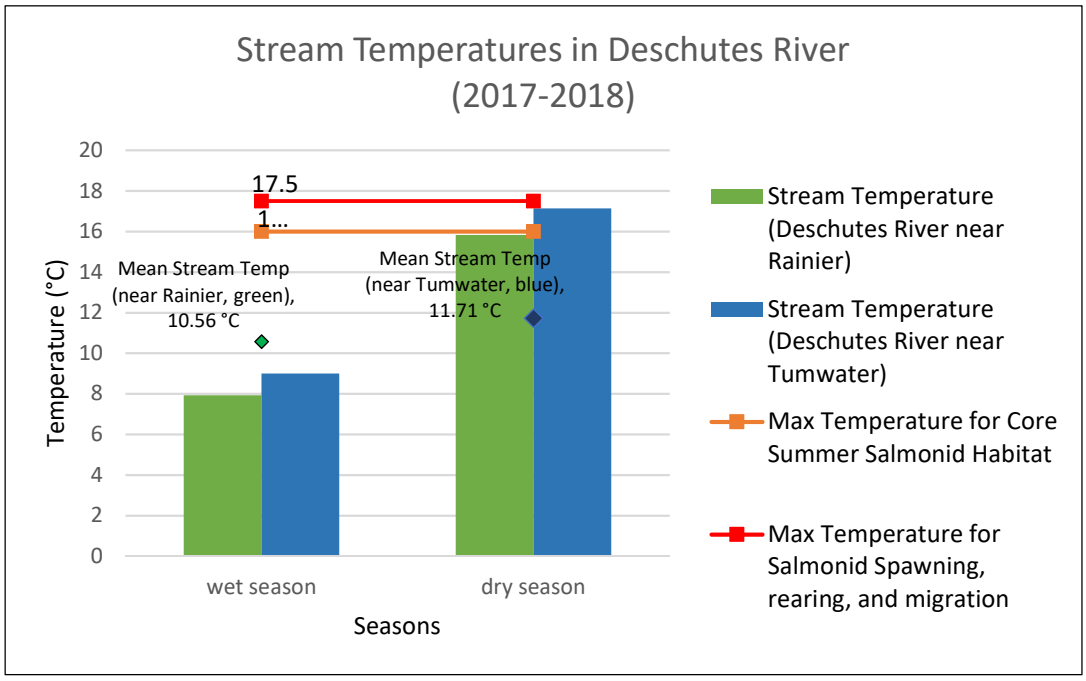

Currently, the water quality of the Deschutes River is deteriorated below TMDL standards. The stream temperature of the Deschutes River has exceeded the TMDL standard, which deteriorated other water quality standards—dissolved oxygen (DO), pH, fecal coliform bacteria, and fine sediment[30] (DoE, 2012; Wagner & Bilhimer, 2015). Warm stream reduces the amount of soluble oxygen in the water and degrades ecological conditions for riverine species and their habitats (Rounds et al., 2013). Enhancing baseflow contribution during a low flow period was one suggested TMDL management strategy (DoE, 2012; DoE, 2015). Improving baseflow from 20% to 40% has a potential to decrease stream temperature by 0.3°C (Table 3), based on a scenario which evaluated

[30] Clean Water Act 303(d)

the changes in baseflow due to anthropogenic influences (domestic exempt wells construction) and climate change (DoE, 2015) (Table 3).

Table 3

Management action scenarios to reduce stream temperature of the Deschutes River. Data from DoE, 2015.

	Management actions	Expected Temperature Change
Streamflow temperature reduction related to Management actions	Restoring mature vegetation	- 4.5°C
	Reducing Channel Width	- 1.3°C
	Improving microclimate	- 0.7°C
	Reducing headwater and tributary temperature	- 0.4°C
	Increasing Baseflow	- 0.3°C

The effect of increasing base flow is seen as a less powerful management action than, for example, restoring vegetation, which is projected to reduce the stream temperature by 4.5°C (Table 3). However, a report on recovering Coho salmon migration on the Deschutes specified that the effect of the baseflow improvement should not be treated as a single variable but with other variables (Cherry Shane Consultant, 2015). This is because the enhanced baseflow contribution has a chain-effect that positively affects other variables in the scenario (Table 3), such as improved microclimate or lowered stream temperature (Cherry Shane Consultant, 2015). The improved base flow yields cooler groundwater while flowing into the surface water system, which benefits fish habitat sites or cool water refugia (Watershed science, 2004; Cherry Shane Consultant, 2015).

2.5.5.1.2: Function 2: Hyporheic Zone, Salmon Habitat

Deteriorated water quality in the Deschutes streamflow has degraded habitat environments for fish. The Deschutes River supports anadromous species, such as sea-

run cutthroat trout, coho, fall Chinook salmon, sea-run and winter steelhead[31] (Conservation & Lead, 2004; Cherry Shane Consultant, 2015). The coho salmon return was once prosperous, however, it has markedly reduced since the 1980s in the mainstem of the Deschutes River; two of the three coho brood lines in the Deschutes have experienced a severe reduction or are "virtually extinct" in the past two decades (Zimmerman, 2010).

Improved baseflow enhances hyporheic exchanges in subsurface water where surface water and groundwater intermix (Wagner & Bilhimer, 2015). Hyporheic exchange is the intermixed flow of groundwater and surface water, where cold groundwater seeps into the surface water system and alleviates stream temperature and improves oxygen exchange (Hayashi & Rosenberry, 2002). The baseflow movement contributes to expanding and activating the hyporheic exchange and the zone. The hyporheic zone (Fig. 19), where the hyporheic exchange occurs, is the "buffer" in the subsurface water in shallow sediments and creates a desirable fish habitat with lower stream temperature and abundant dissolved oxygen (DO)[32].

[31] Anadromous species describes fish "born in freshwater who spend most of their lives in saltwater and return to freshwater to spawn, such as salmon and some species of sturgeon" (NOAA, n.d.).
[32] id

Figure 19

Hyporheic zone. Winter et al., 1998.

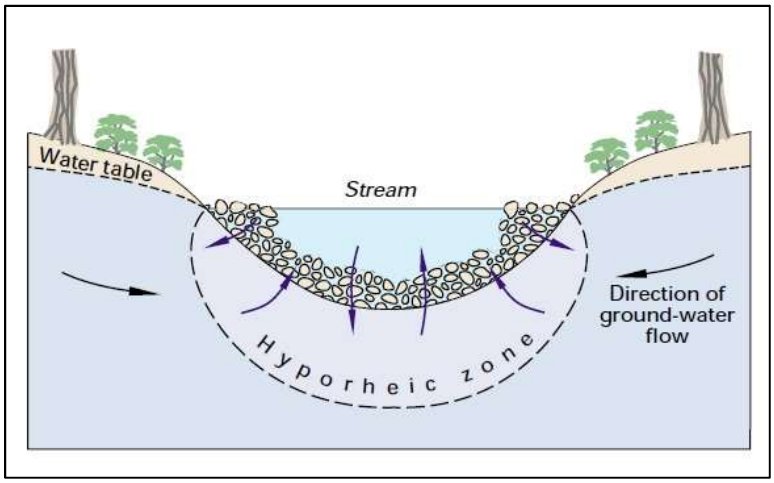

Note. The arrows denote groundwater flow between the underground aquifer, hyporheic zone, and surface stream. The upward arrow denotes baseflow, which contributes from the groundwater to the surface flow.

Under low flow circumstances, baseflow movement is critical in forming hyporheic zones for fish habitats (WRIA 13, 2019). The volume of the hyporheic zone is controlled by ambient groundwater flow (Singh et al., 2018), which is represented as baseflow. The hyporheic exchange contributes to lower the stream temperature as cooler baseflow enters into the surface water system. For example, Roberts et al (2008) concluded that the existing depth of the hyporheic zone was projected to lower the summer stream temperature by 5ºC in Black Lake Ditch and 7 ºC in Percival Creek above the confluence with Black Lake Ditch (Roberts et al., 2008). In the Deschutes River mainstem, doubling the baseflow is projected to lower the stream temperature by 0.9 ºC (Roberts et al., 2008). In contrast, halving the baseflow is projected to increase peak temperatures as much as 0.8 ºC (Roberts et al., 2008). These simulated TMDL managements for the baseflow and hyporheic zone alterations indicate the baseflow is

positively related to lower and healthier surface streamflow, which facilitates better habitat conditions (Roberts et al., 2012; TRPC, 2015).

The baseflow contribution is strongly related to improving water quality (e.g., low stream temperature) and ecological functions (e.g., hyporheic zone formation, healthy fish habitat). Groundwater pumping should be carefully modeled and monitored as the withdrawal reduces groundwater storage, decreases flow and frequency of hyporheic exchange, and degrades potential water quality.

2.6: Well Pumping Mechanism

2.6.1: Cone of Depression

A pumping well affects a stream by reducing groundwater levels and baseflow input (Fig. 20). When groundwater is pumped, the tip of a well can create a gradient, which intercepts surrounding groundwater flow that would have otherwise discharged as baseflow to the surface water. When pumping rates are sufficiently high, declining groundwater induces a 'reverse' flow from the surface water to the aquifer via infiltration. This leads to streamflow depletion as water demand increases (Sophocleous, 2002), particularly during dry periods (Douglas, 2006).

Groundwater pumping generates storage reduction as well as groundwater flow diversion. First, the pumping draws stored groundwater into the head of the well, which results in the formation of a "cone of depression" (Fig. 20-a) (Heath, 1983). The water level around the well begins to decline as the pumping continues, lowering the overall water table and forming a new equilibrium (see section 2.6.2.1). The void space above

the water table is where surface water infiltrates and recharges; however, the complete recharge is not available when withdrawals occur faster than natural recharges. Second, the usual groundwater discharge through baseflow is reduced by well pumping, diverting the groundwater flow, or induced infiltration (Fig. 20-b). In the initial phase, pumping depletes the stored groundwater. As pumping continues and the water table lowers, the groundwater discharge to the surface stream (baseflow) is drawn back toward the head of well and begins to supply the withdrawal. Such continued supply from baseflow causes "baseflow recession", reducing the groundwater that otherwise would have flowed to the surface stream and supplying further withdrawals (Barlow & Leake, 2012).

Figure 20

Cone of depression. Gleeson & Richter, 2018.

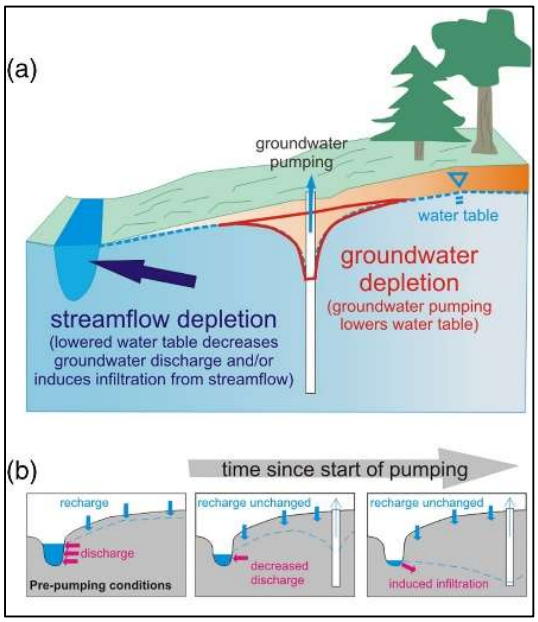

Note. Pumping lowers the water table (dashed line), forming a cone of depression (red line), and induces infiltrating surface water back to the groundwater system.

2.6.2: Residual Depletion and Lag Effect

2.6.2.1: Renewed Equilibrium

The status of hydrologic equilibrium refers to the groundwater storage pursuing a balance between recharge and storage (Theis, 1938). The lower water level throughout the aquifer requires increased recharge to an extent equal to the amount withdrawn by the well, leading to a renewed level of equilibrium in storage (Theis, 1938). Groundwater budget theory provides a quantitative view on groundwater storage in balance (net storage change=0): $Q = dS$, where Q is groundwater discharge, dS is the change in groundwater storage. This means that the groundwater reduction leads to a new and lower equilibrium level.

2.6.2.2: Lowered Groundwater Table and Disconnection from Surface Water

The combined effect of reduced storage impacts the aquifer, both at the time of pumping as well as after the pumping stops due to a "residual effect" (Healy, 1983). When the amount of discharged groundwater due to the pumping effect is greater than the recharged amount, the total groundwater storage reduces and forms the storage in equilibrium. Ultimately, reduced groundwater storage affects the amount of baseflow discharge, which consequently reduces the streamflow. This cycle of continuous withdrawal, groundwater flowing back to aquifer, baseflow recession, and streamflow depletion continue even after pumping ceases.

Depending on the depth and amount of pumping, location of wells, and current groundwater storage condition, the magnitude of residual depletion varies. The bigger the residual effect is, the longer the aquifer will take to recover from the loss even when pumping ceases (Obergfell et al., 2019). This indicates that the effect of pumping does

not stop at the time when pumping ceases; rather, the lagging effect of pumping causes continuous baseflow recession and surface streamflow depletion after pumping stops for additional hours to years (Schneider, 2010). Thus, the groundwater availability should be estimated in advance to when the streamflow depletion occurs.

2.6.3: Losing and Gaining streamflow

Losing surface flow is a final stage that occurs from groundwater pumping. Groundwater depletion causes streams to transform into intermittently or persistently dry streams[33] (Fig. 21-B). Such transformation depends on whether the hydraulic connection between surface water and the groundwater system remains (Barlow & Leake, 2012).

Figure 21

Groundwater depletion and losing surface flow. Barlow & Leake, 2012.

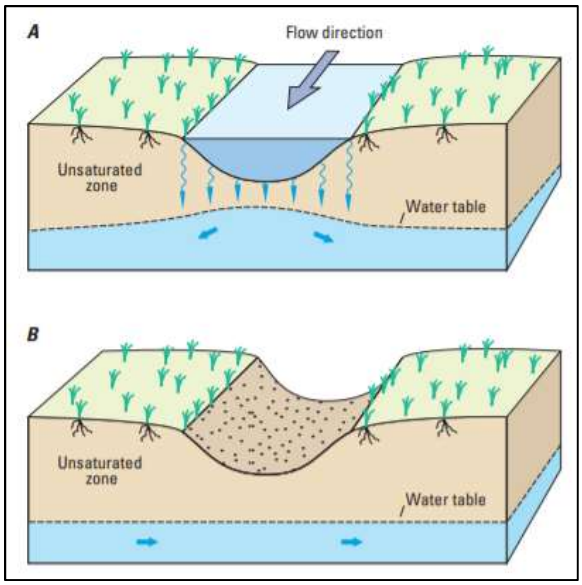

Note. (21-A) Losing stream: Streamflow has become a source of recharge to the underlying groundwater system.

(21-B) Ephemeral stream: Low water table is disconnected from the surface flow so that groundwater does not contribute baseflow to the surface water system.

[33] Ephemeral streams are features that carry "only stormwater in direct response to precipitation with water flowing only during and shortly after larger precipitation events" (Dorney & Russell, 2018).

2.7: Baseflow recession analysis

The recession curve (Fig. 22) explains a theoretical relationship between aquifer structure (i.e., groundwater storage) and groundwater discharge (Thomas et al., 2013). Baseflow recession analyses began with studies by Boussinesq (1877) and Maillet (1950), who developed a theoretical quantification of recession slopes to understand the physical groundwater flow mechanism (Thomas et al., 2013). The groundwater flow involves the behavior of groundwater storage and discharge, and baseflow is a proxy for groundwater discharge to streams (Rumsey et al., 2017). In this study, baseflow indicates groundwater discharge in hydrograph recession analysis as most groundwater discharges to the surface stream under a natural setting.

Figure 22

Recession Curve, period, and segment. Tallaksen, 1995.

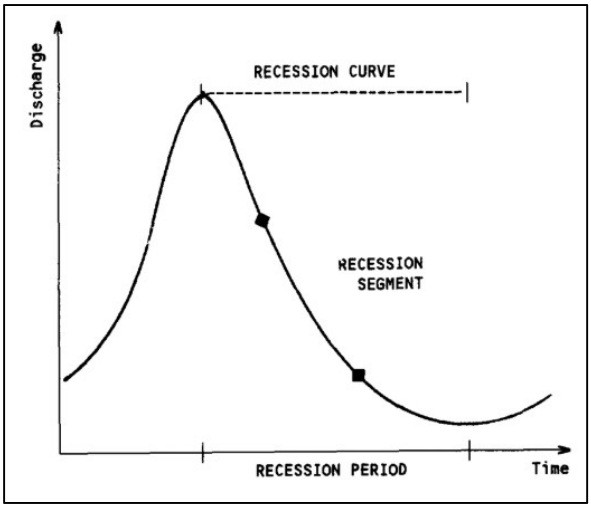

2.7.1: Baseflow Recession Analysis Methods

For an aquifer with no external transfers (Thomas et al., 2013), the groundwater budget theory describes the changing volume of storage (S) over time (t) with the inflow

and outflow of the groundwater system (Theis 1938):

$$dS/dt = I(t) - Q(t) - W(t) - ET(t) \quad (1)$$

where $I(t)$ is recharge to groundwater (normally via precipitation), $W(t)$ is groundwater withdrawal, $Q(t)$ is baseflow, and $ET(t)$ is evapotranspiration from the groundwater table and stream (from plants). We assume that $I(t) = 0$ during the dry summer days of our recession periods. Also, we assume that $ET(t)$ has a negligible impact on the groundwater system during the baseflow recession period (t) (Thomas et al., 2013). Groundwater withdrawals, $W(t)$, describe the impact of groundwater pumping via wells (see section 3.3.2.4.2).

Brutsaert and Nieber (1977) describe the change in storage (S) over time due to baseflow (Q) lost from the groundwater system (see Fig. 2).

$$dS/dt = -Q \quad (2)$$

where dS is the change of groundwater storage (S), dt is the change of time (t), and Q is discharge or baseflow in the research. Previous studies to characterize the groundwater storage and discharge behaviors assumed a power-law relationship between baseflow, Q, and groundwater storage, S (Boussinesq, 1904; Brutsaert & Nieber, 1977; Thomas, 2013):

$$Q = \alpha S^n \quad (3)$$

where S (m^3) is groundwater storage within an aquifer volume, Q $(m^3 d^{-1}, d = day)$ is groundwater discharge (or baseflow) to surface water, and α has units of inverse time (t^{-1}) and n (dimensionless) are constants (Gan & Luo, 2013; Thomas et al., 2013).

Combining (2) and (3) and solving for dQ/dt or $Q(t)$ leads to

$$\frac{dQ}{dt} = -aQ^b \quad (4)$$

where dQ is the change of baseflow (Q), dt is the change of time (t), and a and b are constant values to determine the degree of baseflow recession: $b = (2n-1)/n$ and $a = n\alpha^{1/n}$ (Thomas et al., 2013). The equation (4) replaces S with Q by substituting equation (3) into equation (2) (Brutsaert & Nieber, 1977; Eng&Milly, 2007; Thomas et al., 2013).

Possible solutions to (3) assume that Q is either a linear or a nonlinear function of S. When $n = 1$, there is a linear relationship between S and Q ($b = 1$); nonlinear case is when n is not 1 ($b \neq 1$). Neither a linear or a nonlinear relationship can be generalized in all aquifers because of the unique characteristics of aquifers and geologic traits. The different aspects of an aquifer that affect the groundwater storage-discharge behavior include watersheds that are glacier-dominant or rain-dominant, effects of climate change, and heavy anthropogenic interruption via excessive pumping (Gan & Luo, 2013). Therefore, understanding whether a watershed shows either linear or nonlinear behavior between groundwater storage and discharge should occur prior to a baseflow recession analysis. The linear or nonlinear models of the groundwater storage-discharge relationship are compared and we choose the model that fits better to the natural baseflow status, using linear regression analysis (Gan & Luo, 2013).

2.7.2: Linear or Nonlinear Relationship

We should understand how a given aquifer storage (S) reacts to the baseflow (Q) before identifying the impact of groundwater pumping (W). The linear relationship ($n = 1, b = 1$) between groundwater storage and discharge (or, baseflow, see Fig. 2) has been

widely used for numerous baseflow analyses (e.g., Brutsaert & Nieber, 1977; Thomas et al., 2013). This assumes that the storage reacts in direct proportion to the discharge. Vogel and Kroll (1992) studied 23 watersheds under a low flow status and determined that groundwater showed a linear behavior (Vogel & Kroll, 1992). On the other hand, a nonlinear model has gained attention as there has been significant human interruption on hydrograph in recent years. Thomas et al. (2015) addressed the significance of applying nonlinear equation while current streamflow and aquifer storage is substantially affected by the pumping. These findings deny the traditional applications of linear equations and imply the necessity to assess the aquifer system before applying the linear or nonlinear analysis method.

2.7.3: Recession Constant (K or a)

The recession analysis is a widely recognized method to estimate the baseflow component to the stream hydrograph (Yang et al., 2018). Baseflow "recession constant", is a representative value of the recession analysis, which characterizes the interaction of groundwater and surface water systems (Thomas et al., 2013). The recession constant explains the rate at which baseflow recession (decreasing hydrograph) occurs in each recession period. If the recession constant is bigger, the greater the degree by which baseflow recedes.

A precedent study by Dupuit (1863) and Boussinesq (1877) found solutions for linear and nonlinear groundwater discharge and aquifer storage relationships. The Dupuit-Boussinesq equations (1904) describe groundwater flow in differential equations governing flow in an aquifer, depending on how the aquifer behaves in response to discharge-storage:

When $b = 1$, the linear equation $\frac{dQ}{dt} = -aQ$ is solved by:

$$Q_t = Q_0 e^{-t/c} \qquad (5\text{-}1)$$

When $b \neq 1$, the linear equation $\frac{dQ}{dt} = -aQ^{\,b}$ is solved by:

$$Q_t = Q_0 (1 + \frac{(1-b){Q_0}^{1-b}}{ab} t)^{1/b-1} \qquad (5\text{-}2)$$

where Q_t is groundwater discharge at the time t, Q_0 is the baseflow at the time of initial recession occurrence (Fig. 23), t is the time taken between Q_t and Q_0, and c (5-1) and a, b (5-2) are constants[34]. For convenience, the constant c the is substituted for a nondimensional constant, $K = e^{-\frac{1}{c}}$, which may be used in place of c:

$$Q_t = Q_0 e^{-t/c} = Q_0 K^t$$

Figure 23

Recession Curve, period and segment. Modified from Tallaksen, 1995.

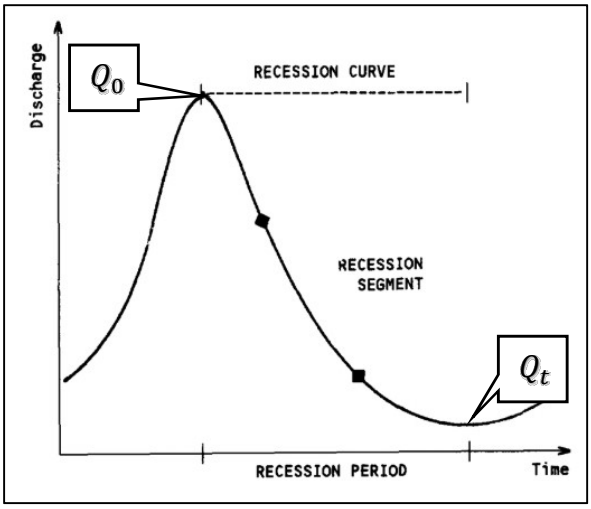

Note. Discharge (y-axis) = Q, Time = t.

[34] Appendix D explains the nonlinear baseflow recession constants.

2.7.3.1: Nonlinear Recession Constant (a)

The nonlinear recession equation (5-2) has two constants: a ($mm^{1-b}d^b$) and b (dimensionless). The nonlinear recession constant, "a" in equation (5-2) depends on the "physical dimensions and hydraulic properties of the aquifer" (Brutsaert & Nieber, 1977, cited in Rupp & Selker, 2006). To solve the equation for the constant a, the value for b is must be chosen. Numerous studies showed various values for b: Clark et al (2008) found the relationship between storage and discharge during the recession is approximately consistent, $b = 1$; Gan & Luo (2013) argued $b = 0.25$ with glacier- and snowmelt-dominated basins (Gan & Luo, 2013); Tague and Grant (2004) showed a negative value of b, which implies a hyperbolic storage-discharge relationship (Kirchner, 2009); Rupp and Selker (2006) found $b = -1$ for early stages of recession and $b = 0$ for later stages (Rupp & Selker, 2006). Finally, Wittenberg (1999) analyzed the recession curves of more than 80 streamflow gauge stations of an unconfined aquifer with an entire watershed and found the mean value of b as 0.49 (Wittenberg, 1999, cited in Wang & Cai, 2009). We use b = 0.5, following Wittenberg (1999), under the assumption that the Deschutes River basin possesses the same hillslope (Harman et al., 2009). This is based on the assumption that the groundwater storage deviates in a relatively negligible degree within the same slope. With these assumptions, the nonlinear recession becomes $\frac{Q_t}{Q_0} = \left(1 + \frac{Q_0^{0.5}}{a} t\right)^{-2}$ or, equivalently, $-2\ ln\left(1 + \frac{t}{a} Q_0^{0.5}\right)$ (Appendix D).

2.7.4: Baseflow Separation Method

As discussed earlier, baseflow contributes to streamflow along with direct runoff (see section 2.3.2). We can directly measure the surface streamflow (e.g., USGS

streamflow gauge stations). In contrast, we can only estimate the baseflow through separating the streamflow into "direct runoff" and "baseflow" via a separation method. This is because groundwater seepage to the surface stream is invisible and highly dependent on the geologic trait of aquifers, which determines the capacity of groundwater interaction with the surface water.

There are two main baseflow separation methods. The graphical method focuses on identifying "the points where baseflow intersects the rising and falling" surface stream hydrograph (Fig. 24; Brodie, 2005). The filtering method focuses on the entire stream hydrograph data to derive baseflow changes (Brodie, 2005). This filtering method provides a reliable baseflow separation analysis in cases of a long period of record over 50 years (Brodie, 2005).

Figure 24

Components of a typical flood hydrograph. Brodie, 2005.

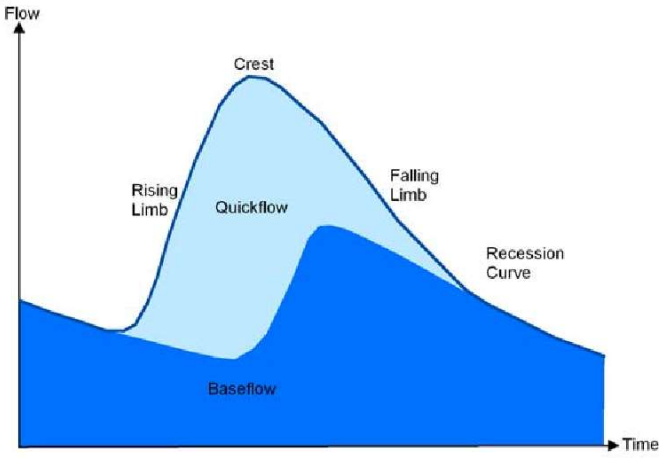

The web-based hydrograph analysis tool (WHAT) is a user-friendly tool to separate baseflow from the streamflow, using two digital filters, BFLOW, and Eckhardt filters (Lim et al., 2005). Here, both BFLOW and Eckhardt filters utilize a maximum

baseflow index (BFI_{max}), which is the maximum value of long-term ratio of baseflow to total streamflow (Lim et al., 2005). First, WHAT is an accessible public domain that separates baseflow from USGS streamflow measurement data by using automated hydrograph filters. Conceptually, the baseflow is an estimated portion of the surface flow without direct runoff. On a hydrograph, the start and end point of the direct runoff determines the portion of streamflow that is directly generated from the excess rainfall.

In contrast, a widely common baseflow separation program from USGS, HYSEP, requires a great deal of "user intervention to prepare input data and run the program" (Lim et al., 2005). In WHAT, the separated baseflow using a combined digital filter of BFLOW and Eckhardt filters generates a high coefficient of determination (R^2) compared with the manual separation of baseflow from streamflow. Lim, et al. (2005) experimented and the filtered baseflow using BFLOW and Eckhardt filters showed a comparable coefficient of determination of 0.83 and 0.9, respectively (Lim et al., 2005). This indicates that the separated baseflow will simulate the natural baseflow if measured.

Lastly, I used a recursive digital filter to represent perennial streams with porous aquifers (WHAT). A recursive digital filtering is a type of digital filter which assumes that the outflow (Q) is linearly proportional to its storage (S). This parameter is chosen for the Deschutes River Basin as the study site is comprised of porous aquifers, rather than other aquifer characteristics: a perennial hard rock aquifer or an ephemeral stream with a porous aquifer. The Deschutes is not an ephemeral stream but is rather perennial.

2.8: Frequency Analysis

Frequency analysis can be used to understand the flow variability over time. The frequency analysis explains how fast current streamflow status reaches a certain flow standard. This differs from baseflow recession analysis in that the amount of recession is identified through 'time', rather than streamflow reduction (e.g., baseflow recession analysis). This temporal approach provides a different view to understand the impact of groundwater withdrawals on the baseflow recession of the Deschutes River.

2.8.1: Low Flow Parameters in the Deschutes

The low flow characteristics of streamflow emphasize the ecological function of the riverine environment from a perspective of quantitative hydrology. In Washington state, the instream flow (see section 2.5.4.1) indicates the ecological function of streamflow. The instream flow in Washington State is determined by different low flow frequency parameter (i.e., 7-day, 10-years flow measurement, or $Q_{7,10}$. See section 2.8.2) and the instream flow incremental methodology (IFIM) regarding available fish habitats (DoE, 2010). As noted earlier, instream flow in the Deschutes River Basin provides regulatory standards (i.e., "closure" of consumptive use). However, the instream flow during a "closed" period does not provide a numeric guidance to compare the baseflow recession under external impacts, such as climate change or groundwater withdrawals. Therefore, this state regulation should include quantitative minimum streamflow during a low flow period to parametrize streamflow, which is subject to various anthropogenic impacts.

2.8.2: A Different Frequency Analysis in Washington State

One low flow analysis parameter, the 7-day, 10-year flow ($Q_{7,10}$), monitors and assesses whether streams in Washington State maintain minimally required streamflow for stream ecology. A widely used low flow metric, $Q_{7,10}$, is defined as the lowest average streamflow that recurs once every 10 years (Curran et al., 2012). Even though the $Q_{7,10}$ metric is a commonly used frequency parameter for the low flow analysis, it is not very applicable to the purpose of this study to analyze past data and predict the future baseflow recession patterns. An empirical study of statistical analysis on 7-day, 10-year indices showed that the $Q_{7,10}$ has weak predictability for future flow prediction (Stuckey, 2006); it had a higher standard error of prediction, which indicates that $Q_{7,10}$ has a larger deviation against the observed streamflow measurement. To predict the future baseflow recession, a different frequency parameter, $Q90$, is used (Gleeson & Richter, 2017).

The $Q90$ refers to a 90% exceedance probability of a set of flows. The value of $Q90$ is the flow rate which is exceeded for more than 90% of time during a certain period. For example, the flow rate that is exceeded more than 9 years among 10 years of time (90% of time) becomes the value for $Q90$. The exceedance probability is a metric to assess the frequency of streamflow against a certain standard. Depending on purposes, the exceedance probability of streamflow can take different measurements other than 90%. In many practices, $Q90$ is used to assess the low flow status as an ecological parameter (e.g., presumptive standards, Gleeson & Richter, 2018).

2.8.3: Environmentally Critical Streamflow

De Graaf et al (2019) conceptualized the minimum streamflow as "Environmental Critical Streamflow (ECS)", which is required to maintain healthy ecosystems (Graaf et

al., 2019). The concept of ECS was derived from a groundwater "presumptive standard" (Gleeson & Richter, 2017). The presumptive standard proposes a percentage-based range around natural flow variability to assess the relationships between hydrologic alterations and ecological responses (Gleeson & Richter, 2017).

The streamflow is at 'risk' that longer supports ecological functions when it reaches or exceeds the ECS (red lines in Fig. 25). With continuous pumping, groundwater and baseflow reduce and lower the surface streamflow during the dry period. The streamflow transforms into a losing stream from a gaining stream when withdrawals reduce the direct runoff of streamflow, which is recharged by rainfall. The losing stream occurs when the depleted groundwater system is no longer connected with the surface flow while the groundwater is being extracted (Fig. 25-B) Groundwater reduction ultimately reduces streamflow, which will reach the environmental flow limit (ECS) at a certain point. The time at which the ECS is reached differs depending on the severity of low flow and the amount of groundwater withdrawals[35].

[35] In Fig. 25, the red lines on the right diagrams indicate the time of when streams meet the environmentally critical flow level, which indicates the stream is at risk of ecological unsustainability.

Figure 25

Continuous pumping and Streamflow reaching the environmental flow limit. Graaf et al., 2019.

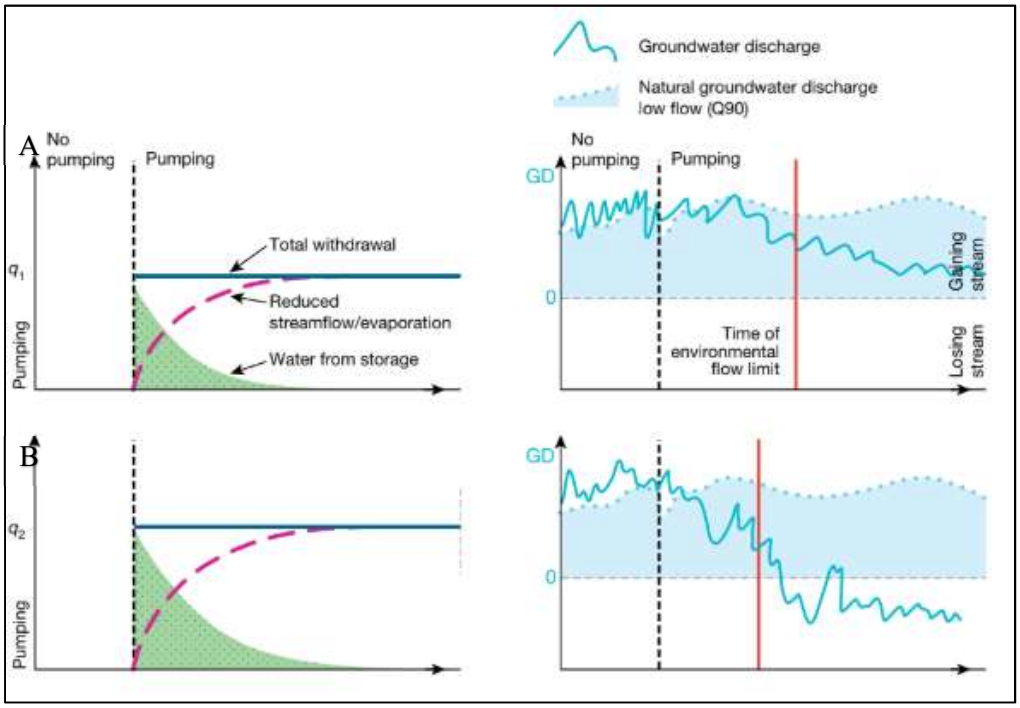

Note. (25-A) After pumping started at a moderate level (q_1 starting at black dashed lines on both graphs), the groundwater discharge (i.e., baseflow) starts to reduce. The streamflow, however, stays as a gaining stream that groundwater storage can still support the withdrawals.

(25-B) With higher groundwater withdrawals (q_2), the time at which reduced streamflow meets the environmental flow limit (ECS) is earlier than with a moderate withdrawal case (25-A). The streamflow transforms into a losing stream with the pumping now intercepts recharged streamflow as groundwater storage is limited.

2.8.3.1: Choice of the Time at which ECS is Impaired

The environmentally critical streamflow (ECS) is a time-sensitive value; the flow which is exceeded 90% of the period of research. De Graaf et al (2019) estimated the ECS as the $Q90$ of monthly baseflow in major rivers in the globe over the past five-year period (i.e., the flow at which is exceeded more than 54 months out of 60 months). Since hydrographic changes occur over five to ten years (e.g., Pacific Decadal Oscillation has

10 years of recurrence), any shorter period than five years may not reflect significant differences in low flow. I adopt this method for the ECB of the Deschutes River since the total study period is similar and long enough: 1954-2069, 116 years.

The ECS is used to assess the impact of groundwater withdrawals of wells (W) by comparing when the ECS is lowered to a certain degree by pumping. The natural ECS is the $Q90$ value of a five-year period. The impacted ECS is calculated from a baseflow recession analysis which incorporated the impact of withdrawal (W). The two predicted ECS (natural versus impacted) scenarios are compared to see if the ECS from the impacted baseflow comprises more than 90% of the natural ECS. The 90% composition is derived from the "method of a presumptive standard" (Gleeson & Richter, 2017): "High levels of environmental protection will be provided if groundwater pumping decreases monthly natural baseflow by less than 10% through time" (Gleeson & Richter, 2017). In other words, the withdrawal impact should comprise less than 10% of the natural Q90 to be ecologically sustainable baseflow.

"Localized baseflow recession analysis" can determine the time when the impacted ECS baseflow exceeds 10% of the natural ECS value. Even if the impact exceeds more than 10% of the baseflow, it must continue for some time to cause "unsustainable" or "impaired" baseflow. To calculate the standard duration of prolonged impaired baseflow, I developed a simple statistical calculation using composition function (C):

$$xCy = 0.01 \quad (6)$$

where x is the average days of recession, y is the number of consecutive days determined to assess the impact exceeded the natural $Q90$, and C is a function for combination, a selection of items from a collection when the order of selection does not matter (Mazur, 2010). Here, the value for x can be found from baseflow recession data. The value 0.01 indicates a 1% probability for y number of successive days occurs to have lower value (here, streamflow) than the $Q90$ value (Graaf et al., 2019). The dependent variable (y) will then assess the ECS of impacted baseflow from withdrawals in the Deschutes River.

2.8.3.2: Environmentally critical baseflow (ECB)

Environmentally critical streamflow (ECS) conceptualizes the minimum streamflow during low flow, addressing the ecological requirement in quantitative streamflow. For the Deschutes River where baseflow dominates the low flow (see section 2.3.3), the minimum streamflow should account for the baseflow contribution as the main criterion. In this case, the ECS for this study transforms into ECB, or "environmentally critical baseflow". The ECB will enable an analysis of baseflow trends and recessions since it accounts for the baseflow as the analysis subject.

2.9: Conclusion

Attention toward the relationship between increased groundwater withdrawals (W) and hydrologic impact on surface streamflow (see section 2.7.1) has soared in recent decades (Wang & Cai, 2009; Thomas et al., 2013; Gleeson & Richter, 2018; Graaf et al., 2019). The impact on groundwater reduction via pumping and consequently lower surface streams is more deleterious during dry seasons when streams are already under

low flow stress. Many global streams have already lost their ecological functions and instream values due to severely lowered streamflow (Graaf et al, 2019). In the 'wet' PNW, many streams have experienced continuously lowered streamflow in low flow periods despite ample precipitations in wet seasons (Georgiadis, 2018). Low flows in PNW are associated with climate changes and groundwater withdrawals, both of which exacerbate reduced baseflow (Q) inflow to the surface water system during dry seasons. Less baseflow inflow, or baseflow recession, is closely related to lowered groundwater storage (S), lower surface flow, degraded water quality, and unsustainable fish habitat environments.

The baseflow recession analyzes low flow characteristics and trends of a stream during dry periods. The baseflow contribution (Q) largely depends on the groundwater storage (S), which implies that groundwater storage status can be analyzed through baseflow recession trends and patterns. Many empirical studies have started to incorporate the impact of groundwater withdrawals on the baseflow recession; the withdrawal (W) is now an essential variable in the differential equation (e.g., equation 1). The baseflow recession slope, or the recession constant K for a linear, or a for a nonlinear aquifer), represents the impact of groundwater withdrawals on the baseflow recession. The baseflow recession constant analysis enables us to predict future trends of baseflow during a low flow period. This is useful in many streams in the PNW which depend largely on the baseflow contribution in dry seasons.

A frequency analysis explains how often streamflow falls below a certain streamflow standard (e.g., environmental flow limit, $Q_{7,10}$) within a certain period. The frequency analysis of low flow is a different tool to understand the baseflow recession

from a perspective of time[36]. While baseflow recession analysis provides how much baseflow will be lost out of the system, the frequency analysis explains how early (in time) the streamflow will reach a hydraulic threshold. The "environmentally critical streamflow" (ECS, or environmentally critical baseflow, ECB) describes how streams with perpetuated groundwater withdrawals will inevitably reach thresholds that will harm the ecological functions of streams.

Using baseflow recession analysis and frequency analysis, I will analyze low flow characteristics and trends of a stream in the PNW, the Deschutes River. A focused study on the relationship between anthropogenic groundwater exploitation and baseflow recession will guide a sustainable groundwater resource management in Washington State for future generations.

[36] E.g., reduced groundwater storage, lowered surface flow, reduced baseflow contribution to the surface water system

Chapter 3: Methods

3.1: Roadmap

The Methods part has two sections: Data description and Formula development. The 'Data description' section describes methods to obtain and analyze 1) streamflow, 2) baseflow separation and selection, and 3) well data. The 'Formula development' section has three sequential steps to analyze the baseflow recession. The first step will analyze baseflow recession and generate recession constants to describe relationships between the starting and ending points of baseflow recession periods. The second step will predict future baseflow contributions to the surface streamflow using the baseflow recession constants derived from the first step. The third step will identify the impact of wells' groundwater withdrawals by finding the time at which the baseflow recession reaches environmentally critical streamflow (ECS). The difference in time of 'natural' baseflow and 'impacted' baseflow (due to withdrawals) represents how much groundwater pumping has an impact on baseflow recession.

3.2: Data Description

3.2.1: Basic Concept of Data Analysis

The goal of our study is to understand the impact of groundwater pumping on the reduced groundwater contribution to the surface water, or baseflow, of the Deschutes River (Fig. 26). Under natural conditions, groundwater flows into the surface stream and maintains minimum flow when there is no rainfall to recharge the stream. This groundwater inflow can be intercepted by groundwater withdrawals through water

pumping wells. The interactive relationship between groundwater and surface water via baseflow will allow us to assess whether current groundwater management is sustainable and ecological.

Figure 26

Groundwater withdrawals and baseflow. Modified from Grannemann et al., 2000.

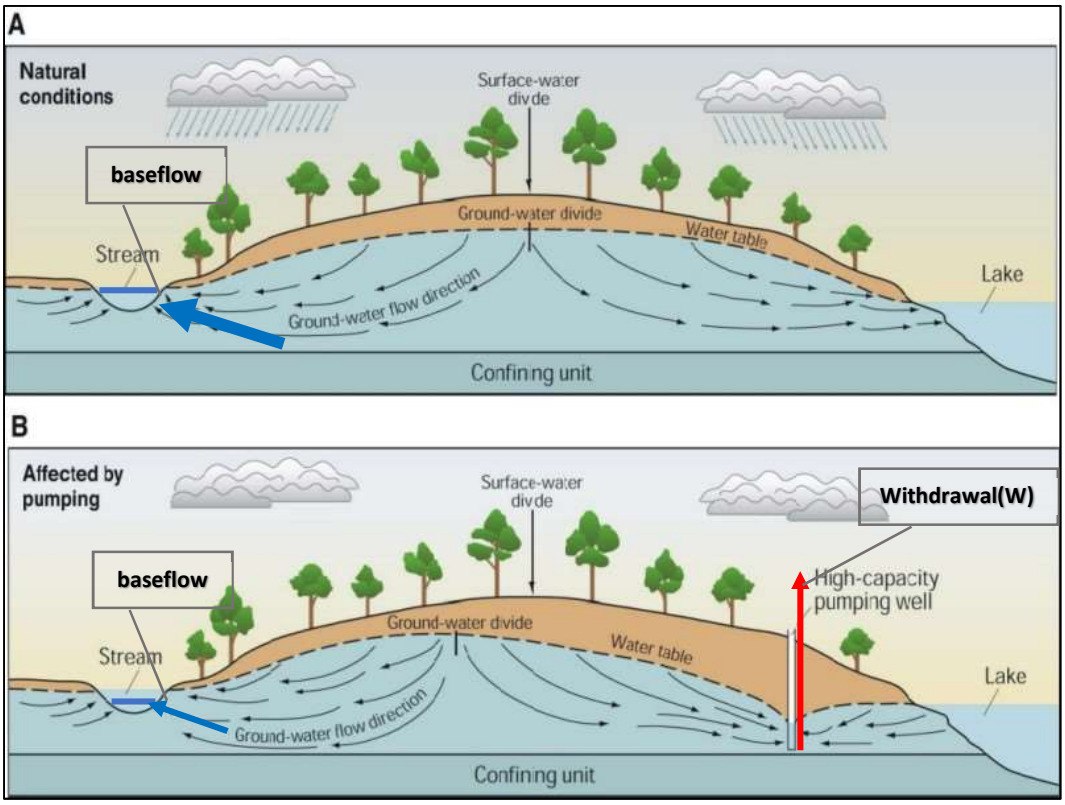

Note. This diagram shows a baseflow contribution from groundwater to surface water under 'natural circumstances' (26-A) and under an 'impacted' condition (26-B). The blue arrows denote the groundwater contribution. The size of the blue arrows signifies different amounts of groundwater contribution to the surface flow. The volume of baseflow into a stream varies depending on the amount of groundwater contribution. The red arrow denotes the groundwater withdrawal through pumping.

3.2.2: Selecting a Streamflow Gauge Station

Streamflow data on the main stem of the Deschutes River was obtained from "USGS Current Water Data for Nation" (USGS, n.d.). In the Deschutes River Basin, two

USGS streamflow gauge stations record continuous streamflow: one near E street in Tumwater (USGS 12080010) and one near the city of Rainier (USGS 12790000). The Tumwater Falls gauge station is in the lower stem of the Deschutes River (river mile, RM, 2.4). This lower gauge station in Tumwater represents the impact of groundwater withdrawals via wells better than the upper station (RM 25.9 near Rainier) (Kimbrough et al., 2005). Located at a lower elevation, the lower gauge station can catch the hydraulic impact of groundwater withdrawals from higher elevations. For this reason, I selected the Tumwater Falls gauge station to represent the baseflow change under natural and impacted conditions[37].

3.2.3: Baseflow Separation and Selection

'Baseflow' and 'direct runoff' constitute total surface flow (Fig. 27; baseflow + direct runoff = surface flow). I separated baseflow from the surface flow using "Web-based hydrograph analysis tool (WHAT)" (see section 2.7.4). A hydrograph shows change in the hydrologic variables (e.g., streamflow, baseflow) over time.

[37] The Tumwater gauge station (USGS 12080100) measured streamflow from 1945 to 2019. The data is not continuous that there are missing periods: from 1955 to 1956 (2 years) and from 1964 to 1990 (27 years). The streamflow data during these missing periods are predicted using Interpolation in order to treat the data of the whole period as continuous.

Figure 27

Surface Streamflow Components.

Streamflow data from NWIS streamflow gauge station USGS 1280010 near Tumwater.

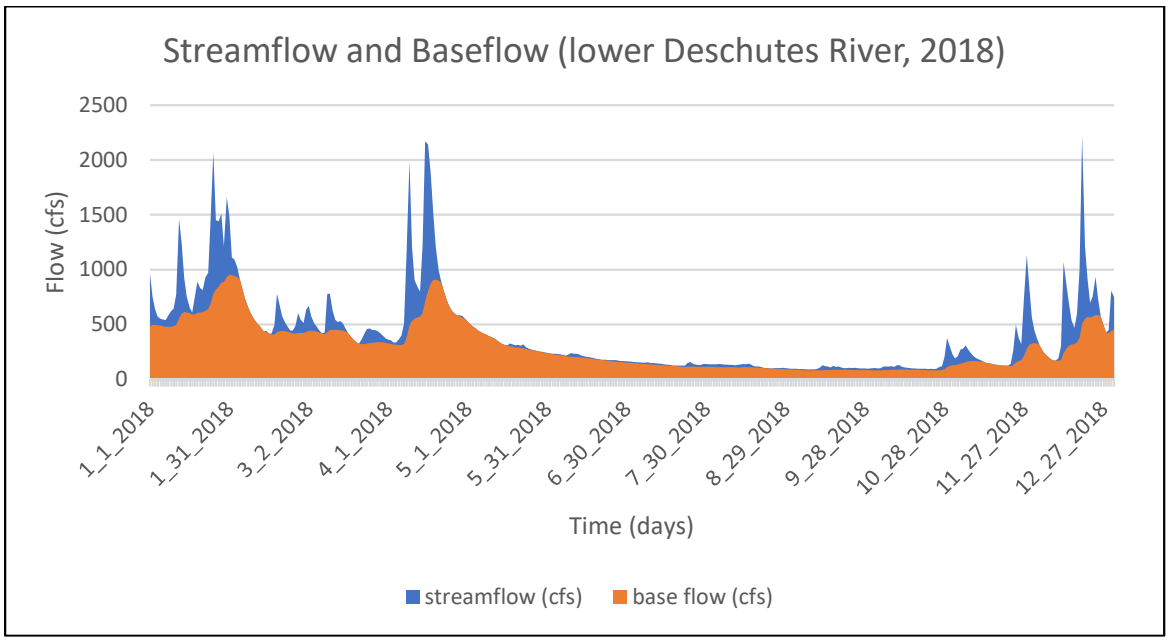

Note. This chart displays a hydrograph of streamflow (blue) and baseflow (orange) between January 1st, 2018 to December 31st, 2018[38]. The streamflow hydrograph encompasses the baseflow part (orange) along with direct runoff (blue area without the orange area).

Only selected periods of baseflow data were utilized for the baseflow recession analysis. First, I selected a dry season, from June to October, when the lowest streamflow occurs and baseflow constitutes most of the surface flow. Second, only the dates that show declining "three-day average moving streamflow" were selected to highlight the baseflow recession (Vogel and Kroll, 1996). The three-day average baseflow movement is the averaged flow rate of three days, which was calculated for each day[39]. Then, I selected sets that had a minimum of 10 days of recession (Fig. 28)

[38] Streamflow data obtained from USGS Current Streamflow database Water Watch (USGS, n.d.)
[39] Example of three-day average moving streamflow in Appendix E

(Kirchner, 2009). This enabled more substantial analysis with data that showed recession trends because I eliminated some days with the increasing flow in the hydrograph during selected dry months. The data used for the recession analysis incorporated these conditions (three-day average decline, minimum 10 days recession).

Figure 28

Baseflow data description and selection. Streamflow data from NWIS.

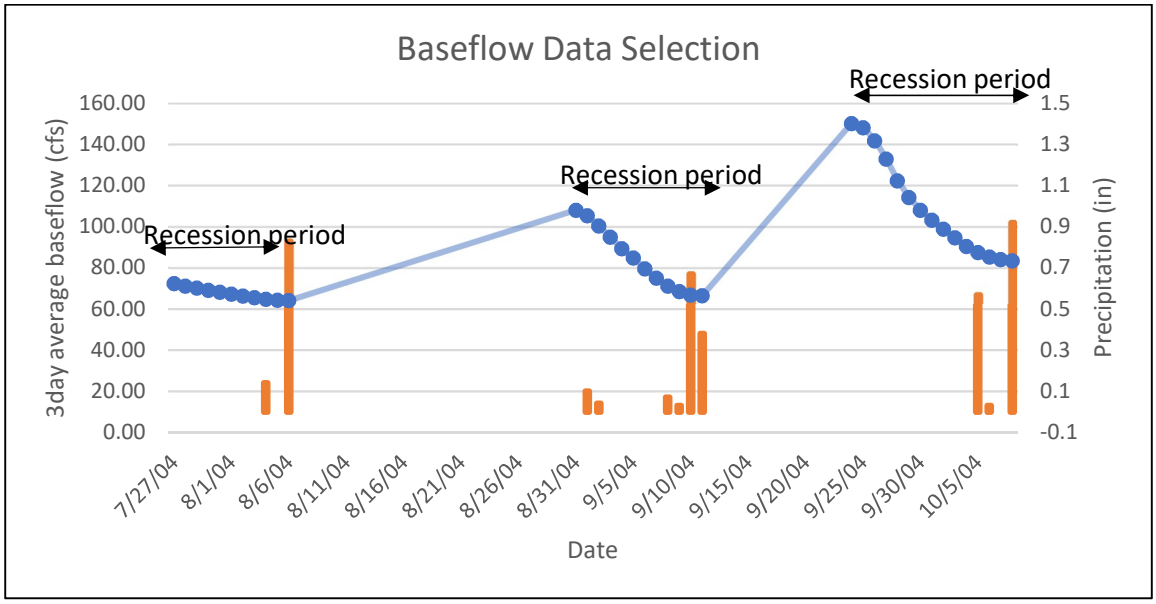

Note. This hydrograph shows selected baseflow recession data during the summer of 2004 in the Lower Deschutes River. Three-day average baseflow movement (cfs, cubic feet per second): blue marker and blue line. Precipitation (in, inch): orange column. Recession periods: black arrows. Each recession period is more than 10 days.

3.2.4: Well Data

3.2.4.1: Location

Well data is required to estimate the impact of groundwater withdrawals on the reduced baseflow. The amount of well pumping is the 'impact', which is the lost amount of groundwater storage from an aquifer. Lost groundwater storage means less baseflow inflow from the groundwater to the surface stream. The impact of groundwater

withdrawals is more pronounced during a low flow period when there is little to no precipitation to recharge the surface flow system.

The secondary well data was collected from the Thurston County Water Planning department (Thurston County Water Planning, 2019). The data included some groundwater pumping wells and their withdrawal amounts in Thurston County, which had hydraulic connectivity to the surface flow of the Deschutes River (Hansen, 2018). I separated wells based on through which aquifers the wells pump groundwater: either unconsolidated or consolidated rocks of the Puget Sound aquifer[40] (Wallace & Molenaar, 1961) (Table 4). The wells located where unconsolidated rocks are revealed on the surface have a direct hydraulic connection to the surface stream of the Deschutes River. Using the ArcGIS Online program (AGOL), I selected wells that were located on unconsolidated aquifer layers (Qa, Qad, Qgd in Table 4) in order to understand their impact on lowering baseflow and surface streamflow (Fig. 29). On the other hand, wells located on consolidated aquifer layers (Tm, Tv(c), Tn in Table 4) were excluded from the analysis as I assumed these wells pumped groundwater from confined aquifers, which were not hydraulically connected with the surface flow of the Deschutes River.

[40] Unconsolidated sand and gravel aquifers have intergranular porosity, which enables groundwater flow. Glacial deposits of coarse gravel and sand are permeable medium. The consolidated layer includes high volume of clay and silt along with some sand, pebbles, cobbles, and boulders. High density in clay and silt generates the aquifer to be confined and impermeable that groundwater flow is limited within the consolidated aquifers.

Table 4

Aquifer layers in Deschutes River Watershed. Schuster, 2015.

	Geologic code	Geologic unit	Geologic Description
Included	Qa	Quaternary alluvium	Moderately sorted deposits of cobble gravel, pebbly sand, and sandy silt along rivers and streams. Also includes alluvial fans, common particularly where streams reach the coastline. Surfaces generally unvegetated.
	Qgd	Pleistocene continental glacial drift	Till and outwash clay, silt, sand, gravel, cobbles, and boulders deposited by or originating from continental glaciers; locally includes peat, nonglacial sediments, modified land, and artificial fill
	Qad	Pleistocene alpine glacial drift	Till, outwash, and glaciolacustrine sediments; locally includes loess, talus, and lacustrine deposits
Excluded	Tv(c)	Tertiary volcanic rocks, Crescent Formation	Siltstone, sandstone, and conglomerate; fossiliferous, concretionary, and carbonaceous
	Tm	Tertiary marine sedimentary rocks	Lithofeldspathic or feldspatholithic sandstone and siltstone; common claystone, shale, and mudstone; minor conglomerate and breccia; locally tuffaceous; local basaltic sandstone and poorly sorted basal conglomerate.
	Tn	Tertiary nearshore sedimentary rocks	Siltstone, sandstone, and conglomerate; fossiliferous, concretionary, and carbonaceous

Figure 29

Aquifer layers in Deschutes River Watershed – Included or Excluded.

Map created using ArcGIS Online. ESRI ArcGIS Online Layer sources: WSDOT, 2012; Bilhimer, 2014; City of Tacoma GIS, 2019.

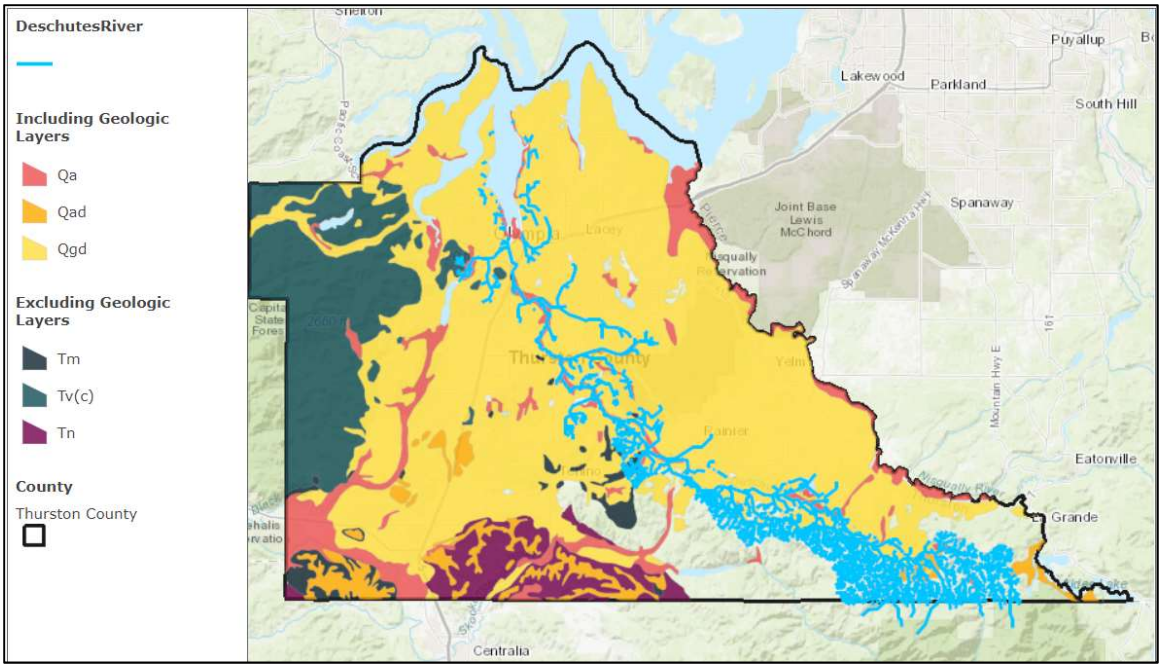

Note. The "Included geologic layers" (Qa, Qad, Qgd) represent the geologic scope of the Deschutes Watershed that incorporates wells that overlie these layers. The "Excluded geologic layers" (Tm, Tv(c), Tn) represent the geologic scope where wells overlying on these layers are excluded from the study area.

3.2.4.2: Calculating Withdrawals

In order to calculate the annual withdrawal amounts, I used three steps to sort the wells, add all wells' withdrawal by each year, and multiply the annual withdrawals by the wells' lifetime to obtain the cumulative withdrawal amount.

3.2.4.2.1: Yearly Withdrawal Amounts

First, the wells and withdrawal amount were sorted by years to understand the yearly trend of the groundwater pumping amount. This applies to all permitted wells that had known withdrawal rates.

I calculated the total withdrawal amount as of a given year by multiplying the rates by the well's lifetime. The cumulative withdrawal at any (y_k) is then the sum of withdrawals (x_i) in previous years (i) up to the year of interest (year k):

$$y_k = \sum_{i=1}^{k} x_i$$

The starting year of the analysis was fixed at 1945 (the starting year of the baseflow data record). The result of this cumulative sum solved for y_k will be the total withdrawal up to year ys, for example:

$$y_1 = x_1,\ y_2 = x_1 + x_2,\ y_3 = x_1 + x_2 + x_3,\ \dots,\ y_k = x_1 + x_2 + x_3 + \cdots + x_k$$

The well withdrawal data included wells from 1860 to 2019. I used Thurston County's well withdrawal data as a variable (W) in my baseflow recession analysis, which is x_i from above. The baseflow data existed from 1945 and the starting point of the withdrawal data should align with the same starting year (1945). In order to include the total impact from all wells, the withdrawal data preceding 1945 (1860-1944) was included as a 'base' withdrawal; the base withdrawal was included in the following year's withdrawal amount; for example:

$$y_{1945} = (x_{1860} + x_{1861} + \cdots + x_{1944}) + x_{1945}$$

where the withdrawal amount for the year 1945 involves all the preceding withdrawals.

3.2.4.2.2: Permit-exempt Wells Withdrawal

Second, the withdrawal amount was calculated for the wells that had measured pumping rates or estimated for the other wells that do not have recorded withdrawal rates. All wells were categorized into two groups: permitted or exempted wells, depending on whether the withdrawal rates were known or unknown, respectively. Permitted wells are the wells that acquired groundwater permits to pump groundwater from the Department of Ecology; exempted wells (hereafter "permit-exempt") did not require permits as their withdrawals were expected to be "small" and considered to have an insignificant impact on surface water (DoE, 2015). From earlier sections, recall that exempt wells, however, may pump up to 5,000 gallons per day.

A majority of groundwater withdrawal in the study area of the Thurston County was attributed to domestic and public supply purposes. The public supply wells were divided into group A and B depending on the septic connection system (DoH, 2018); Group A wells were permitted while group B wells were mostly permit-exempt wells. Also, domestic wells, referring to the water supplies to single or group homes, were exempted and included in the permit-exempt well. Over half of total the withdrawals were comprised of permit-exempt wells, which were mainly domestic and public supply group B wells (Fig. 30).

Figure 30

Purposes of groundwater withdrawals in Thurston County.

Well withdrawal data from Thurston County Water Planning.

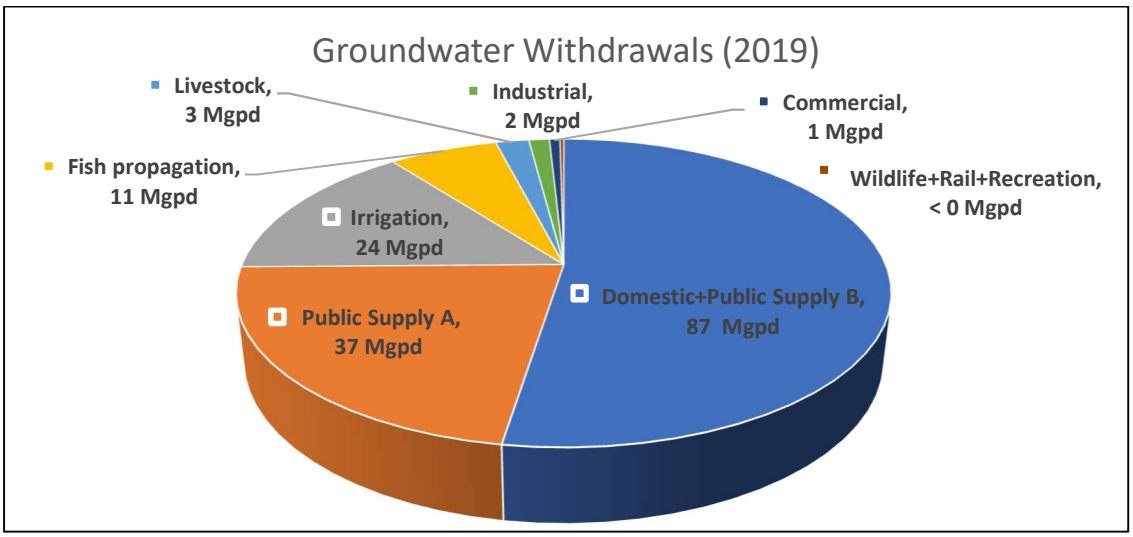

Note. Mgpd: million gallons per day (Mgpd).

3.2.4.2.3: Yearly Cumulative Withdrawal

Third, I added the yearly estimated withdrawal amount by multiplying the withdrawal rates to the well's lifetime, which produced the 'impact' of wells. The impact of wells is the lost amount of groundwater that would have been a potential baseflow contribution to the surface stream. The total withdrawal amount of a certain year was the cumulative withdrawal sums of the years in the past and the withdrawal amount of the very year; for example, the withdrawals in 1946 were the summation of withdrawals of 1945 and 1946. This assumed that all wells from the well data were "active" wells that had been pumping groundwater since the year they were constructed (Hansen, 2018).

After calculating the total withdrawal amount of all wells in the study area of Thurston County, I will next use this as the withdrawal impact to calculate the baseflow

recession of the lower Deschutes River. The future withdrawal amount was projected to increase in Thurston County[41] (TRPC, n.d.). The estimated future withdrawals are expected to increase with population growth[42]. The estimated future withdrawals will then be used to 1) test baseflow recession models (see section 3.3.2.4) and 2) assess future baseflow recession against the environmentally critical streamflow threshold (see section 3.3.3.1).

3.3: Formula Development

3.3.1: Step 1. Baseflow Recession Analysis

Baseflow describes interconnected hydrology between groundwater and surface water systems. A baseflow analysis is useful to understand the low flow period of a stream when groundwater contribution (i.e., baseflow) dominates the surface flow. Low flow, again, refers to the period when groundwater contribution governs the surface streamflow as there is little to no precipitation input on the stream (Stuckey, 2006). The change in the quantity of baseflow should be carefully analyzed during the low flow period since surface flow relies mostly on baseflow to maintain ecological flow for aquatic species and other ecosystem functions. The reduction in baseflow, referred to as "baseflow recession", delineates the decreasing patterns of groundwater discharge (baseflow) and groundwater storage (groundwater in aquifers) in a metric relationship.

[41] Population changing rate = (Population projection in 2025)/(Population in 2015)
[42] Estimated future withdrawals = (Population changing rate[6]) * (Cumulative Withdrawal Total of the withdrawals from the closest year)

To characterize the baseflow recession pattern, I employed the Boussinesq-Dupuit equation (1904, cited in Hall, 1968). Reviews by Hall (1968) and Tallaksen (1995) explained how the Boussinesq-Dupuit equation was developed through model experiments and case studies. The baseflow recession assumed a power-law relationship between baseflow (Q) and groundwater storage (S) (Brutsaert & Nieber, 1977) [43]. The baseflow recession patterns were categorized into two groups: linear or nonlinear relationships (Tallaksen, 1995). The linear relationship assumed that the groundwater storage (S) changes in proportion to the baseflow (Q). The nonlinear relationship assumed that the groundwater storage (S) changes proportional to the power of the baseflow (Q).

3.3.1.1: Model Development

To characterize the relationship between the groundwater storage (S) and baseflow (Q), I adopted the simple decay model (Hall, 1968; Brutsaert & Nieber, 1977, cited in Thomas et al., 2013), which compared the flow rate at the beginning of the baseflow recession (Q_0) to that at the end of the baseflow recession (Q_t) after a certain period of time (t) passed. The Q_0 and Q_t represent the groundwater discharges at different times, either at the beginning or end of recession periods. This will either be linear or nonlinear, such as the relationship between the groundwater storage and discharge. Using Q_0 and Q_t, we can predict the pattern of groundwater discharge patterns

[43] In literature, Q is "groundwater discharge", which refers to the amount of groundwater released or lost from the groundwater system. In this study, Q represents "baseflow" as it means the amount of groundwater contributed or "lost" to the surface water system. This study focuses on the low flow period when there is hardly other components in the streamflow or groundwater discharge than baseflow. I can estimate the baseflow through observed streamflow separation that baseflow provides a physical value to the concept of groundwater discharge.

without having to calculate total groundwater storage, which is nearly impossible without a precise groundwater modeling (Thomas et al., 2013).

I assume that the selected recession periods have no external input from precipitation (I) and negligible evapotranspiration (ET) (see section 2.7.1). Brutsaert and Nieber (1977) defined the relationship between the change in storage (S) over time as the amount of baseflow (Q) in a negative form, which indicated the direction of groundwater being lost from the groundwater system. Both linear and nonlinear relationships between S and Q assume a simple differential equation for baseflow (Q), when $I = 0$, $ET = 0$, and $W = 0$ (see section 2.7.1):

$$\frac{dQ}{dt} = -aQ^b \quad (4)$$

3.3.1.1.1: Linear Baseflow Recession Model

The linear relationship between groundwater storage-baseflow is the case with $b = 1$. The solution is a simple exponential decay (Boussinesq, 1877; Hall, 1968):

$$Q_t = Q_0 e^{-t/c} \quad (7)^{44}$$

$$Q_t = Q_0 K^t \quad (8)$$

where Q_t ($m^3 d^{-1}$) is baseflow at time t, Q_0 ($m^3 d^{-1}$) is the value when baseflow starts to show a decline on hydrograph, and c is a baseflow constant with the dimension of time. The equation (8) defines (7), the recession constant $K = e^{-1/c}$. The baseflow recession constant (K) indicates the groundwater storage (S) behavior against the baseflow (Q). In other words, this form of solution for Q_t assumes that the baseflow consistently decreases

[44] The equation (5-1) (see section: 2.7.3) and the equation (7) are identical but explained in section 2.7.3.

at a constant rate (K) during the recession period (Yang et al., 2018). The estimation of K is required for many hydrologic models as it describes the interconnectivity between groundwater and surface water system (Thomas et al., 2013). In sum, the equation (7) and (8) describes the exponential decay of Q_t assuming a linear relationship between Q_t assuming a linear relationship between Q and S.

3.3.1.1.2: Nonlinear Baseflow Recession Model

Followed by the equation (4) with a case when b is not 1 ($b \neq 1$) leads to a nonlinear baseflow recession; groundwater storage (S) changes in a nonproportional way against the discharge (Q) (Wittenberg, 1999, Gan & Luo, 2013). If we assume a linear power-law relationship between Q and S ($b \neq 1$), the solution for Q takes the form:

$$Q_t = Q_0\left(1 + \frac{(1-b){Q_0}^{1-b}}{ab}t\right)^{1/b-1} \qquad (9)^{45}$$

where a is a constant ($mm^{1-b}d^b$) and b is a constant (dimensionless) which describes the power-law relationship between Q and S. In a nonlinear groundwater storage-discharge relationship, the degree of baseflow recession cannot be represented with a single constant value. In this case, the hydrograph curve is not a straight line that there cannot be a single value of slope (it is not a straight line for the exponential decay, either, unless we take the logarithm form). Therefore, nonlinear constant values ('a' and 'b') represent the storage property, which describe to which degree the baseflow (Q) reduces over time (Rupp & Selker, 2006).

[45] The equation (5-2) (see section: 2.7.3) and the equation (9) are identical but explained in section 2.7.3.

Many studies explore the values for the constant b, or the slope of baseflow recession (see section 2.7.3.1). Wittenberg (1995) found $b = 0.5$ in 23 unconfined watersheds (Wittenberg, 1999). Fixing b enables us to find the constant value for 'a', when the baseflow at the beginning (Q_0) and the ending (Q_t) are known (Equation 10). The form of the solution for the nonlinear case with b = 0.5 is (Appendix D):

$$Q_t = Q_0(1 + \frac{{Q_0}^{0.5}}{a}t)^{-2} \qquad (10)$$

I will calculate the baseflow constant 'a' each year from 1945 to 2019 by solving equation (9) for 'a'. We can find the ratio of Q_t/Q_0 for the special case of b = 0.5 (11-1, 11-2) (Wittenberg, 1995):

$$\frac{Q_t}{Q_0} = (1 + \frac{{Q_0}^{0.5}}{a}t)^{-2} \qquad (11\text{-}1)$$

$$\ln\left(\frac{Q_t}{Q_0}\right) = -2\ln(\frac{a+{Q_0}^{0.5}t}{a}) \qquad (11\text{-}2)$$

where a is a constant ($mm^{1-b}d^b$).

3.3.1.2: Use of Baseflow Recession Constants

Baseflow recession constants indicate how fast baseflow decreases. The decay rate is K for the linear model and a for the nonlinear model. I can use the recession constants to predict future baseflow values at the ending point of the recession hydrograph (Q_t). First, I substitute data for the beginning (Q_0) and the ending (Q_t) recession points into the linear and nonlinear equations to obtain recession constants (K for the linear and a for the nonlinear equation)[46]. Next, I plot a set of recession constants

[46] Existing baseflow recession data from 1945 to 2019

against time to get the trend of changing recession constants (K and a). The recession constant trends 1) determine how the degree of baseflow recession changed and 2) are used to extrapolate future baseflow recession constants[47]. Finally, using the predicted future recession constants, the future baseflow values will be estimated. This future baseflow will ultimately assess the low flow status in the Deschutes River surface stream against ecological threshold called, environmentally critical baseflow (ECB, discussed in "Environmentally Critical Baseflow").

3.3.2: Step 2. Data Preparation and Prediction

Prior to linear and nonlinear baseflow recession analyses, the primary baseflow data and recession constants should be prepared to predict future baseflow recession data. First, the primary baseflow is the baseflow data separated from the measured USGS streamflow data through the WHAT (1945-2019). Next, three different methods estimated values for the future independent variables. The future independent variables from the most reliable method estimates produce the future dependent variable, the minimum baseflow (Q_t). Finally, the most reliable set of independent variable and resultant dependent variable is determined by statistical testing (e.g., low p-value and high coefficient of determination, R^2).

3.3.2.1: Variables

The trend of recession constants enables us to predict future recession constant values. The dependent variable is then Q_t while the independent variables were the estimated recession constants (K for linear and a for nonlinear), time (t), and the

[47] Prediction for recession constants made from 2020 to 2069

baseflow value at the start of recession periods (Q_0)[48]. Here, the future dependent variable (Q_t between 2020-2069) was predicted using a 'forecast' function[49]; the independent variables (Q_0 and t) were predicted using three different methods: average, forecast function, and trendline (section 3.3.2.2.2; Table 5). Linear regression analysis determines which set of Q_0 and t predicts future minimum baseflow (Q_t) that fits most to the 'forecasted future Q_t'.

3.3.2.2: Data Prediction

3.3.2.2.1: Missing Data Treatment

The existing data (1945-2019) should be continuous to generate future (2020-2069) Q_0 and Q_t. However, the baseflow data (separated from streamflow measurement, USGS streamflow gauge station 12080010) had missing data sets[50]. I used a "linear interpolation" to estimate these missing data. Linear interpolation assumed that a trend of two distant data points is proportionally estimated (Bayen & Siauw, 2015):

$$n\ (years) = 1957 - 1954 = 3,\ Q_{t,1954} = 80,\ Q_{t,1957} = 110$$

$$Q_{t,1955} = Q_{t,1954} + \frac{Q_{t,1957} - Q_{t,1954}}{n} = 80 + \frac{110 - 80}{3}$$

$$Q_{t,1956} = Q_{t,1954} + \frac{Q_{t,1957} - Q_{t,1954}}{n} * 2 = 80 + \frac{110 - 80}{3} * 2$$

[48] Linear model ($Q_t = Q_0 K^t$), Nonlinear model ($Q_t = Q_0(1 + \frac{(1-b){Q_0}^{1-b}}{ab} t)^{1/b-1}$)

[49] See section 3.3.2.2.2

[50] Missing data between 1955-1956, 1964-1990.

3.3.2.2.2: Predicting Future Data

I used a continuous data set between 1945 to 2019 to predict future independent and dependent variables between 2020 to 2069. I used three combinations of a method to determine the future independent variables, $Q_0 \; and \; t$: averages, forecast function, and a trendline. After that, I used linear regression to decide which set of the $Q_0 \; and \; t$ calculates minimum future baseflow (Q_t) that has the highest correlation with the dependent variable (Q_t).

First, I used the 'average' of past data of the independent variables ($Q_0 \; and \; t$) to represent the future estimation.

Second, I used the 'forecasted' past data using a 'forecast' function to represent the future independent variables estimation. This function uses a linear equation between independent (x) and dependent (y) variables to predict future trends, $y = ax + b$, where a is a cross-correlation constant:

$$a = \frac{\sum(x - \bar{x})(y - \bar{y})}{\sum(x - \bar{x})^2}$$

and b is calculated from averages of existing data:

$$b = \bar{y} - a\bar{x}$$

where $\bar{x}$ = average of existing x values and $\bar{y}$ = average of existing y values. The predicted future value (y) is a continuation of the historical values of a specified period of time, which should be a continuation of the timeline (Microsoft, n.d.).

Third, the 'trend' of past data ($Q_0 \; and \; t$) was used to estimate the future independent variables ($Q_0 \; and \; t$).

3.3.2.3: Model Fitness: Linear vs Nonlinear

The linear and nonlinear baseflow recession models were tested for their fitness to the 'forecasted future Q_t' data (2020-2069). Here, a 'forecast' function of Microsoft Excel generated the 'forecasted future minimum baseflow (Q_t)'. This 'forecasted future Q_t' functions as a 'control' case, which we use to compare the Q_t values calculated from linear and nonlinear models. By comparing them against the future forecasted Q_t, using linear regression analysis, we can determine which model is more reliable to predict future Q_t. For example, each case of the calculated Q_t is an independent variable (x-axis) and the 'forecasted future Q_t' is a dependent variable (y-axis) on a linear regression plot (Fig. 31). The model with a higher coefficient of determination (R^2) has a higher goodness-of-fit and was chosen to further the baseflow analysis under the impact of groundwater withdrawal effect (see section 3.3.2.4).

Figure 31

Model fitness through linear regression. Gan & Luo, 2013.

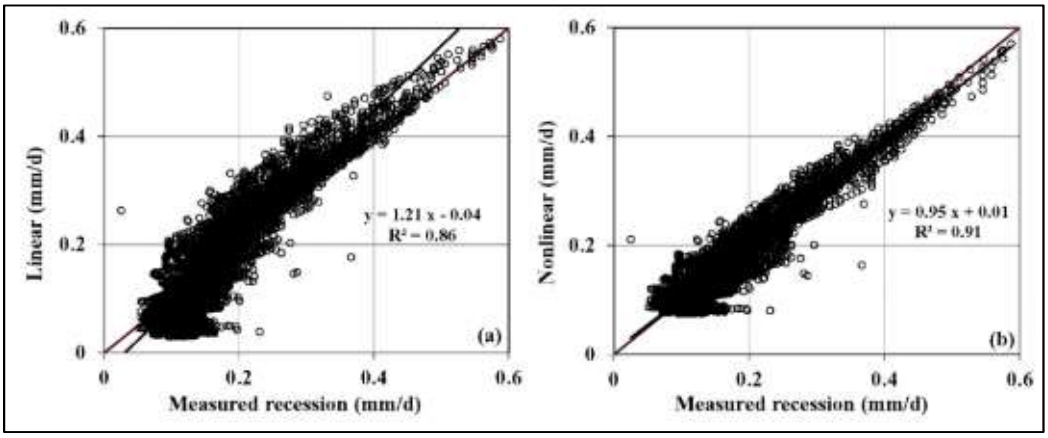

Note. Comparison of the simulated and observed recession data: (left) using the linear aquifer storage-discharge relation model; (right) using a nonlinear aquifer storage-discharge model (Gan & Luo, 2013).

In sum, the three methods to estimate future Q_0 and t, two recession models (linear and nonlinear) to test more fitted model, and forecasted baseflow recession constants (K or a) generate six different cases of potential future minimum baseflow (Q_t) (Table 5). The six cases of Q_t will be compared and statistically analyzed (two-sample Student's t-test)

Table 5

Six cases of modeled future minimum baseflow (Qt)

Q_0 and t Estimating Methods	Baseflow Recession Models	Baseflow Recession Constants (K or a)	Cases
Averages	Linear	Estimated from the Forecast Function (compared against Trendline)	1. Averaged Q_0 and t, Linear Model
			2. Averaged Q_0 and t, Nonlinear Model
Forecast function			3. Forecasted Q_0 and t, Linear Model
	Nonlinear		4. Forecasted Q_0 and t, Nonlinear Model
Trendline			5. Q_0 and t from Trendline, Linear Model
			6. Q_0 and t from Trendline, Nonlinear Model

3.3.2.4: Natural vs Impacted

3.3.2.4.1: A Different Perspective

After evaluating the model fitness, we will choose either a linear or nonlinear model to predict future minimum baseflow (Q_t). Now we add the impact of groundwater withdrawal[51] (W) into the future Q_t in order to assess the impact of pumping on the baseflow recession. Typically, we subtract W from the modeled Q_t to generate the 'impacted' Q_t values ($W \neq 0, W > 0$). However, I will use an inverted approach to the conventional way of subtracting withdrawals from the Q_t for convenience in the

[51] Section 2.7.1 equation 1

calculation. This means that I will leave the modeled Q_t to represent the 'impacted' case while I will add the W to the modeled Q_t to represent the 'unimpacted' or 'natural' case.

The predicted future baseflow was categorized into two groups, one with a 'natural' flow and the other with groundwater withdrawal 'impact' from wells. First, I assumed the 'natural' flow was without groundwater pumping effects ($W = 0$). The natural flow theoretically represented a scenario when groundwater withdrawals did not occur. The withdrawals (W) were constant values (see section 3.2.4.2), estimated from the annual average withdrawal amount assuming the withdrawal rate per unit time has not changed. By contrast, the 'impacted' flow represented the baseflow values from the existing streamflow ($W \neq 0$). This was because the existing streamflow measured from the USGS gauge station already includes the impact of groundwater withdrawals (W).

Adding the withdrawal impacts to the virtual case of naturally flowing baseflow without pumping effect ($Q_t + W = Q_{t,natural}$) is a different approach from previous literature. This method is useful to calculate the baseflow as the impact (W) is added as a positive value than to subtract the impact (W) from the baseflow (Q_t). It ensures the baseflow result with the impact ($W \neq 0$) does not become a negative value that calculation becomes easier (e.g., taking negative value in a logarithm is not possible). This is useful when the withdrawal is larger than the baseflow amount ($Q_t < W$). Also, the impacted baseflow ($Q_{t,impacted}$) represented the existing streamflow and baseflow that were under pumping effects. This informed how current groundwater pumping practices would result in the future baseflow ($Q_{t,impacted}$) with the existing baseflow trends. Thus, the existing method in the literature to add the withdrawals (W) to the

impacted scenario ultimately resulted in subtracting the impact of withdrawals (W) twice as the streamflow already incorporated the impact of withdrawals (W). Therefore, the new perspective to represent the natural flow as a virtual scenario without pumping effect would represent the baseflow recession trends more realistically.

3.3.2.4.2: $Q_{t,natural}$ and $Q_{t,impacted}$

The natural baseflow ($Q_{t,natural}$) included the groundwater withdrawals to represent the scenario when there was no groundwater withdrawal existed. On the other hand, the impacted baseflow ($Q_{t,impact}$) was derived from the existing baseflow data which already incorporated the groundwater pumping via wells. To specify the impact of groundwater withdrawal impact on the baseflow, I adopted Wang and Cai's method (2009). Thomas et al (2013) estimated the baseflow recession constant under the impact of withdrawals, which deplete aquifer storage:

$$\frac{dS}{dt} = -Q_t - W_t \qquad (12)$$

where W_t is withdrawal rate at the same period of the occurrence of Q_t, baseflow.

Combining equation (3) and (11) using $k = {}^{1}/_{\alpha}$,

$$\frac{d(kQ_t)}{dt} = -Q_t - W_t \qquad (13)$$

Here the groundwater withdrawals were constant during each individual recession hydrograph (Thomas et al., 2013); the secondary withdrawal data involved a fixed

pumping rate as an averaged per-day withdrawals (Hansen, 2019). The equation was linearized[52] in a logarithmic form

$$\ln(Q_t + W) = \ln(Q_0 + W) + tln(K) \qquad (14)$$

The equation (14) is a linear model with a dependent variable $\ln(Q_t + W)$, independent variable time t, intercept $\ln(Q_0 + W)$, and slope $ln(K)$ (Thomas et al., 2013). Ultimately, the exponential form of the (13), $(Q_t + W) = (Q_0 + W)e^{-t/c}$, equated the form of precedent Boussinesq equation of $Q_t = Q_0 e^{-t/c}$, or $Q_t = Q_0 k^t$ with $k = -\frac{1}{c}$.

Under the assumption the groundwater storage-discharge showed a linear behavior, the baseflow at the lowest point was categorized into natural ($Q_{t,natural}$) or impacted ($Q_{t2} = Q_{t,impacted}$) flow scenarios (Table 6).

[52] Multiplying the integration factor $e^{t/k}$ leads to $ke^{\frac{t}{k}}\frac{dQ^t}{dt} + e^{\frac{t}{k}}Q_t = -e^{\frac{t}{k}}W$. Using the chain rule and integration leads to $Q_t = \frac{-Wk\left(e^{\frac{t}{k}}-1\right)+kQ_0}{ke^{\frac{t}{k}}} = -W(1-K^t) + Q_0K^t$, where Q_t (ft^3s^{-1}) is the lowest baseflow and Q_0 (ft^3s^{-1}) is the highest baseflow, k (unit of time) is the baseflow recession constant, and W is the rate of withdrawal (ft^3s^{-1}).

Table 6

Baseflow recession analysis equations under Natural or Impacted scenarios and Linear and Nonlinear models

Equations derived and modified from Boussinesq-Dupuit (1903) and Thomas et al. (2013).

	Natural flow (Q_{t1})	Withdrawal impacted (Q_{t2})
Linear model ($Q_{ti,L}$)	$Q_{t1,L} + W = (Q_{01} + W)\, {K_1}^t$ (15-1)	$Q_{t2,L} = (Q_{02}){K_2}^t$ (8)
Nonlinear model ($Q_{ti,N}$)	$Q_{(t1,N+W)} = (Q_{(01+W)})(1 + \frac{0.5(Q_{(01+W)})^{0.5}}{0.5a_1}t)^{-2}$ (15-2)	$Q_{t2,N} = Q_{02}(1 + \frac{0.5{Q_{02}}^{0.5}}{0.5a_2}t)^{-2}$ (10)

Note. Equations used for Natural and Impacted baseflow with linear or nonlinear assumptions on aquifer behavior. $Q_{ti,L}$, $Q_{ti,N}$ (ft^3s^{-1}): i is baseflow under natural (Q_{t1}) or impacted (Q_{t2}) models, L is linear model, N is nonlinear model with a special case when $b = 1/2$. ${K_1}^t$: coefficient of linear model under natural flow. ${K_2}^t$: coefficient of the linear model under wells' withdrawal impacts. a_1: constant of the linear model under natural flow. a_2: constant of the nonlinear model under wells' withdrawal impacts. W is a withdrawal amount from well pumping activity (ft^3s^{-1}).

3.3.2.5: Statistical Testing

The difference between $Q_{t,natural}$ and $Q_{t,impacted}$ will be statistically tested. The simulated baseflow calculated from a chosen model at the lowest point (Q_t) on a hydrograph were tested using two-sample Student's t-test. I hypothesized the difference between current and future $Q_{t,natural}$ and $Q_{t,impacted}$ show the significant differences due to the effect of groundwater withdrawals (W). The null hypothesis was that there was no difference in mean values (μ) in the natural verses impacted baseflow (Q_t)with the confidence interval of 95%:

$$\mu_{natural} = \mu_{impacted}$$

3.3.3: Step 3. Withdrawal Impact on Ecological Functions of a River

Baseflow contribution to the surface flow sustains an ecological function of a river during a low flow period. Previous baseflow recession analyses focused on the assessing methods (e.g., linear or nonlinear groundwater storage-discharge relationship, Thomas et al., 2013) or quantifying the human's withdrawal impact on baseflow recession (Wang & Cai, 2010). In detail, the impact of groundwater withdrawal is usually expressed in the flow rate that is "lost" from the baseflow or surface streamflow. This study extended the baseflow recession analysis to future baseflow recession prediction between 2020 and 2069. Ultimately, the predicted future baseflow provided a different interpretation of the baseflow recession phenomenon, in relation to the stream's ecological function.

The ecological function of streamflow during low flow was assessed by comparing the predicted future baseflow contribution on the streamflow to a parameterized threshold that was required to sustain the ecological river function. The former was derived from the baseflow recession analysis. The latter was derived from conceptualized minimum streamflow standards, which were "Ecologically critical streamflow (ECS)" (de Graaf et al., 2019) and "Presumptive standards" (Gleeson & Richter, 2018), from which ECS derived. Ultimately, the ECS is the threshold that is required for streamflow to maintain its ecological function and can serve as a standard whether future predicted baseflow recession reaches this threshold. The time when the baseflow recession reaches the required threshold (ECS) in the future will be when baseflow contribution no longer supports the environmentally sustainable streamflow under low flow.

3.3.3.1: Environmentally Critical Baseflow (ECB)

3.3.3.1.1: What and Why?

Environmentally Critical Baseflow (ECB) is a threshold baseflow contribution level to the surface flow which sustains streams' ecological function during the low-flow period. The ECB is an altered concept adopted from "Environmentally critical streamflow (ECS, de Graaf et al., 2019)" for the purpose of this study focused on the baseflow. The ECB assumes that the baseflow contribution during the low flow period in Deschutes River Watershed dominates the surface streamflow. Therefore, 'baseflow' can substitute the 'streamflow' during a low flow period.

The environmentally critical streamflow is derived from "Presumptive Standards (Gleeson & Richter, 2017)", which assessed the relationships between hydrologic alterations (e.g., decreased baseflow) and ecological responses (e.g., eroded ecological function) (Gleeson & Richter, 2018) as a result. While these two low flow parameters—ECS and Presumptive Standards—focus on the surface streamflow as the assessment objective, ECB pays attention to the baseflow recession and its reducing contribution to the surface water system. The time at which the 'impacted' future baseflow meets the ECB will be compared to the time when the 'natural' future baseflow meets the ECB. Comparing the 'time' at which each future baseflow meets the ECB will be the 'impact' of the groundwater withdrawals on the baseflow recession. This provides a different perspective to understand the degree of withdrawal impact on the baseflow recession. Such an approach may help us communicate the adverse impact of groundwater withdrawal to a variety of audiences.

3.3.3.1.2: How?

Following the recent work of de Graaf. et al on the environmentally critical streamflow (ECS) (2019), the environmentally critical baseflow (ECB) adopted the exceedance probability (Q) every 5 years (de Graaf et al., 2019). First, the threshold or ECB was determined to be the value of the baseflow which is exceeded 90% of the time for each 5 years, referred to as $Q90$. The baseflow between the study period (1945-2069) was sorted in descending order to calculate the 90% exceedance probability value ($Q90$). The probability exceedance was calculated as follows:

$$P=100\{m/(n+1)) \qquad (16)$$

where P=exceedance probability (%), m=rank of baseflow among 5 years of record, n=total number of baseflow record.

Next, the $Q90$ of natural baseflow contribution assessed whether the impacted baseflow (baseflow with the withdrawal impact, W) was above the environmentally critical baseflow (ECB). According the Gleeson and Richter (2018), impact of groundwater withdrawal was identified to be environmentally harmful at a time when the groundwater pumping decreased natural baseflow by more than 10% through time (Gleeson & Richter, 2018). Therefore, the time when estimated baseflow under groundwater withdrawal impact (Q_{t2} or $Q_{t,impacted}$, see section 3.3.2.4.2) was lower than 10% of the $Q90$ is when the ECB was exceeded. When the ECB was exceeded, the baseflow contribution was too low to maintain the stream's ecological function during low flow. To calculate this, the maximum ECB will be set as the 90% of the $Q90$ value (Fig. 32).

Figure 32

Environmentally Critical Baseflow (ECB) of the Deschutes every 5 years. Q**90** *and ECB calculated from streamflow data (NWIS).*

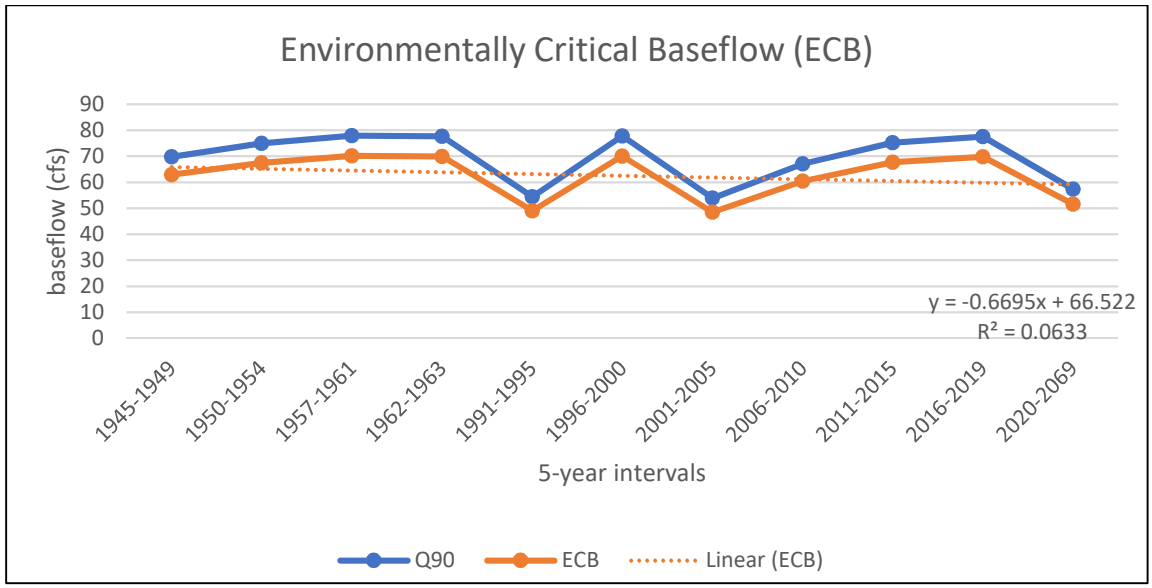

Note. The ECB is 90% of the $Q90$. The trend of ECB shows decline (linear regression with a negative slope of -0.6695)

Also, the time of reaching the ECB was determined to be at which the yearly baseflow falls 10% below the natural $Q90$ for at least two consecutive years (de Graaf et al., 2019). The two consecutive years criterion was motivated by the assumption that at least two years are needed before water management strategies are changed (de Graaf et al., 2019). This criterion substantiated as the baseflow recession is sensitive to time (Thomas et al., 2013).

Lastly, the impact of groundwater withdrawal against ECB was determined to be when the impacted baseflow reached the ECB. Likewise, the natural future baseflow from the observed data was analyzed for when it reached the ECB. Comparing the two times when natural and impacted future baseflow met the ECB addressed the

groundwater withdrawal impact in a perspective of time. I hypothesized that the ECB will be reached by the impacted baseflow (Q_{t2} or $Q_{t,impacted}$) earlier than the natural baseflow (Q_{t1} or $Q_{t,natural}$) in the future.

Chapter 4: Results

4.1: Roadmap

Results are organized into four sections: 1) groundwater withdrawal data analysis, 2) baseflow recession models, linear and nonlinear, 3) baseflow recession analyses with 'impacted' and 'natural' scenarios, and 4) assessing the baseflow against environmentally critical baseflow, the threshold for the river to maintain ecological function. The first three sections are sequentially related that each step leads to the next baseflow recession analysis. The fourth section provides a different perspective of baseflow recession data using frequency analysis.

4.2: Groundwater withdrawals

4.2.1: Yearly Groundwater Withdrawals

The cumulative groundwater withdrawal amount of each year has continuously increased in Thurston County[53] (Fig. 33). Yearly cumulative withdrawal of the starting year (1945) was 7.02 cubic feet per second (cfs) and the ending year (2019) was 78.65 cfs, which is an increase of more than tenfold over the 75 years. The increase in groundwater withdrawals tracks the increase in population of Thurston County.

[53] The withdrawal amount values of each year: see Appendix F

Figure 33

Relationship between population and groundwater withdrawals in Thurston County.

Decadal Population Data from the U.S. Census Bureau, Withdrawal Data from Thurston County Water Planning.

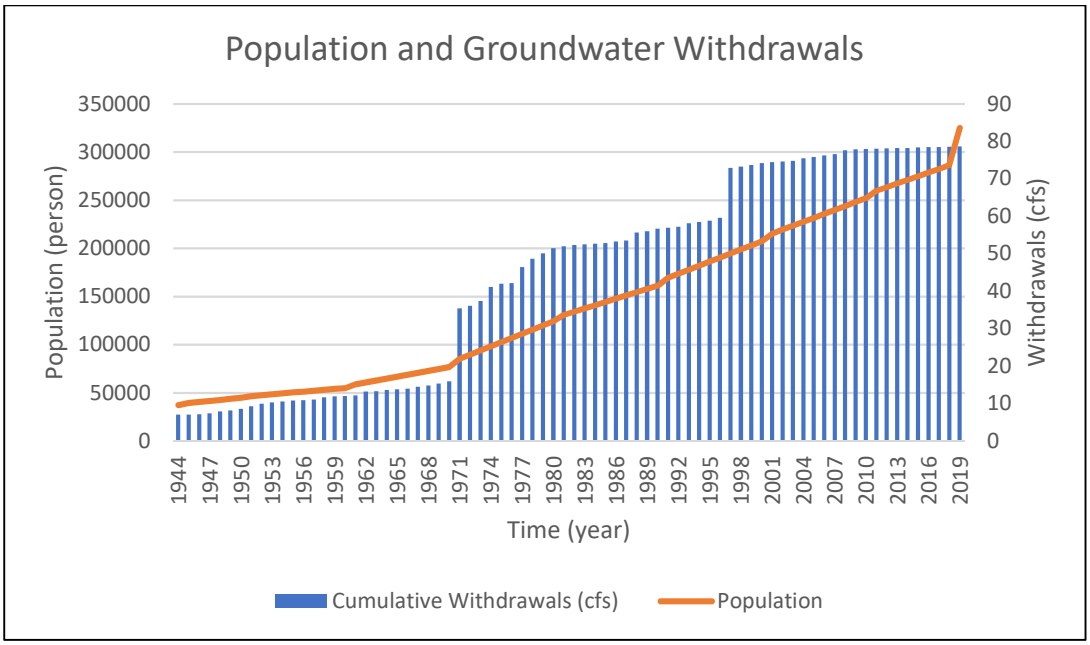

Note. The population between each decade was extrapolated by using linear regression.

Withdrawal rates of the year 1971 and 1997 showed a sharp increase. Unlike the gradual withdrawals of the rest of the period, the increases of two years are rather abrupt, which could be because of data issues. The year 1971 was when the Department of Ecology (Ecology) started managing received well reports (DoE, n.d.). Ecology had received the well reports since the 1930s but not managed them until 1971 (DoE, n.d.). There could have been missing withdrawal data that occurred before 1971, but this cannot be confirmed without existing well data. For the year 1997, there was no information to explain a sharp increase in the withdrawals. This could be due to a population growth of 61.6% in 1990-2000, which was higher than the mean annual

growth rate of 47% between 1870 to 2000 (U.S. Census Bureau, 2014). This is a viable conjecture as the population growth and the groundwater withdrawal rates are positively correlated[54].

The population increase is related to the gradual increase in groundwater withdrawals in the area. Among the groundwater withdrawals dedicated to residential uses, water uses through "domestic uses" and "public supply" composed nearly 75% of total withdrawals in 2019 (see section 3.2.4.2.1; Fig, 34). Residential and public water uses differ in withdrawal amount. The "public supply group A" refers to the water supply service for at least 25 people or a minimum of 15 connections. The "public supply group B" serves fewer than 15 connections or 25 people; most of Group B systems use the groundwater permit exemption (see section 2.5.3.1; Table 2). In 2019, public supply group B (exempt wells) pumped over half of the total groundwater withdrawal amount with 87 Million gallons per day (Mgpd) (Fig. 34). These permit-exempt wells were initially for "small withdrawals" in areas where public supply is not available (DoE, n.d.)[55]. Under the Groundwater Code (Chapter 90.44.050 RCW), these permit-exempt wells are not mandated to record or report the withdrawal rates of pumping; the pumping rates or withdrawal amount can be only estimated with averaged water use amounts (see section 3.2.4.2). The increase of these permit-exempt wells in the area was expected as the population in Thurston County was projected for continuous growth (OFM, 2012). Thurston County Water Planning estimates the withdrawal rates from permit-exempt wells by averaging public water use of the area.

[54] Two-sample Student's t-test between yearly cumulative withdrawals and the population showed a significant difference between the two groups (p-value <2.2e-16, CI=95%).
[55] In this study, permit-exempt wells include the "domestic" and "public supply group B" wells.

Figure 34

Groundwater Withdrawals by Water Use Purposes.

Withdrawal data from the Thurston County Water Planning.

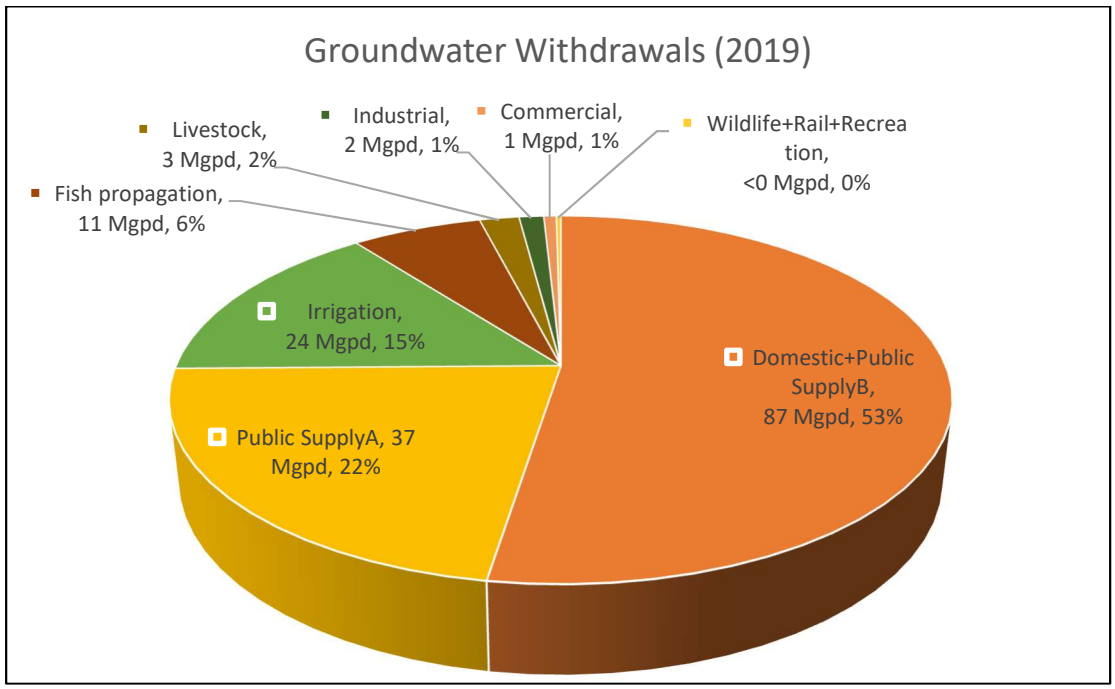

Note. Groundwater withdrawal portions in amount (Million gallons per day (Mgpd)) and percentage (%).

4.2.2: Concentrated Withdrawal Locations

Groundwater withdrawals intensified in different locations. Due to rural developments, the withdrawal from the southwest region has increased dramatically from around 1975 (Fig. 35, Map-B). Major urban areas in Tumwater, Lacey, and Olympia in the center to the north of the county have shown consistently increasing withdrawals, at lower rates. The spatial extent for urban development of the three major cities (Tumwater, Lacey, and Olympia) started around 1975 and intensified afterward, highlighting recent development and sprawl in Lacey (Fig. 35, Map-C).

Additionally, the pumping effect created by wells in the mid- to lower Deschutes River was expected to be higher than the upper river. The selected wells for this analysis were situated on geological layers that are hydraulically interconnected with the stream (Fig. 35, Map-D). This means the increase in groundwater withdrawals from such units will have an adverse impact on lowering the Deschutes surface stream.

Figure 35

Groundwater withdrawal concentrations in the study area of Thurston County

Withdrawal data from Thurston County Water Planning. Heat map created using ArcGIS Online. ESRI ArcGIS Online Layer sources: WSDOT, 2012; City of Tacoma GIS, 2019. Withdrawal amount data source: the Thurston County Water Planning.

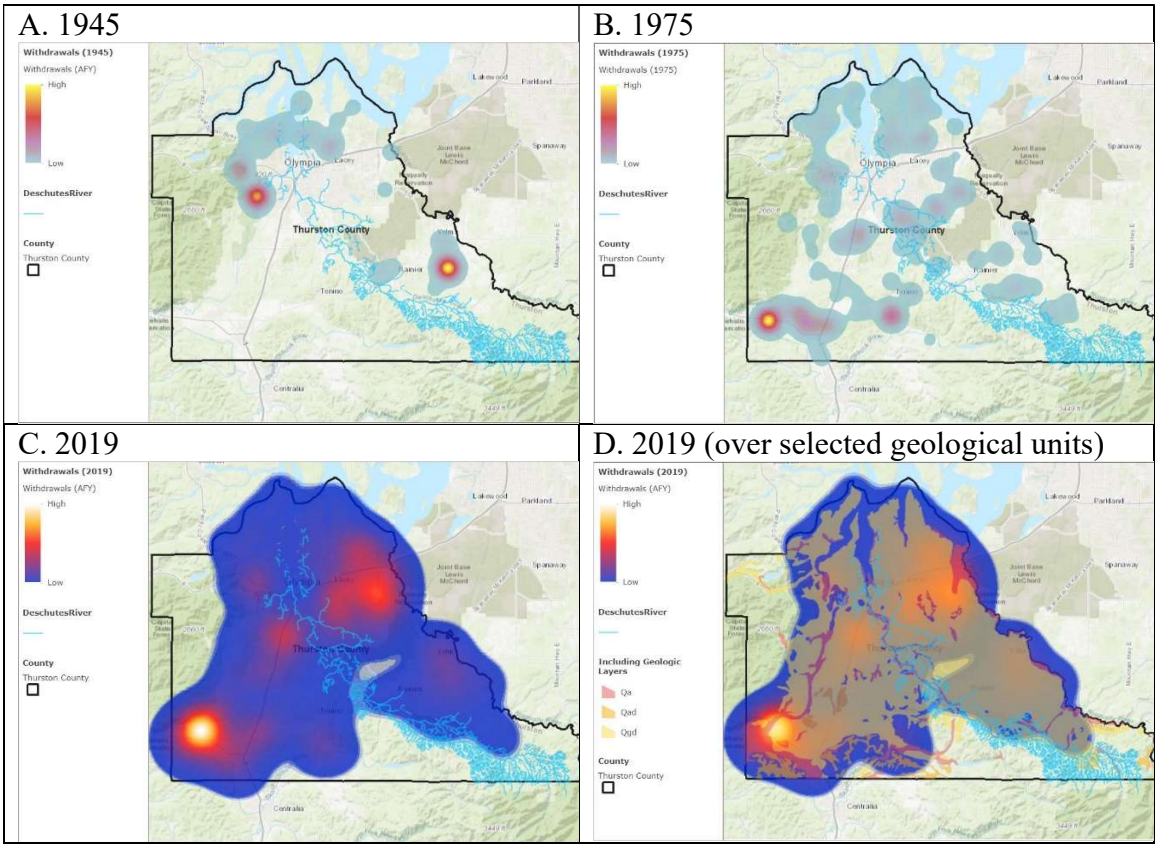

Note. Maps showing locations of concentrated groundwater withdrawals (A: 1945, B: 1975, C: 2019, D: 2019 with hydraulically connected geological units). Blue tint denotes a lower withdrawal rate; red, yellow, white shows a higher withdrawal rate. The withdrawal rate is acre-feet per year (AFY).

4.3: Model fitness

I used linear and nonlinear models and calculated the baseflow recession constants to estimate the annual future Q_t between 2020 and 2069. Using linear regression, the linear- or nonlinear- modeled Q_t were tested for their goodness-of-fit against the predicted 'future forecasted Q_t', which is the future Q_t value forecasted from the past Q_t (see section 3.3.2.3). The selected model, either linear or nonlinear, will represent the future baseflow and recession regime in section 4.3.2.2.

4.3.1: Data preparation

Data is estimated and prepared to predict future Q_t under linear and nonlinear models. For the time period 2020 to 2069, I estimated the baseflow at the beginning of recession periods (Q_0), the length of recession period (t), and baseflow recession constants (K and a). I then estimated independent variables for the future, including Q_0 and t by 1) averages, 2) forecast function, and 3) linear trend relationship. Briefly, there are six cases of modeled minimum baseflow (Q_t) that I generated, compared, and chose for the best-fit model to the 'forecasted future' minimum baseflow data, Q_t (Table 5[56]).

[56]

Q_0 and t Estimating Methods	Baseflow Recession Models	Baseflow Recession Constants (K or a)	Cases
Averages	Linear	Estimated from the Forecast Function (compared against Trendline)	1. Averaged Q_0 and t, Linear Model
			2. Averaged Q_0 and t, Nonlinear Model
Forecast function			3. Forecasted Q_0 and t, Linear Model
	Nonlinear		4. Forecasted Q_0 and t, Nonlinear Model
Trendline			5. Q_0 and t from Trendline, Linear Model
			6. Q_0 and t from Trendline, Nonlinear Model

4.3.1.1: Determination of Q_0

I obtained different future estimations of the maximum baseflow at the beginning of baseflow recession periods[57] (Q_0).

First, the average value of the past Q_0 data from 1945 to 2019 is of $Q_0 = 151$ (cfs). I averaged data from 1945 to 2019 to find the mean of Q_0:

$$mean\ Q_0\ value = \frac{\sum_{1945}^{2019} Q_0}{n}$$

where n is the number of recession periods (t).

Second, I found a linear trend of the past baseflow Q_0 (1945-2019) between baseflow and time: $Q_0 = 0.5935t - 1025.6$ (Fig. 36, blue trendline). The positive slope indicates that Q_0 increases with time by 0.59 cfs per day. The trend of Q_0 between 1945 to 2019 showed a gradual increase, as the maximum baseflow at the beginning of each recession period grew higher in recent years. I expected that this will continue to grow in the future (Fig. 36, orange line) because of the increasing trend of the past data.

Third, the forecast function from Microsoft Excel estimated the future Q_0 and showed a similar value to the averaged Q_0 (Fig. 36, gray line). This forecast function differs to the two methods, the average and trendline, in that it uses a "process for measuring the similarity of one time series (i.e., past) to another time series (i.e., future)" (Onajite, 2013). The forecast function assumes a linear relationship of the independent

[57] The future maximum baseflow (Q_0) and recession period (t) in the future (2020-2069) were estimated based on historic data (1945-2019) using three different methods: average, forecast function, and trendline. The estimated future Q_0 and t is in Appendix G.

(x-axis) and dependent (y-axis) variables to predict future estimations (see section 3.3.2.2.2).

Figure 36

Maximum baseflow ($\boldsymbol{Q_0}$) of recession periods (1945-2019) estimated from the trendline and forecast function.

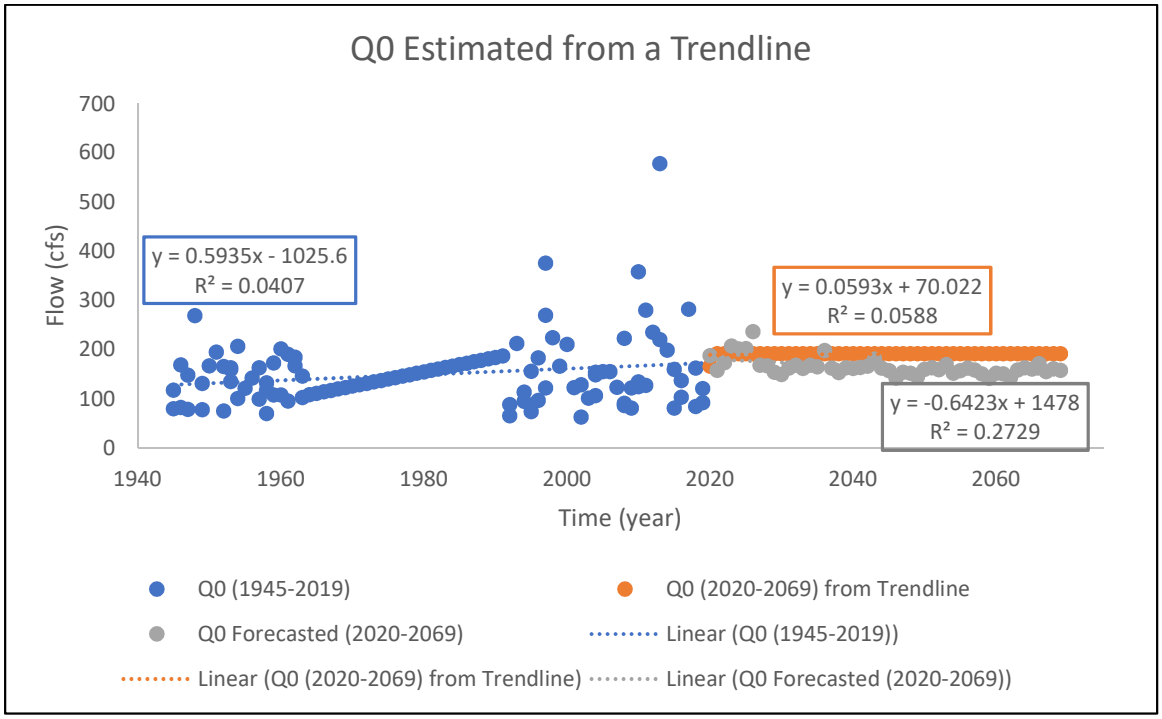

Note. The future prediction on Q_0 estimated from trendline (orange line) is higher than the Q_0 estimated from the forecasted function (gray line). The highly scattered data causes a low coefficient of determination ($R^2 = 0.0407$). The values between 1964 to 1990 were missing and they were estimated from linear interpolation.

As a result, I will use these three different methods to predict future (2020-2069) Q_0 and determine which one will produce the future Q_t that fits most to the forecasted future Q_t, using a Student's t-test (Table 7).

4.3.1.2: Determination of recession period (t)

The three different methods described above (see section 4.3.1.1) applied to estimate the lengths of future recession periods (t) [58]. The lengths of recession periods indicated how many days the recession occurred during each low flow period.

First, the averaged recession period between 1945 and 2019 was 64 days (Fig. 37, blue markers).

Second, the linear trend of the recession period showed a gradual increase, with a positive rate of change of 0.075 days. The recession periods varied from 10 days (minimum) to 122 days (maximum) with an average of 64 days. The estimated recession period in 2020 (future) is 62 days while the estimated recession period between 2021 and 2069 is 65 days (Fig. 37, orange line). On average, the future recession period was 63.5 days (≈ 64 days) when I calculated the mean of 62 days (recession period in 2020) and 65 days (recession period between 2021 and 2069).

Third, the forecast function estimated the future recession period (the forecast function method is described in section 3.3.2.2.2). The mean value of the forecasted future baseflow is 64 days, which is the same as the averaged baseflow of the past days (1945-2019). The forecasted recession periods ranged from 64 days (minimum) to 65 days (maximum) (Fig. 37, gray markers). Overall, the three methods to estimate the future recession periods (t) generated a similar result of 64 days. The similarity of the

[58] The future maximum baseflow (Q_0) and recession period (t) in the future (2020-2069) were estimated based on historic data (1945-2019) using three different methods: average, forecast function, and trendline. The estimated future Q_0 and t is in Appendix G.

estimated results from these two methods indicate that these are reliable tool to predict the future recession period.

As a result, I assumed the recession period (t) will remain as 64 days in the future prediction between 2020 and 2069. The historic data (1945-2019) of the recession period showed a gradual increase with a positive rate of 0.1406 days (blue trendline in Fig. 37). However, the future prediction from three methods, including averaged data, trendline, and the forecast function produced a static or marginally increasing recession period. One reason for the static or marginally diverting estimations in the future may be because of the relatively short predicting period of 40 years (2020-2069). Also, the historic data had a high variability ($R^2 = 0.01$, blue trendline in Fig. 37) that finding a fluctuating trend may be less reliable than estimating the future data with a static value of 64 days. Therefore, a future recession period is estimated with 64 days for the 2020-2069 prediction.

Figure 37

Recession period (t) of the historic data (1945-2019) and future (2020-2069) estimated from the trendline and forecast function (2020-2069).

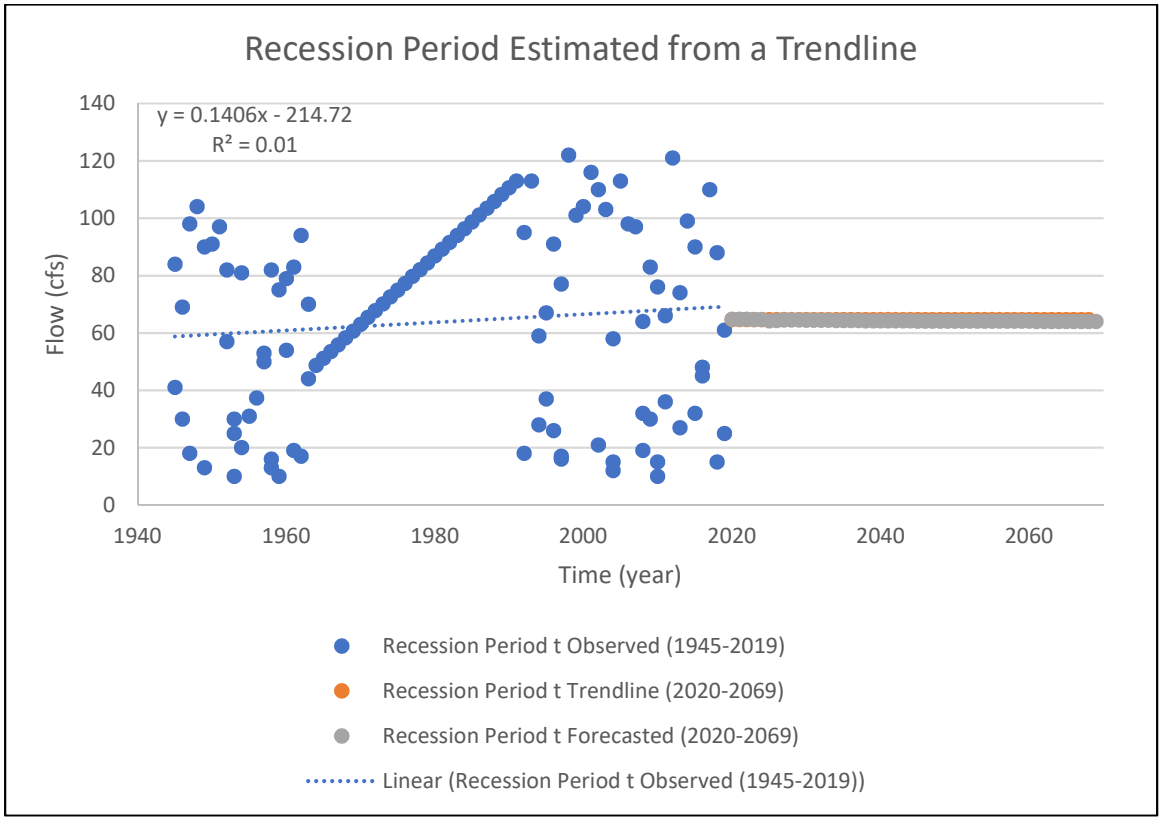

Note. The predicted future recession period (t) estimated from the trendline (orange line) and the forecast function (gray line) show an almost identical pattern. The historic data is represented as 'observed' data (blue scatters). The values between 1964 to 1990 were missing thus estimated from linear interpolation.

4.3.1.3: Determination of Recession Constants (K and a)

The baseflow recession constants parametrize the degree to which future minimum baseflow (Q_t) changed over time. The constants, K (dimensionless) and a ($m^{-1}s^{-1}$), represent the slope of the baseflow recession in a linear model and in a

nonlinear model[59]. The baseflow recession constants show the hydrological property of the groundwater-surface water interaction in a nonlinear model (Rupp & Selker, 2006), respectively. The forecast function (see section 3.3.2.2.2) estimated the future recession constants for the linear model (K) and the nonlinear model (a) (Fig. 38).

Figure 38

Trend of recession constants

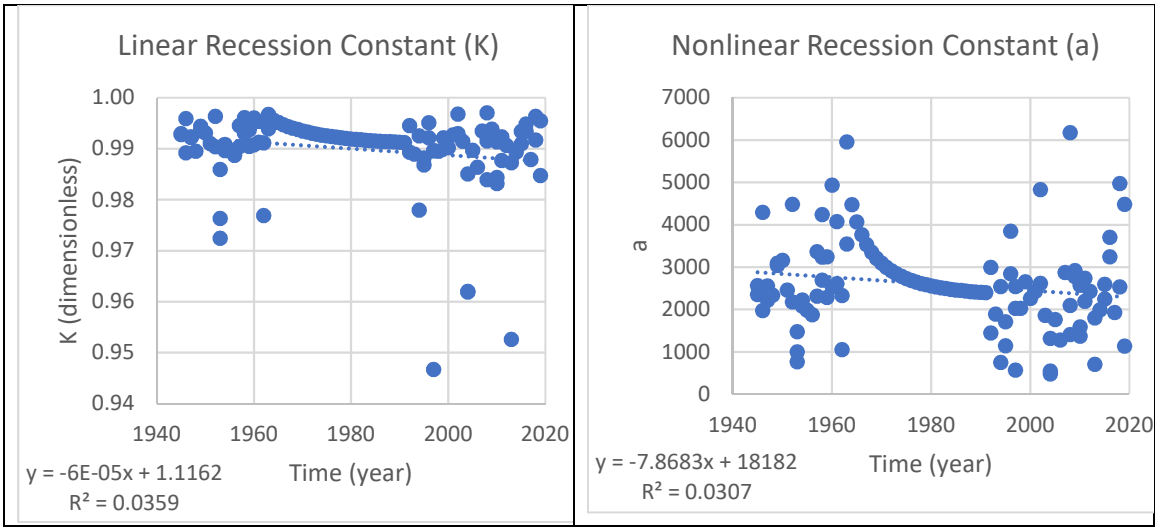

Both linear and nonlinear recession constants estimated from the trendline of historic data (1945-2019) showed high variability and low predictability: low coefficient of determination ($R^2 \approx 0.03$). This means that historic data (1945-2019) can predict future values at about 3% of probability, which is low predictability. Then, the future estimation of the recession constant using the trend of the past data is unreliable. As an alternative, the recession constant is predicted from the forecast function, which "smooth out" highly variable historic data (Fig. 39) (Microsoft Office, n.d.).

[59] Linear model: $Q_t = Q_0 K^t$, Nonlinear model: $Q_t = Q_0(1 + \frac{(1-b){Q_0}^{1-b}}{ab}t)^{1/b-1}$ (see section 3.3.1.1). The constants are K (linear) and a (nonlinear).

Figure 39

Estimated recession constants (1945-2069)

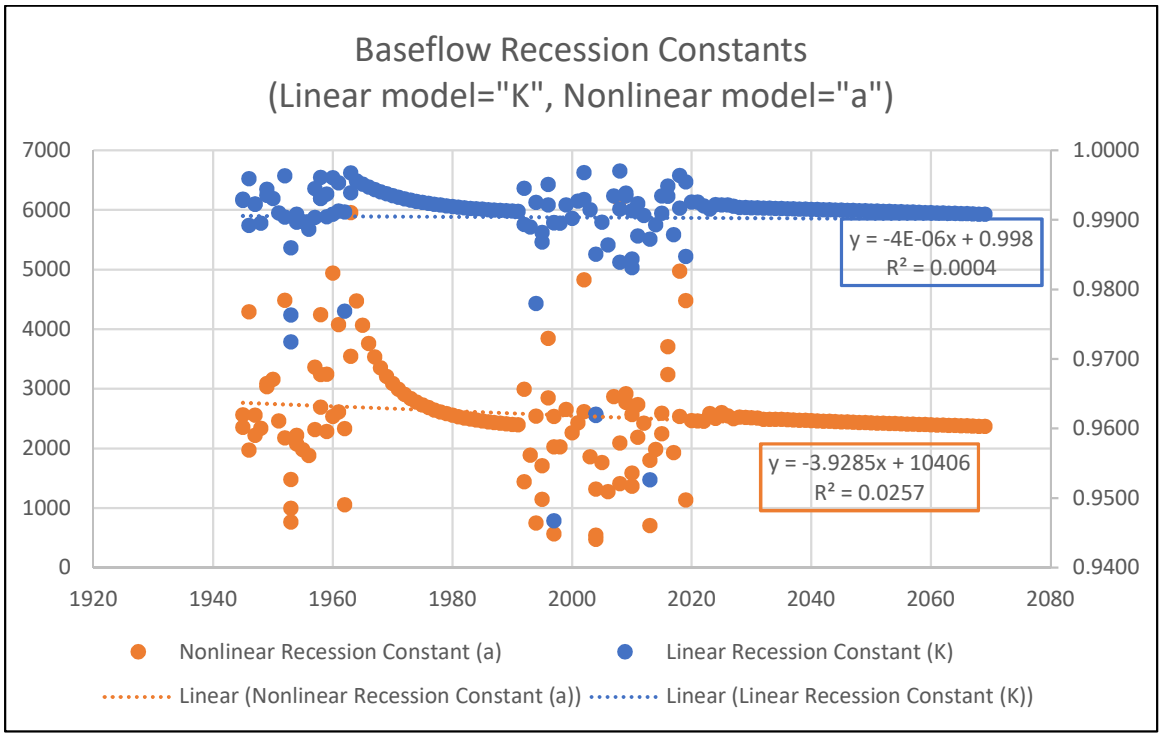

Note. The future baseflow recession constants for both linear and nonlinear models were estimated using the forecast function. For the linear recession constant (K), the baseflow decreases with -4E-06 in every time period (day). For the nonlinear recession constant (a), the baseflow decreases with -3.9285 in every time period (day). However, both linear and nonlinear recession constant data have high variability that its predictability and power of determination (R^2) is 0.04% and 2.6%, respectively.

As a result, I chose to use Excel's forecast function to predict the future baseflow recession constant values. Using the forecast function, the estimated future baseflow recession constants (linear model=K, nonlinear model=a) between 2020 and 2069 show a slight decreasing trend as seen in Fig. 39[60]. The reducing recession constant values indicate the slope of recession will become greater, or the degree of recession will

[60] The linear and nonlinear baseflow recession constant values estimated using the forecast function is displayed in Appendix H.

increase. It means the future minimum baseflow (Q_t) will be reducing at a faster degree. I will discuss the future minimum baseflow (Q_t) in the following section.

4.3.2: Choosing a Model

4.3.2.1: Future Estimation of Data

The goodness-of-fit of linear and nonlinear models were tested to choose which model—linear or nonlinear—had a higher correlation to the 'forecasted future baseflow' Q_t. Linear regression was used to test the fitness of the models. To do this, historic Q_t data (1945-2019) was not applicable as the Q_t from the linear model and the measured Q_t are the same. This is because I used the measured Q_t to calculate the linear recession constant (K), which then is used to estimate the Q_t with the linear model. Therefore, I will use the future Q_t data (2020-2069) to compare and assess the most fitted model to the forecasted future Q_t.

4.3.2.1.1: Future Minimum Baseflow (Q_t)

The forecasted future baseflow at the lowest point (Q_t), obtained from the forecast-functioning the past Q_t, showed a declining trend in the future (Fig. 40). This indicates that the predicted minimum baseflow in the future decreases, resulting in lower streamflow during dry seasons. The reduced minimum baseflow casts a concern over drier streamflow, which might be exacerbated in the face of climatic and anthropogenic impacts.

Figure 40

Forecasted future minimum baseflow ($\boldsymbol{Q_t}$). Baseflow data separated from the streamflow data obtained from NWIS.

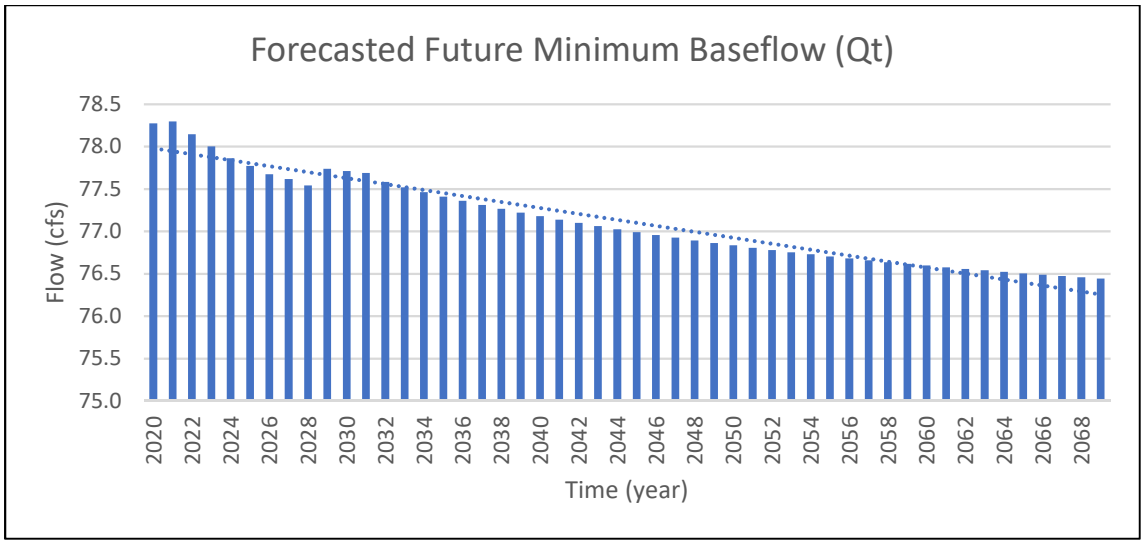

Note. Future baseflow at the lowest point (Q_t), estimated with the forecast function.

4.3.2.2: Model Selection

4.3.2.2.1: Linear Regression Analysis

The linear regression between modeled Q_t (linear, nonlinear) versus forecasted Q_t (2020-2069) identified which model best explained and predicted the relationship between the estimated values of Q_t. For each case, the null hypothesis was: The slope of linear regression is not zero between the estimated Q_t from a model (response variable) and the forecasted Q_t (explanatory variable); The confidence interval (CI) was 95% and the significance level at 0.05 (p-value). Depending on the estimated maximum recession baseflow (Q_0), five out of six cases showed a significant relationship between the explanatory and response variable (Table 7).

As a result, we obtained our best fit to forecasted Q_t with the Q_t estimated through a 'linear' baseflow regression model and 'averaged' Q_0 with 'averaged' t (1st case in Table 7). The low p-value (< 2e-16) of this linear model lets us reject the null hypothesis that the slope of the linear regression between the linear model Q_t and the forecasted future Q_t was not zero (slope ≠ 0). This means that there is a significant difference in two variables of the 'forecasted future Q_t' and 'Q_t from a linear model'; a high coefficient of determination ($R^2 = 0.906$) showed the 'linear model Q_t' predicts the forecasted future Q_t well:

Table 7

Minimum baseflow (Qt) estimation from different methods and models

Estimating Methods	Models	Single Linear Regression expression	P-value	Coefficient of Determination (R^2)
Averaged Q_0 and t	Linear	$y = 4.3x - 248$	$< 2.2e-16$	0.906
	Nonlinear	$y = 0.8x + 55.4$	$2.081e-14$	0.7075
Forecast function (Q_0 and t)	Linear	$y = 14.8x - 1042.5$	$4.667e-07$	0.414
	Nonlinear	$y = 12.9x - 870.9$	$5.918e-05$	0.2878
Trend of Q_0 and t	Linear	$y = 4.4x - 230.4$	$3.625e-12$	0.6381
	Nonlinear	$y = -0.3x + 168$	0.6507	0.0043

Note. For each single linear regression, the x represents future Q_t estimated from the forecast function; y represents future Q_t calculated by plugging Q_0 and t (estimated by three methods: average, forecast, or trend) into either linear or nonlinear models.

Light green denotes statistical significance to explain the model and the observed baseflow data. Red denotes statistical insignificance between variables. Dark green signifies the most predictable model on the observed baseflow.

4.3.2.2.2: Model Validation

Linear models showed a consistently higher R^2 than nonlinear models across all six different scenarios (Table 7). While two nonlinear models (2nd and 4th in Table 7) showed statistical significance, these had low R^2 values. Therefore, the linear model with the highest R^2 was chosen to be the representative model that fits best to the 'future

forecasted' baseflow. Each model is compared against the future, minimum baseflow (Q_t) calculated from the forecast function. The future Q_t functions as a 'control' case as it is simply forecasted from the historic data (1945-2019) without model processes. Finally, the future Q_t compares the six modeled cases to determine which model fits closest to it and is most predictable for future Q_t predictions[61].

The linear regression analysis showed that the linear model predicts the future Q_t better than the nonlinear model. The linear regression between the forecast and the 'linear model' shows high relatedness (Fig. 41; Fig. 42). When different statistical parameters (i.e., mean, median, minimum, and maximum values of data) were compared between the 'forecasted future' and 'linear or nonlinear' models, the linear model produced estimations of future Q_t that are closer to the 'forecasted future' case (Fig. 42).

Figure 41

Linear regression analysis of the linear and nonlinear model.

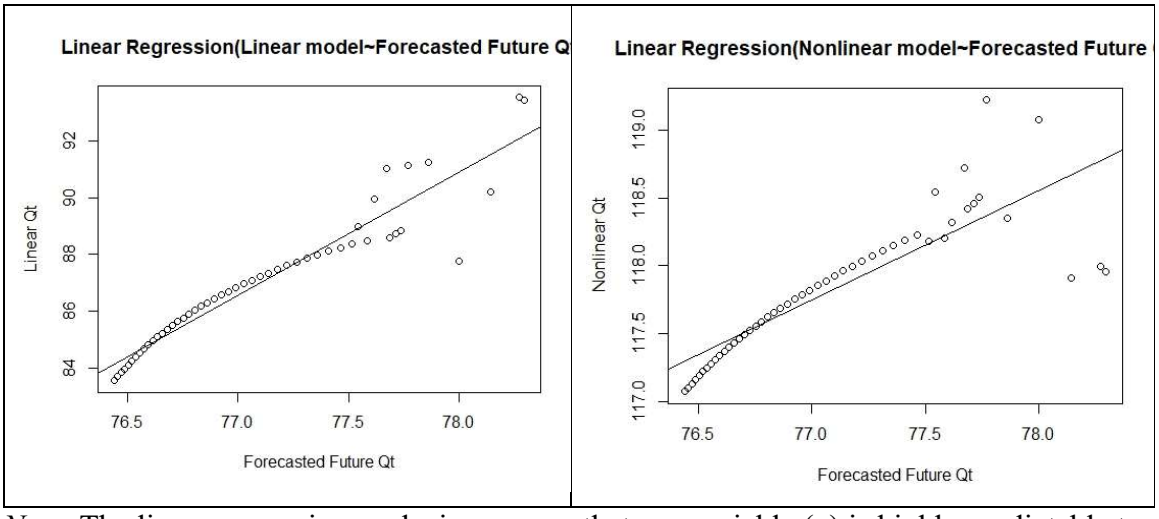

Note. The linear regression analysis assumes that one variable (y) is highly predictable to the other variable (x) when data scatters near the projected linear regression line.

[61] The estimated future minimum baseflow (Q_t) depending on the linear/nonlinear model and the method to determine the maximum baseflow (Q_0)—trend or average: see in Appendix I

Figure 42

Statistical comparisons of the $\boldsymbol{Q_t}$ estimations from the linear and nonlinear model

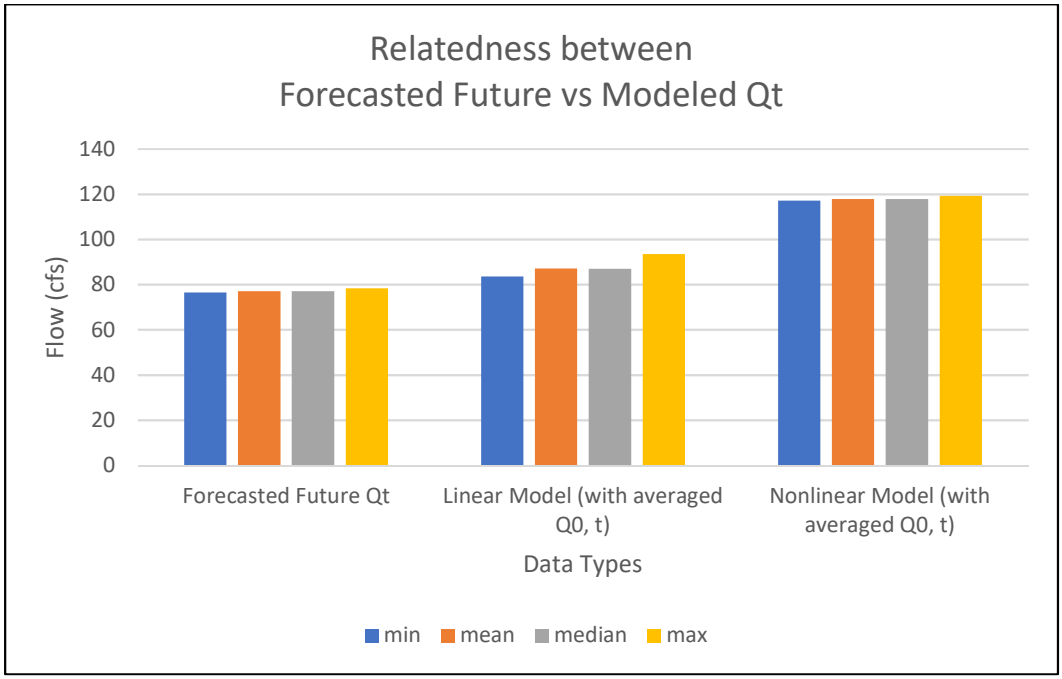

4.3.2.2.3: Residual Analysis

The residuals analysis of the two linear regression analyses in Fig. 41 signified which model has more consistent and predictable data. Four types of tests addressed the fitness of models. First, the residual vs fitted plot suggested that linear and nonlinear models were linearly positive to the forecasted future Q_t (Fig. 43-A). Second, the normal probability (Q-Q) plot showed that both linear and nonlinear modeled data showed normal distribution (Fig. 43-B). Third, the scale-location plot suggested the residuals were spread equally during the earlier phase but sprawling in a greater degree in the later phase (Fig. 43-C). This meant the estimated Q_t via both linear and nonlinear models showed greater variability over time. Lastly, the residual vs leverage plot suggested there was a difference in influential cases (e.g., outliers). The linear model did not show an influential case as the major trendline did not intervene with the Cook's distance (a red

dashed line). However, the nonlinear model showed the data could include some influential cases as the trendline crossed the Cook's distance (Fig. 43-D). This indicated that the baseflow data estimated by a nonlinear model could potentially be less predictable of the forecasted future baseflow (Q_t). Overall, the linear model was more reliable with data distribution and predictability. Therefore, we chose linear model for further baseflow recession analysis with the impact of withdrawals.

Figure 43

Residuals analysis of the linear and nonlinear models.

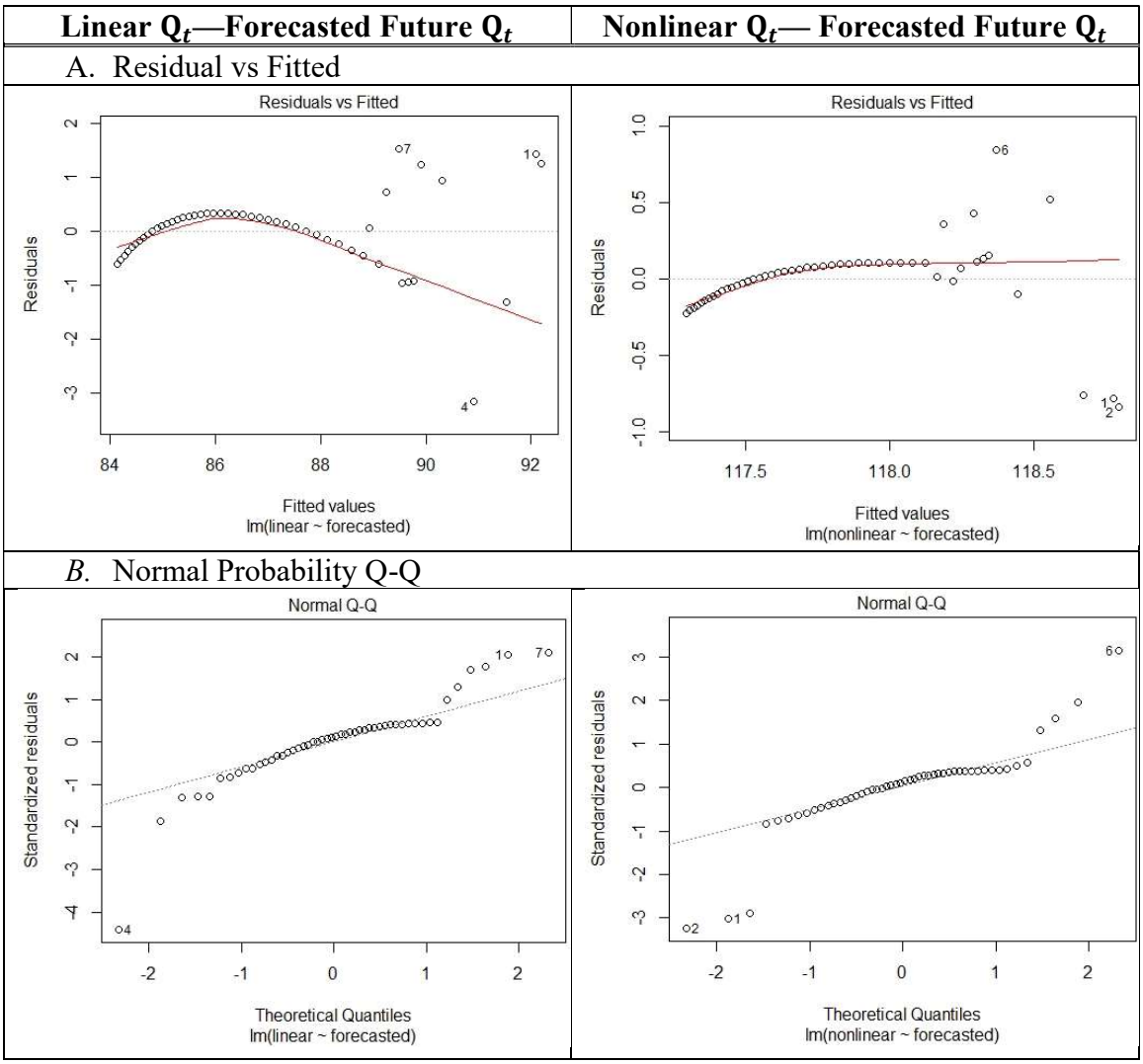

C. Scale-Location ($\sqrt{\text{Standard residuals}}$)

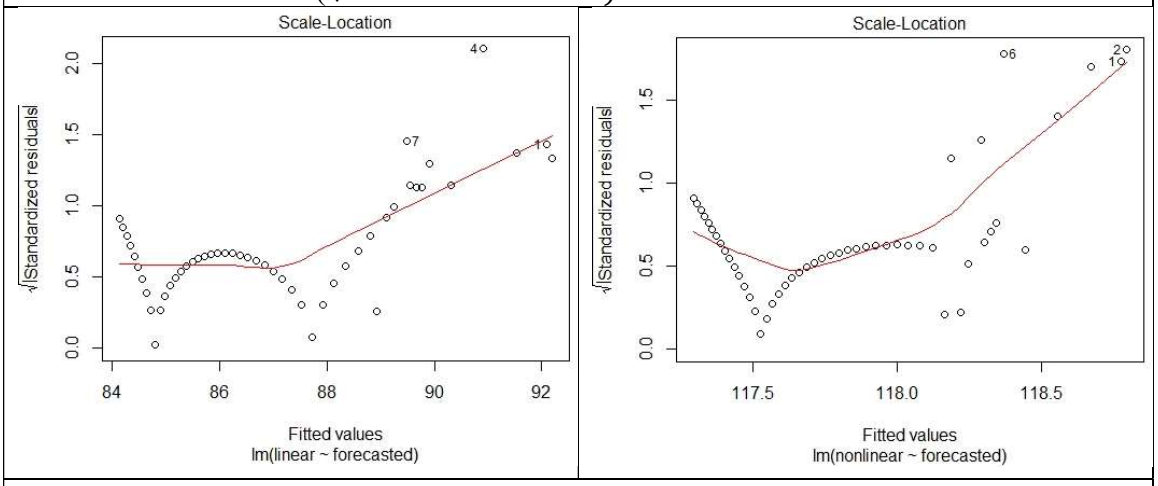

D. Residual vs Leverage

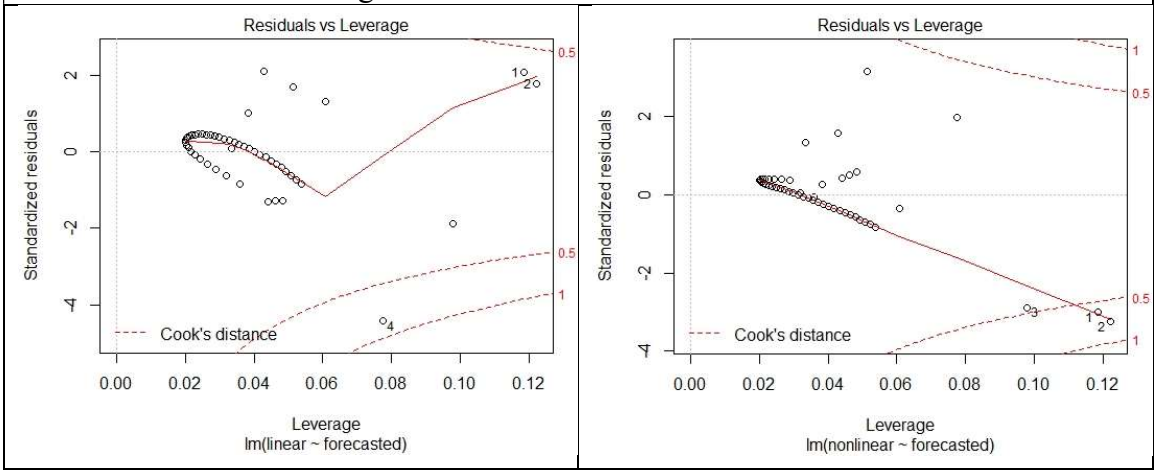

4.4: Baseflow Recession Analysis

4.4.1: Existing "Impacted" Baseflow Recession

The 'impacted' baseflow ($Q_{t,impacted}$) in this study refers to the baseflow that already added the groundwater withdrawals. In other words, the baseflow portion of the observed streamflow (via USGS gauge station at Tumwater) was measured while groundwater pumping occurred and is the baseflow under the 'impacted' scenario.

The baseflow recession constant "K" under a linear mode showed a very slightly decreasing trend in the past and the future estimation (Fig. 44). The decreasing constant (K) derived from the reduction in the minimum baseflow (Q_t) data from 1945 to 2019 (Fig. 44, blue column). Consequently, the decreasing trend of recession constant (K) resulted in reducing the future Q_t (Fig. 44, gray column), assuming more baseflow recession occurrences and less baseflow contribution to the future surface flow.

Figure 44

Recession constant of the linear model (K) and minimum baseflow ($\boldsymbol{Q_t}$) (1945-2069). Streamflow data from NWIS, separated using WHAT.

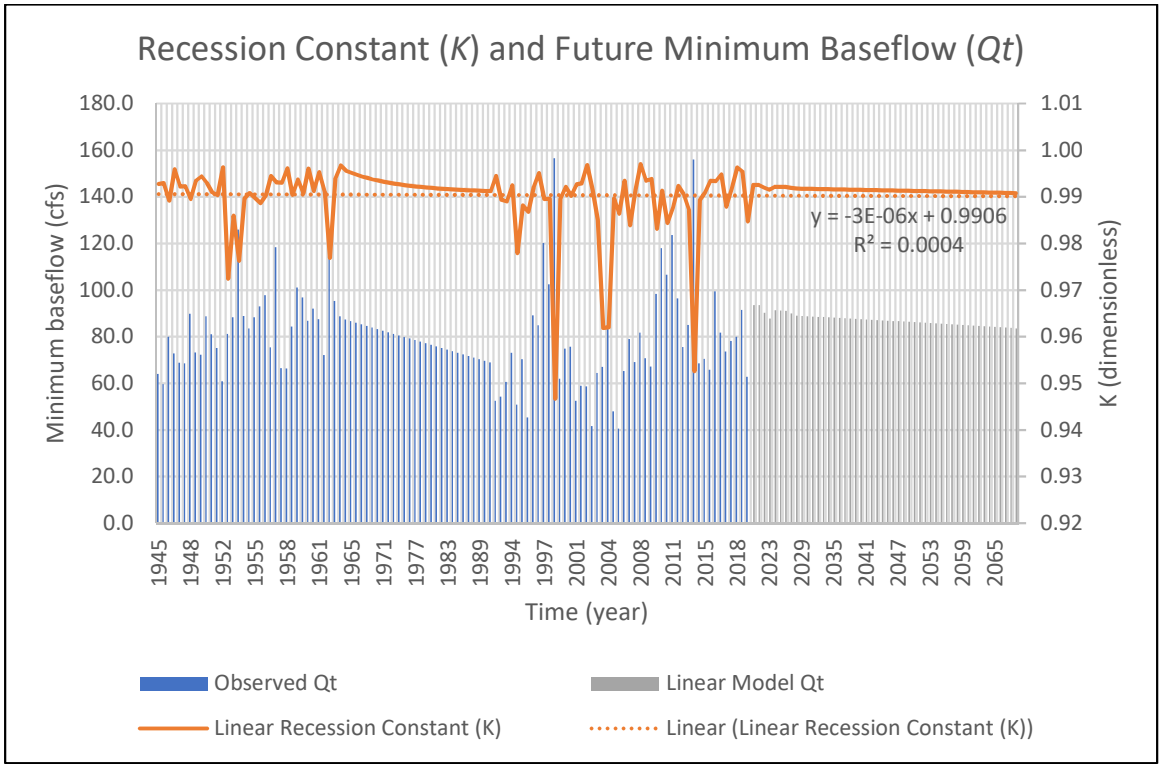

Note. The past minimum baseflow (Q_t, blue column) and future minimum baseflow (Q_t, gray column) decrease. The trendline of the linear recession constant (K, orange line) has a negative coefficient, showing a decrease in the future baseflow. On the linear regression equation of the trendline $y = -3E-06x + 0.9906$, 'x' is time (year) and 'y' is constant K (dimensionless).

4.4.2: Hypothetical "Natural" Baseflow Recession

The baseflow under a 'natural' condition is a hypothetical setting as if there have not been any groundwater withdrawals; we calculate this by adding withdrawals to the baseflow ($Q_t + W = Q_{t,natural}$). The null hypothesis of this section is that there is no significant difference between minimum baseflow (Q_t) under the 'impacted' and 'natural' conditions. The alternative hypothesis is that there is a significant difference between Q_t under the impacted and natural conditions. Here, I categorized the 'natural' condition into two groups with different estimations of future withdrawals: 1) In one case, the withdrawals from 2020 to 2069 would increase in proportion to the population growth. 2) In the other, the withdrawal would stay equivalent to that of 2019. In contrast, the baseflow under an 'impacted' condition was estimated from the existing streamflow data; the observed streamflow data and its baseflow portion was affected by the withdrawals ($Q_{t,impacted}$). The groundwater withdrawals on baseflow recession suggested has a significant impact in baseflow with the withdrawal effects (W) (Table 7).

4.4.3: Statistical Analysis on Groundwater Withdrawal Impact

4.4.3.1: Present Data Analysis (1945-2019)

The groundwater withdrawals in the study area of the Thurston County showed the baseflow recession from 1945 to 2019 (see section 4.3.1.3). The impact of withdrawals found from the two-sample Student's t-test between the $Q_{t,impacted}$ and $Q_{t,natur}$ showed the baseflow recession between 1945 and 2019 was significant (p-value < 2.2e-16, CI=95%) (Table 8. 3-B in the following section 4.4.3.2). The withdrawals comprised from 8 to 189 % of the minimum baseflow. This tells that almost double the amount of existing baseflow (i.e., 189%) was potentially lost as an impact of

groundwater withdrawal (Fig. 45). The decreasing minimum baseflow (Q_t) represented that baseflow contribution has lowered over time, which relates to the lack of the sole source of surface water recharge during dry season. The depletion of baseflow due to perpetuated groundwater withdrawal already started in the early 2000s (Fig. 45).

Figure 45

Minimum baseflow ($\boldsymbol{Q_t}$) and withdrawals (W) (1945-2019).

Baseflow Data separated from the streamflow data obtained from NWIS. Withdrawal data from Thurston County Water Planning.

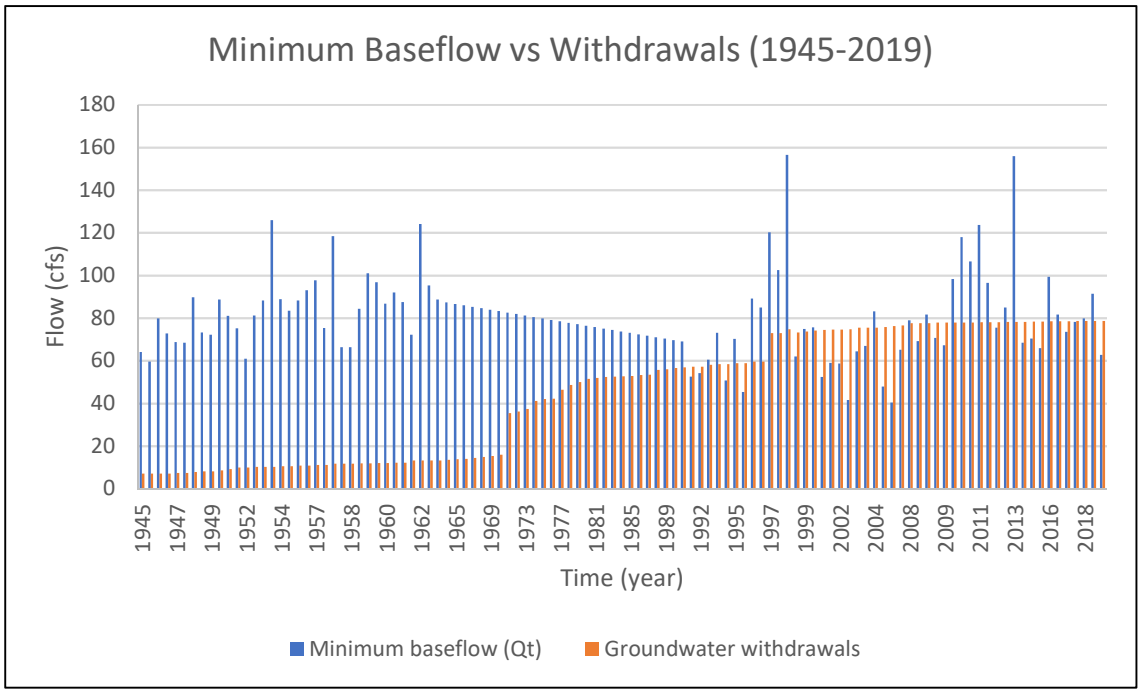

Note. The trend in past minimum baseflow contributions to the Deschutes Streamflow (blue column). During recession periods when withdrawals (orange column) exceeded baseflow (blue column), the baseflow was virtually eliminated from the streamflow, as evident from comparing two columns from early 2000s[62].

[62] An abrupt increase in the groundwater withdrawals (orange column) in early 1970s is most likely attributed to the transitioning in data management (explained in section 4.2.1)

4.4.3.2: Entire Period Analysis (1945-2069)

The future minimum baseflow of the natural scenario ($Q_{t,natural}$) versus the impacted scenario ($Q_{t,impacted}$) showed a substantial discrepancy in mean values in both the past (1945-2019) and the future (2020-2069) (Fig. 46). The mean of 'natural' baseflow ($Q_{t,natur}$) was 125 (cubic feet per second, cfs), while the mean of 'impacted' baseflow ($Q_{t,impacted}$) was 80 cfs. The difference of mean baseflows was more than a half of the mean of 'impacted' baseflow, which implied the impact of withdrawals was as much as half of the mean flow of the 'impacted' baseflow ($125 - 80 = 45; 45 > (\frac{80}{2} = 40)$).

Figure 46

Minimum baseflow ($\boldsymbol{Q_t}$) comparisons between the Impacted versus Natural scenarios.

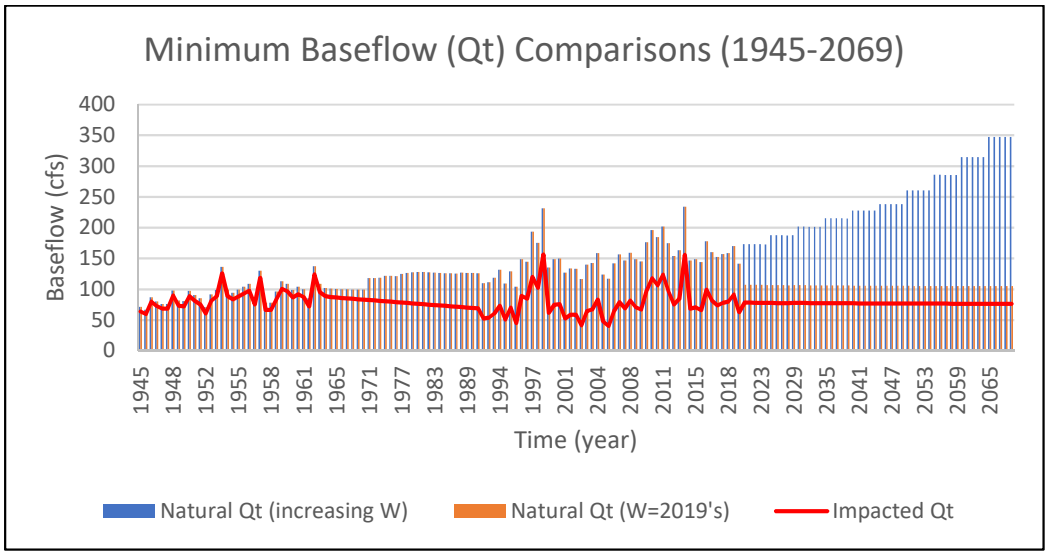

Note. The 'impacted' baseflow (Q_t) (red line) is compared against the two hypothetical 'natural' baseflow (Q_t) cases with increasing withdrawals (blue column) and constant withdrawal (orange column) values in the future[63].

[63] The estimated minimum baseflow under impacted, natural (with increasing withdrawal), and natural (fixed withdrawal at 2019's) are displayed in Appendix J.

The groundwater withdrawal was correlated with the present (1945-2019) and the projected future (1945 to 2069) baseflow recession. First, a two-sample Student's t-test on the minimum baseflow of the natural scenario of the present groundwater withdrawals ($Q_{t,natural}$) versus the impacted scenario without the withdrawals ($Q_{t,impacted}$) showed a significant difference in the mean baseflow (Model B: p-value < 2.2e-16, CI=95%, Fig. 47 and Table 8). The groundwater withdrawals in the Model B includes the increasing withdrawals that is proportional to the population growth in the past. The mean 'natural' baseflow ($Q_{t,natural}$, 1945-2019) was 125.2 cfs, while the mean 'impacted' baseflow ($Q_{t,natural}$, 1945-2019) was 80.1 cfs. This indicates that the minimum baseflow has been impacted over 45 cfs lost flow due to the past and present groundwater withdrawals from 1945 to 2019. This impact is over half of the mean flow of the impacted minimum baseflow ($Q_{t,impacted}$).

Second, a two-sample Student's t-test comparing the minimum baseflow of the future natural scenario ($Q_{t,natural}$) to the impacted scenario ($Q_{t,impacted}$) showed a significant difference in the mean baseflow (Model C: p-value < 2.2e-16, CI=95%, Fig. 47 and Table 8). The groundwater withdrawals in the Model C includes the increasing withdrawals that is proportional to the projected population growth. The mean 'natural' baseflow ($Q_{t,natural}$, 1945-2069) was 162.4 cfs, while the mean 'impacted' baseflow ($Q_{t,natural}$, 1945-2019) was 79.2 cfs. This indicates that the minimum baseflow has been impacted by 83.2 cfs ($162.4 - 79.2 = 83.2$) lost flow due to the past and present groundwater withdrawals from 1945 to 2019. The impact (83.2 cfs) is bigger than the mean impacted minimum baseflow ($Q_{t,natural}$, 1945-2069), which implies that the

baseflow influx would have doubled without withdrawals. The impact was between 110% and 190% of the estimated future baseflow (Table 8. 3-C).

Third, a two-sample Student's t-test comparing the minimum baseflow of the future natural scenario ($Q_{t,natural}$) to the impacted scenario ($Q_{t,impacted}$) showed a significant difference in the mean baseflow (Model D: p-value < 2.2e-16, CI=95%, Fig. 47 and Table 8). The groundwater withdrawals in the Model C includes the same amount of withdrawals in 2019, assuming the future groundwater withdrawal will remain the same amount as that of in 2019. The mean 'natural' baseflow ($Q_{t,natural}$, 1945-2019) was 119.1 cfs, while the mean 'impacted' baseflow ($Q_{t,natural}$, 1945-2019) was 79.2 cfs. This indicates that the minimum baseflow has been impacted by almost 40 cfs lost flow due to groundwater withdrawals from 1945 to 2019. The impact is about half of the mean flow of the impacted minimum baseflow ($Q_{t,impacted}$). A constant withdrawal rate at 2019 levels would still be more than 100% of the estimated baseflow discharge. This indicates that even in our more conservative case (model C), the impact could deplete the entire baseflow to the surface water. In conclusion, the groundwater withdrawal impact on the current and future baseflow recession from 1945 to 2069 was projected to reduce over half of the current baseflow given the constant withdrawals, and more than double the current baseflow given increasing withdrawals.

Figure 47

Two-sample Student's t-test analysis between Models

Model B: $Q_{t,impacted}$ vs $Q_{t,natural,\ \ increasing\ present\ W}$ (1945−2019)

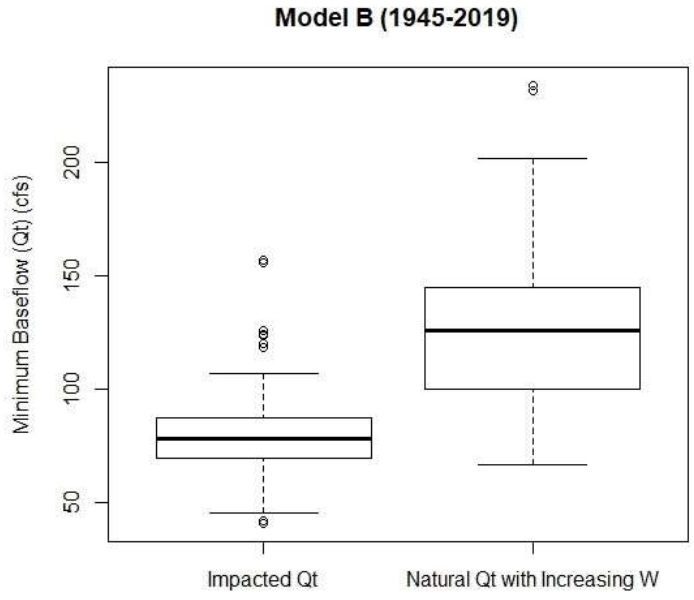

Model C: $Q_{t,impacted}$ vs $Q_{t,natural,\ \ increasing\ future\ W}$(1945−2069)

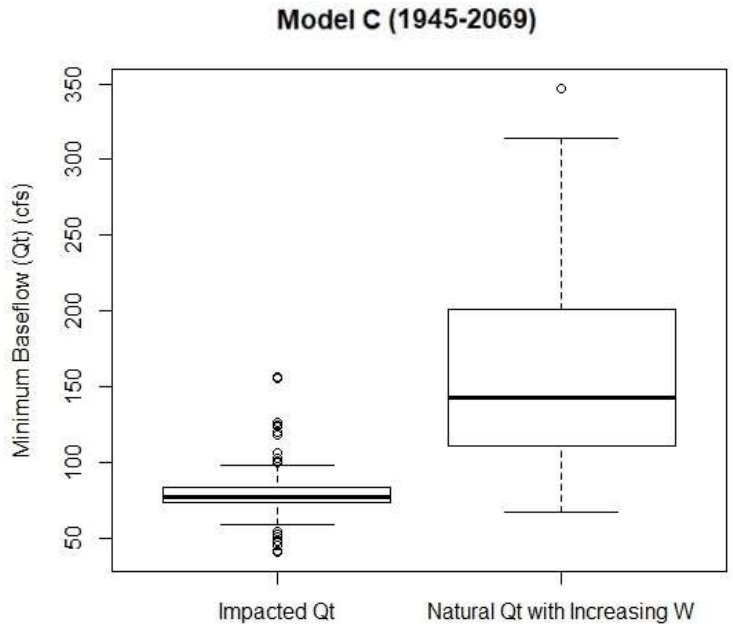

Model D: $Q_{t,impacted}$ vs $Q_{t,natural,\ fixed\ W=2019}$

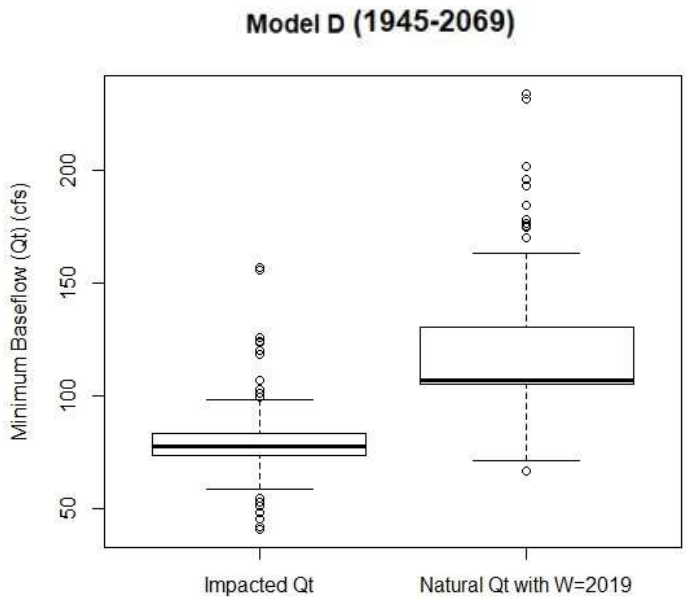

Table 8

*Statistical comparison between the minimum baseflow (Qt) under the Impac*ted scenario (model A) and Natural scenarios (model B, C, and D).

	A		B	C	D
	$Q_{\ t,impacted}$ (1945−2069)		$Q_{t,natural,W=increase}$ (1945−2019)	$Q_{t,natural,W=increase}$ (1945−2069)	$Q_{t,natural,W=2019}$ (1945−2069)
p-value			p < 2.2e-16	p < 2.2e-16	p < 2.2e-16
Mean (cfs)	80.1 (1945-2019)	79.2 (1945-2069)	125.2	162.4	119.1
% of W within Q_t[64]			8 ~ 189 % (mean 61 %)	110 ~ 191 % (mean 147 %)	100 ~ 103 % (mean 102 %)

Note. A: the impacted baseflow is the standard to which we compared three other models of B, C, and D. B: hypothetical "natural" baseflow scenario between 1945 and 2019, with increasing withdrawals proportional to population growth. C: hypothetical "natural" baseflow scenario between 1945 and 2069 with increasing withdrawals proportional to population growth. D: hypothetical "natural" baseflow scenario with the 2019 withdrawal rate held constant into the future (2020-2069).

[64] The ratio of withdrawals to the minimum baseflow (Qt) is in Appendix K.

4.5: Environmentally Critical Baseflow (ECB)

4.5.1: Future Baseflow Recession and Ecological Threshold

Environmentally critical baseflow (ECB) identifies when the impact of groundwater withdrawals finally interrupts the baseflow inflow. Once the amount of groundwater withdrawal reaches or exceeds a certain threshold (i.e., ECB) required to sustain riverine ecology, summer flows when the river rely on baseflow the most is considered at risk. Determining the time at which the groundwater withdrawals will exceed the ECB provides a temporal perspective of the impact of groundwater pumping. This is a different approach to project the level of future baseflow recession from the baseflow recession analysis (section 4.3; 4.4).

I projected that the impacted future baseflow trend would be exceeded by ecological thresholds, ECB, during low flow periods. The future baseflow was estimated by the forecast function and was compared against the 90% of the exceedance probability that occur 90% of a given period, or Q90[65]. The 90% of the Q90 indicates the minimum threshold to sustain a healthy ecological function.

I used the analyzed baseflow estimation from Model A of the baseflow recession analysis for the 'future baseflow' data (Table 8). The Model A includes baseflow estimation with the impact of groundwater withdrawals, necessary to assess the ecological function in the future by comparing it against the ECB.

[65] The 'Q' symbol used here represents a low flow parameter, not the 'baseflow' or 'groundwater discharged as I used in previous sections for the baseflow recession analysis.

4.5.2: Different Estimation and Interpretation of ECB

To assess whether future baseflow may fall under the threshold, different techniques to estimate the ECB were used. In method 'median', I used the median value of the past ECB value (1945-2019) and used it as the ECB in the future (2020-2069). In method 'mode', I used the most frequently emerging value of the past ECB (1945-2019) as the future ECB (2020-2069). In method 'forecast', I used the forecast function (Microsoft Office, n.d.) to project the future ECB (2020-2069) from the past (1945-2019) ECB levels. These three methods will estimate the future trend of ECB that we can determine whether the future Q_t will fall below the ECB.

First, with the ECB estimated by the median value of ECB levels between 1945 and 2019 (63 cfs) (method 'median'), the future baseflow did not fall under the ECB levels (Fig. 48, green line). Second, with the ECB estimated by the mode value of ECB levels in the past (70 cfs) (method 'mode'), the future baseflow did not fall below under ECB levels (Fig. 48, orange line). Third, however, we projected that the forecasted ECB levels would exceed the estimated baseflow (Fig. 48, yellow line). The forecasted value of ECB levels based on the past ECB levels (method 'forecast') showed a slight increase near the 2060s. This may be due to varied trend of the past ECB level on which the future series relies and projects the future dataset. The first year when minimum baseflow (Q_t) is projected to exceeded by the ECB at least for 2 years was 2061, when baseflow will reach 77.75 cfs, which is about 2 cfs lower than the mean minimum baseflow of 79.19 cfs. Combined with the perpetuated recession, the baseflow on 2061 will be exceeded by an ecological threshold, or ECB.

Figure 48

Future Impacted baseflow and ECB (mode, mean, and forecasted of the past records).

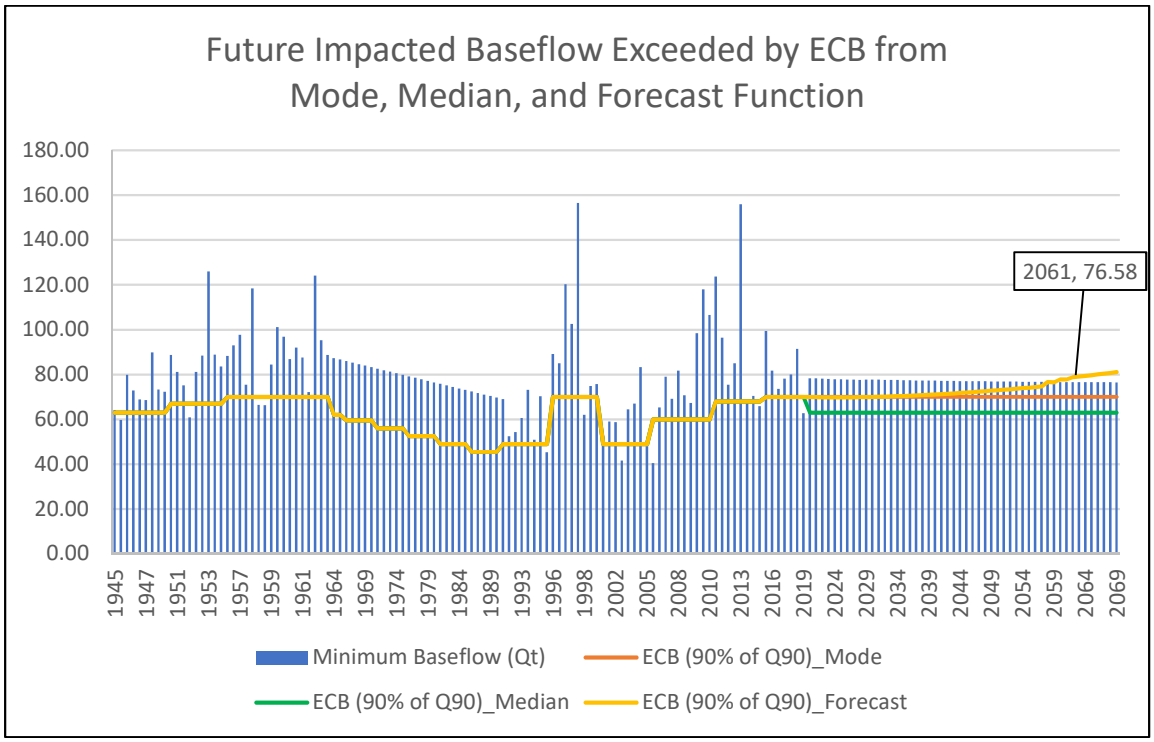

Note. Future estimations on the minimum baseflow (Q_t, blue column) from the mode (orange line), median (green line), and forecasted (yellow line) past ECB records. Compared to the forecasted future ECB (yellow line), the Q_t at 2061 is exceeded by the ECB, falling below the ecological threshold.

Two estimations (method 'median' or 'mode') showed different results for future baseflow falling below the ecological threshold, or ECB. Also, the pattern or trend of future baseflow fluctuation was rather flat (less variant than the method 'forecast'). This can change as the baseflow trends in the past shows high variability; the future baseflow may fall under the ECB estimations.

Chapter 5: Discussion, Limitations & Suggestions, Conclusion

This paper finishes with discussion, limitations and suggestions, and a conclusion. In the Discussion section, I interpret the significance of the results and explain their implications in relation to the theoretical framework addressed in section 2.5.2. In the Limitations and Suggestions section I address the limitations of the study and suggest future research to enhance the applicability and validity of this research. Finally, I summarize and offer concluding remarks.

5.1: Discussion

This study demonstrated a correlation between groundwater withdrawals via well pumping and the baseflow recession in the Deschutes River. Statistically, the baseflow recession had a high correlation with the estimated groundwater withdrawals as shown in section 4.4.2.1. The yearly groundwater withdrawal has increased more than tenfold in the past 75 years (1945-2019), which implicated potentially reduced groundwater storage. Such a decrease in groundwater showed lower streamflow as the deficit in groundwater will lead to less baseflow input to the surface flow. An exponential increase of groundwater withdrawals over time worked as a strong driver of baseflow recession, as pumping extracts a large amount of groundwater and intercepts the groundwater flow, lowering the groundwater table.

This study focused on the minimum baseflow of each recession period (Q_t) between the 'natural' versus 'impacted' scenarios (see section 3.3.2.4). I defined the 'natural' baseflow to be a hypothetical status with no groundwater withdrawals. In this

case, the withdrawal (W) is added to the measured baseflow, which was separated from the existing streamflow data via the web-based hydrograph analysis tool (WHAT). The 'impacted' baseflow, without added withdrawals, showed a noticeable reduction compared to the 'natural' baseflow starting in the 1970s. This coincided with an abrupt increase of recorded groundwater withdrawals in 1971 due to a shift in well-log management (see section 4.2.1). In conclusion, the significant difference in the minimum baseflow of the 'impacted' versus 'natural' scenario indicates that decreased baseflow influx has reduced the minimum baseflow (Q_t) level over time. This raises concerns about whether the baseflow may remain at a sustainable level to support the riverine ecosystem of the Deschutes River stream in dry seasons, which rely heavily on baseflow. Therefore, the decreasing minimum baseflow (Q_t) has an ecological implication on the low flow period.

The overall decrease of baseflow influx during dry seasons is supported by other indicators, including recession constant (K) for each recession period (t). The recession period has increased over time between 1945 to 2019 (section 4.4.1). A longer recession period indicates that baseflow reduction periods are longer than in the past, which potentially addresses drier and lower flow in recent summers than in the past. The dry months of June to October in future years are expected to become drier due to climate change; with longer recession periods, there will be more days with less baseflow input. The longer recession period (t) indicates added stress on aquatic species relying on areas with lower flow, higher stream temperature, and degraded water quality (section 2.5.5.1.1). Additionally, the decreasing trend of recession constant (K) supports lower baseflow and drier streams (section 4.4.1). The baseflow recession constant lets us

predict the amount of baseflow recession in the future. Baseflow is projected to decline, yielding less surface streamflow during dry periods.

The maximum baseflow at the beginning of each recession period (Q_0) showed an increase between 1945 and 2019 (Fig. 36). This suggests that the streamflow is higher in recent years than the past, potentially due to extreme precipitation events and climate change which produced higher flow in the river. The maximum baseflow (Q_0), at the beginning of each recession period, has become higher than before, meaning the baseflow after precipitation in the study period (June-October) has increased. This may be due to the higher variability of Q_0 values in later years (1991-2019) than in the early years (1945-1964). Also, the precipitation pattern in early summer (April, May) and the intermittent rainfall during dry seasons (June-October) might have positively affected the increase in higher baseflow input at the beginning of recessions. Baseflow is highly affected by the amount of precipitation as rainfall recharges the surface water, which then replenishes the groundwater and increases the potential baseflow. This shows the effect of climate change and extreme precipitation patterns on the baseflow in the Pacific Northwest.

More importantly, the relationship between the maximum (Q_0) and minimum baseflow (Q_t) under the impact of groundwater withdrawals (Model A) showed that recession has increased more in recent years than in the past. The gap between Q_0 and Q_t has grown greater over time, as the maximum baseflow increased while the minimum baseflow decreased. This shows a growing gap in the actual level of the recession, indicating less baseflow input in recent years and potentially in the future. On the other hand, the decreasing trend of the minimum baseflow (Q_t) happened even though the

maximum baseflow (Q_0) showed an increasing trend. This indicates that the effect of precipitation recharging surface water and groundwater systems might happen more slowly, until it cannot compensate for reduced groundwater and baseflow input on the stream. As a groundwater deficit lowers surface flow, there is a delayed impact because groundwater in an aquifer must travel between sedimentary pores (see section 2.6.2). The groundwater deficit can reach a level threatening significantly reduced baseflow contribution before surface flow shows a depletion (see section 2.8.3). Therefore, the increasing gap between the maximum (Q_0) and minimum baseflow (Q_t) in a recession period is a salient parameter to assess the groundwater-surface water relationship.

The future baseflow recession in the Deschutes, estimated from the linear model, is projected to reach or exceed the environmentally critical baseflow (ECB) level in 2061 (see section 4.5.2). The year in which future minimum baseflow (Q_t) may exceed the ECB depends on the method of determining the ECB. The future Q_t fell below the forecasted ECB in year 2061, while it was not reached when determined with either the mode or the median of the past ECB records. Despite these differences in ECB projections, the future minimum baseflow (Q_t) shows a consistent decrease and approaches the ECB values estimated from the all three methods. Continued future baseflow recession causes groundwater deficits due to withdrawals, and threatens the ecological function of groundwater, which the Deschutes relies on to recharge surface water in low flow periods. Overall, estimating the time when decreasing baseflow exceeds the ECB offers a temporal perspective on how early the Deschutes may face the degraded function of the baseflow recession. This has implications for management of groundwater deficits and withdrawal practices.

5.2: Limitations and Suggestions

There are two limitations of this study related to 1) defining the 'impacted' and 'natural' baseflow and 2) determining the level of an ecological function via the environmentally critical baseflow (ECB). First, the past baseflow recession trend showed a relatively gradual and small decrease compared to the extent of withdrawals. Though there was a tenfold increase of groundwater withdrawal over 75 years, the minimum baseflow (Q_t) did not decrease tenfold (Fig. 45). The difference between groundwater withdrawals and the baseflow recession could be attributed to the difference time between pumping and the groundwater traveling within the aquifer. For example, the 'natural' baseflow scenario assumes the amount of groundwater "impacted" or "lost" would have remained in the aquifer if there was no pumping occurred. Some of this "lost" groundwater could have discharged to the surface water in the form of baseflow gradually travelling vertically through the aquifer. Therefore, the impact of such lost groundwater could be more accurately calculated using the vertical hydraulic traveling time, rather than the withdrawal amount itself. This vertical movement relates to the concept of "hydraulic conductivity" in a permeable porous aquifer by using the hydraulic gradient (Sinclair & Bilhimer, 2007). Therefore, the actual impact of annual groundwater withdrawal would be more in a distributed form rather than an instant total withdrawal, resulting in a much smaller impact of "lost" groundwater in each recession period. Even though the total amount of impact or withdrawal may increase (as described in section 4.2.1), the hydraulic gradient and conductivity will delay the flow. I did not include the impact of hydraulic conductivity on groundwater withdrawals (Sinclair & Bilhimer, 2007). With a further study, the yearly impact from withdrawals could be estimated with

the consideration of the hydraulic conductivity. To that end, the hydraulic conductivity would adjust the withdrawal amount with the hydrogeologic consideration of groundwater movement within the aquifer.

Second, the unique value of the environmentally critical baseflow (ECB) at which the healthy ecological function is maintained should be assessed for the Deschutes River. Derived from the environmentally critical streamflow (ECS), the ECB was used to demonstrate whether the river maintained a minimum streamflow from the baseflow contribution. While ECB could be a substitute for the ECS during the dry season, when baseflow comprises most of the surface flow (see section 2.3.3), the ECB estimation has not been tested for potential errors. Additionally, this research introduced the concept of the ECB adopted from the ECS. The low flow parameter in Washington State utilizes the 7-day, 10-year ($Q_{7,10}$) method, which is different from the $Q90$ applied to calculate the ECS and ECB. Therefore, further research on validating the low flow parameter to determine the value for the ECS and ECB would clarify the standard by which the future baseflow can be compared and assessed.

5.3: Conclusion

The impact of groundwater withdrawals on baseflow recession during low flow periods has become a major element in streamflow changes. The two research questions in this work assessed the impact of groundwater withdrawal on baseflow recession in the past and the future of the Deschutes River, WA. A quantitative analysis using the baseflow recession constant attempted to explain and predict baseflow recession trends,

which were then used to assess the sustainable and ecological function of the river in the future.

The methods employed in this research explored an association between baseflow recession and a variety of variables. The main variable, groundwater withdrawal (W), showed an impact on the baseflow recession via statistical testing (two-sample Student's t-test). Other variables such as recession constants (K for a linear model and a for a nonlinear model), maximum baseflow at the beginning of recession periods (Q_0), and time (t) fitted to baseflow trends. Additionally, the baseflow recession analysis from 1945 to 2019 required assessment of the ecological function of the stream using a threshold ('environmentally critical baseflow', or 'ECB'). Different methods to determine the ECB produced different results for the time when the future baseflow recession fall below the ecological threshold. ECB predicted from one method (forecast function) indicated the river cannot sustain a minimum flow to sustain the riverine ecosystem as the baseflow input weakens with less groundwater storage. Two other methods to estimate the ECB (using the mode and the median from the past ECB trend) showed less baseflow recession. Regardless of the different methods, future baseflow was predicted to decline.

The method to compare and assess the groundwater withdrawals on the baseflow recession extend the theoretical framework presented in section 3.3.2.4.1. In the literature, the 'impacted' baseflow subtracts withdrawals from baseflow ($W \neq 0, W \leq 0$) while the 'natural' baseflow does not incorporate the withdrawals ($W = 0$). In contrast, this research considered the 'impacted' baseflow as the existing baseflow from measured streamflow (W not included in the baseflow recession equation: equation 7, 9), and

estimates for the 'natural' baseflow assumed that there were no groundwater withdrawals ($W \geq 0$: equation 14-1, 14-2). This inverted perspective facilitated our estimation of the impact of groundwater withdrawals on the baseflow.

This research analyzed the baseflow recession phenomenon in association with the impact of groundwater withdrawals and the ecological function of the streamflow. The first research section (Ch 4.4) assessed the correlation between groundwater withdrawal and baseflow recession on the lower Deschutes River streamflow. The second research section (Ch. 4.5) revealed that perpetuated baseflow recession in the future may threaten the ecological function to sustain the riverine ecosystem. One ECB estimate predicted the baseflow recession would exceed baseflow discharge in the year 2061, indicating that low flow in the stream would not likely sustain ecological status. These two findings demonstrated that current practices of groundwater pumping deserve our attention regarding sustainable streamflow in the present and future.

In order to properly analyze the impact of groundwater withdrawal, a more accurate baseflow model is needed. The anthropogenic impact of withdrawals should account for the hydrogeologic characteristics of different aquifers, using the hydrologic traveling time of withdrawals through the hydraulic conductivity of the aquifer. Additionally, the findings of this research related to the second research question could be improved with a more accurate estimation of the impact on the baseflow. This highlights the need for successive research on modeling the impact of withdrawal on baseflow in time, and the capacity to predict the impacted streamflow in the future.

The findings of this research suggest that we should be more cautious with the quantity of water in relation to the quality of the Deschutes River stream. The

anthropogenic impact of groundwater withdrawals has become a major element in groundwater depletion and streamflow alterations. This work intends to bridge the influenced groundwater system and the streamflow on the surficial level via baseflow recession. Future studies on groundwater management should build upon our findings to help us further understand the impact of current groundwater appropriation on the sustainable baseflow contribution to the surface water. This can help researchers, groundwater resource managers, and environmentalists adapt analyses and policies to the river's ecological values and functions for future groundwater resource management. That can move us closer toward intergenerational sustainability in streamflow management to preserve the instream values of the Deschutes River for future generations.

Chapter 6: References

Washington State Office of the Attorney General (AGO). Water-Water Rights-Wells-Status in water rights system of exempt groundwater withdrawals. AGO 1997 No. 6-Oct 10, 1997. *Attorney General Christine Gregoire.* Retrieved from https://www.atg.wa.gov/ago-opinions/water-water-rights-wells-status-water-rights-system-exempt-ground-water-withdrawals

Anderson, B., Anderson, C., Christensen, D., Inman, R., & Marti, J. 2015 Drought Response Summary Report, 16-11-0012015 (2016). Olympia, WA.

Barlow, P.M., and Leake, S.A., 2012, Streamflow depletion by wells—Understanding and managing the effects of groundwater pumping on streamflow: U.S. Geological Survey Circular 1376, 84 p. Retrieved from http://pubs.usgs.gov/circ/1376/

Bayen, A. M., & Siauw, T. (2015). Interpolation. *An Introduction to MATLAB® Programming and Numerical Methods for Engineers*, 211–223. doi: 10.1016/b978-0-12-420228-3.00014-2

Bilhimer, D. (2014). Surface Water Quality Standards for rivers and streams within the Deschutes River TMDL boundary. [ESRI ArcGIS Map Layer]. *Washington State Department of Ecology Water Quality Program*. Retrieved from http://services.arcgis.com/6lCKYNJLvwTXqrmp/arcgis/rest/services/Deschutes_SWQS_v2/FeatureServer

Bracken, N. (2010). Exempt Well Issues in the West, *Environmental Law,* Vol. 40:1. Retrieved from https://law.lclark.edu/live/files/4541-40-1bracken

Brutsaert, W., and Nieber, J. L. (1977), Regionalized drought flow hydrographs from a mature glaciated plateau, *Water Resource. Res.*, 13(3), 637– 643, doi:10.1029/WR013i003p00637.

Chapter 173-513 WAC. (1988).

Chapter 246-291 WAC. (March 27th, 2014). Group B Public Water System.

City of Bellevue Utilities. (n.d.). Water Source. Retrieved from https://bellevuewa.gov/city-government/departments/utilities/manage-your-utility-services/water/water-source

City of Tacoma GIS. (2019). *Geology (WADNR)* [ESRI ArcGIS Map Layer]. Washington Division of Geology and Earth Resources. Retrieved from https://gis.dnr.wa.gov/site1/rest/services/Public_Geology/WADNR_PUBLIC_WGS_Surface_Geology/MapServer

Conservation, T., & Lead, D. (2004). Salmon Habitat Protection and Restoration Plan for Water Resource Inventory Area 13. July.

Curran, C. A., Eng, K., & Konrad, C. P. (2012). Analysis of Low Flows and Selected Methods for Estimating Low-Flow Characteristics at Partial-Record and Ungaged Stream Sites in Western Washington. 56.

Dieter, C.A., Maupin, M.A., Caldwell, R.R., Harris, M.A., Ivahnenko, T.I., Lovelace, J.K., Barber, N.L., and Linsey, K.S., 2018, Estimated use of water in the United States in 2015: *U.S. Geological Survey* Circular 1441, 65 p., https://doi.org/10.3133/cir1441. [Supersedes USGS Open-File Report 2017–1131.]

Washington State Department of Ecology (DoE). (n.d.). Well Construction and Licensing Search Tools. History of the Well Report (Well Report). https://appswr.ecology.wa.gov/wellconstruction/map/WCLSWebMap/siteinformation.aspx#hire

Washington State Department of Ecology (DoE). (2010). An Overview of the Instream Flow Incremental Methodology (IFIM). *Water Resources Program.* Retrieved from https://fortress.wa.gov/ecy/publications/documents/qwr95104.pdf

Washington State Department of Health (DoH). (2018, September). Design Information for New and Expanding Group B Water Systems. *Group B Water System Design Guidelines.* https://www.doh.wa.gov/Portals/1/Documents/Pubs/331-467.pdf

Dorney, J., & Russell, P. (2018). North Carolina Division of Water Quality Methodology for Identification of Intermittent and Perennial Streams and Their Origins. *Wetland and Stream Rapid Assessments*, 273–279. doi: 10.1016/b978-0-12-805091-0.00014-1

Douglas, T. (2006). Review of groundwater-salmon interactions in British Columbia. November, 19. Retrieve from https://www.watershed-watch.org/publications/files/Groundwater+Salmon++hi+res+print.pdf

United States Environmental Protection Agency [EPA]. (2016, December 22). Climate Impacts in the Northwest. Retrieved from https://19january2017snapshot.epa.gov/climate-impacts/climate-impacts-northwest_.html

United States Environmental Protection Agency [EPA]. (2018, October 19). Definition and Characteristics of Low Flows. Retrieved February 21, 2020, from https://www.epa.gov/ceam/definition-and-characteristics-low-flows

United States Environmental Protection Agency [EPA]. (n.d.). Overview of Total Maximum Daily Loads (TMDLs). Retrieved April 18, 2020, from https://www.epa.gov/tmdl/overview-total-maximum-daily-loads-tmdls

United States Environmental Protection Agency [EPA]. (2018, August 20). How Your Septic System Works. Retrieved February 20, 2020, from https://www.epa.gov/septic/how-your-septic-system-works

Essington, T., Klinger, T., Conway-Cranos, T., Buchanan, J., James, A., Kershner, J., Logan, I., West, J. (2010). The Biophysical Condition of Puget Sound. *Puget Sound Science Review.* Retrieved from https://www.eopugetsound.org/science-review/biophysical-condition-puget-sound-physical-environment

Famiglietti, J. The global groundwater crisis. *Nature Clim Change* 4, 945–948 (2014). https://doi.org/10.1038/nclimate2425

FORECAST.ETS function. (n.d.). Retrieved January 26, 2020, from https://support.office.com/en-us/article/forecast-ets-function-15389b8b-677e-4fbd-bd95-21d464333f41.

Gan, R., & Luo, Y. (2013). Using the nonlinear aquifer storage–discharge relationship to simulate the baseflow of glacier- and snowmelt-dominated basins in northwest China. *Hydrology and Earth System Sciences*, *17*(9), 3577–3586. doi: 10.5194/hess-17-3577-2013

Georgiadis, Nicholas. (2018). Are low flows changing in Puget Sound streams?. *University of Washington Puget Sound Institute; Encyclopedia of Puget Sound*.

Gleeson T, Richter B. How much groundwater can we pump and protect environmental flows through time? Presumptive standards for conjunctive management of aquifers and rivers. *River Resource Applic.* 2018; 34:83–92. https://doi.org/10.1002/rra.3185.

Gleick, P. H., 1996: Water resources. In Encyclopedia of Climate and Weather, ed. by S. H. Schneider, *Oxford University Press, New York, vol. 2, pp. 817-823.*

Golder Associates. (2015). Technical Memorandum. Johns Creek Tributary Area and Predictive Scenarios.

de Graaf, I.E.M., Gleeson, T., (Rens) van Beek, L.P.H. *et al.* Environmental flow limits to global groundwater pumping. *Nature* 574, 90–94 (2019) doi:10.1038/s41586-019-1594-4.

de Graaf, I.E.M., van Beek, L.P.H., Wada, Y., Bierkens, M.F.P., 2014. Dynamic attribution of global water demand to surface water and groundwater

resources: Effects of abstractions and return flows on river discharges. Adv. *Water Resour.* 64, 21–33. https://doi.org/10.1016/j.advwatres.2013.12.002

Grannemann, N.G., Hunt, R.J., Nicholas, J.R., Reilly, T.E., Winter, T.C. (2000). The Importance of Ground Water in the Great Lakes Region. U.S. Geological Survey. Water-Resources Investigations Report 00-4008. Retrieved from https://pubs.usgs.gov/wri/wri00-4008/pdf/WRIR_00-4008.pdf

Gustard, Alan., Tallaksen, Lena. (2008). Chapter 2. Estimating, Predicting, and Forecasting Low Flows. Manual on Low-flow Estimation and Prediction. *World Meteorological Organization*.

Hall, F. R. (1968), Base-Flow Recessions—A Review, *Water Resource. Res.*, 4(5), 973– 983, doi:10.1029/WR004i005p00973.

Hamlet, A.F. 2010. Assessing water resources adaptive capacity to climate change impacts in the Pacific Northwest region of North America. *Hydrology and Earth System Sciences* 7(4): 4437-4471, doi:10.5194/hessd-7-4437-2010.

Hansen, K. (2018). Methods Used to Calculate the Pumping Rates, Locations and Open Intervals of Active Groundwater Wells in Thurston County, Washington. *Thurston County Water Resources Technical Memorandum #8.*

Hayashi, Masaki & Rosenberry, Don. (2002). Effects of Ground Water Exchange on the Hydrology and Ecology of Surface Water. *Ground water*. 40. 309-16. 10.1111/j.1745-6584.2002.tb02659.x.

Hydrology Report No. 50. Retrieved from http://www.wmo.int/pages/prog/hwrp/publications/low-low_estimation_prediction/WMO%201029%20en.pdf

Kimbrough, R.A., Ruppert, G.P., Wiggins, W.D., Smith, R.R., Kresch, D.L. (2005). Water Resources Data-Washington Water Year 2005. *U.S. Geological Survey Water Data Report* WA-05-1. Retrieved from https://pubs.usgs.gov/wdr/2005/wdr-wa-05-1/

Kavanaugh, R. (1980). Deschutes River Basin Instream Resources Protection Program including Proposed Administrative Rules (Rater Resource Inventory Area 13). *Water Resource Policy Development Section Washington State Department of Ecology.* Retrieved from https://fortress.wa.gov/ecy/publications/documents/80irpp13.pdf

Konikow, L.F., 2013, Groundwater depletion in the United States (1900−2008): U.S. Geological Survey Scientific Investigations Report 2013−5079, 63 p., http://pubs.usgs.gov/sir/2013/5079.

Kormos, P. R., Luce, C. H., Wenger, S. J., & Berghuijs, W. R. (2016). Trends and sensitivities of low streamflow extremes to discharge timing and magnitude in Pacific Northwest mountain streams. *Water Resources Research*, *52*(7), 4990–5007. https://doi.org/10.1002/2015WR018125

Lambert, J. (2019, October 9). Too much groundwater pumping is draining many of the world's rivers. *Science News*. Retrieved from https://www.sciencenews.org/article/too-much-groundwater-pumping-draining-many-earth-rivers

Lane, R.C., and Welch, W.B., 2015, Estimated freshwater withdrawals in Washington, 2010: U.S. Geological Survey Scientific Investigations Report 2015-5037, 48 p., http://dx.doi.org/10.3133/sir20155037.

Luce, C. H., Abatzoglou, J. T., & Holden, Z. A. (2013). The Missing Mountain Water: Slower Westerlies Decrease Orographic Enhancement in the Pacific Northwest USA. *Science*, *342*(6164), 1360–1364. doi: 10.1126/science.1242335

Luce, C. H. and Z. A. Holden. 2009. Declining annual streamflow distributions in the Pacific Northwest United States, 1948-2006. *Geophysical Research Letters 36.*

Mazur, D. R. (2010). Combinatorics: a guided tour. Washington, DC: Mathematical Association of America.

Microsoft Office. (n.d.). FORECAST.ETS function. Retrieved May 11, 2020, from https://support.microsoft.com/en-us/office/forecast-ets-function-15389b8b-677e-4fbd-bd95-21d464333f41r

Miller, M. P., Buto, S. G., Susong, D. D., and Rumsey, C. A. (2016), The importance of base flow in sustaining surface water flow in the Upper Colorado River Basin, *Water Resour. Res.*, 52, 3547– 3562, doi:10.1002/2015WR017963.

National Water Information System: Web Interface. (2015). USGS Water Use Data for Washington. Retrieved February 20, 2020, from https://waterdata.usgs.gov/wa/nwis/wu

NOAA. (n.d.). What does anadromous mean? Retrieved March 28, 2020, from https://www.fisheries.noaa.gov/node/8071

Nolan, K., & Hill, B. (1990). Storm-runoff generation in the Permanente Creek drainage basin, west central California — An example of flood-wave effects on runoff composition. *Journal of Hydrology*, *113*(1-4), 343–367. doi: 10.1016/0022-1694(90)90183-x

Onajite, E. (2014). Seismic Data Analysis Techniques in Hydrocarbon Exploration. Waltham: Elsevier.

Population Forecast: 2010-2040: Washington Office of Financial Management (OFM) medium series forecast for Thurston County, 2012. 2045 - TRPC's extrapolation of OFM's forecast. Retrieved from https://ofm.wa.gov/sites/default/files/public/legacy/pop/gma/projections12/GMA_2012_county_pop_projections.pdf

Office of the Washington State Climatologist [OWSC]. (2009). Drought-like Conditions in Washington. Retrieved February 21, 2020, from https://climate.washington.edu/events/2009drought/

Osborn, R. P. (2013). Native American Winters Doctine and Stevens Treaty Water Rights: Recognition, Quantification, Management. *American Indian Law Journal.* Vol 2, Issue 1.

Panza, C., Manetti, S., & Brunelli, A. (2015). "Venir meno" ovvero una sincope. In *Quaderni ACP* (Vol. 22, Issue 1).

Pelto, M.S. (2011). Skykomish River, Washington: impact of ongoing glacier retreat on streamflow. *Hydrol Process* 25:3356—3363. Doi: 10.1002/hyp.8218

Pitz, C. F. (2016). Predicted Impacts of Climate Change on Groundwater Resources of Washington State. Washington State Department of Ecology. No. 16-03-006. https://fortress.wa.gov/ecy/publications/documents/1603006.pdf

Poole, G.C. and Berman, C.H. (2001) An Ecological Perspective on in-Stream Temperature: Natural Heat Dynamics and Mechanisms of Human-Caused Thermal Degradation. *Environmental Management*, 27, 787-802. http://dx.doi.org/10.1007/s002670010188

Rasmussen, P. (2014). What happened to the Steh-chass people?

Roberts, Mindy., Ahmed, Anise., Pelletier, Greg., Osterberg, David. (2008). Deschutes River, Capitol Lake, and Budd Inlet Temperature, Fecal Coliform Bacteria, Dissolved Oxygen, pH, and Fine Sediment Total Maximum Daily Load Water Quality Study Findings (Issue 09).

Roberts, M., A. Ahmed, G. Pelletier, and D. Osterberg. (2012). Deschutes River, Capitol Lake, and Budd Inlet Temperature, Fecal Coliform Bacteria, Dissolved Oxygen, pH, and Fine Sediment Total Maximum Daily Load Technical Report: Water Quality Study Findings. Publication No. 12- 03-008. Washington Department of Ecology. Olympia, WA

Rounds, S.A., Wilde, F.D., and Ritz, G.F. (2013). Dissolved oxygen (ver. 3.0). *U.S. Geological Survey Techniques of WaterResources Investigations*, book 9, chap. A6, sec. 6.2, http://water.usgs.gov/owq/FieldManual/Chapter6/6.2_v3.0.pdf.

Rumsey, CA, Miller, MP, Schwarz, GE, Hirsch, RM, Susong, DD. The role of baseflow in dissolved solids delivery to streams in the Upper Colorado River Basin. *Hydrological Processes*. 2017; 31: 4705– 4718. https://doi.org/10.1002/hyp.11390

Rupp, D. E., and J. S. Selker (2006), On the use of the Boussinesq equation for interpreting recession hydrographs from sloping aquifers, *Water Resource. Res*., 42, W12421, doi:10.1029/2006WR005080.

Schuster, E.J. (2005). Geologic Map of Washington State. Washington Division of Geology and Earth Resources Geologic Map GM-53. Retrieved from https://people.wou.edu/~taylors/g492/WA_geo_explain.pdf

Sinclair, K., Pitz, Charles. (1999). Estimated Baseflow Characteristics of Selected Washington Rivers and Streams. *Washington State Department of Ecology.* http://www.wa.gov/ecology/biblio/99327.html

Singh, T., Wu, L., Gomez-Velez, J. D., Lewandowski, J., Hannah, D. M., & Krause, S. (2019). Dynamic Hyporheic Zones: Exploring the Role of Peak Flow Events on Bedform-Induced Hyporheic Exchange. *Water Resources Research*, *55*(1), 218–235. doi: 10.1029/2018wr022993

Smith, A. (2010). Runoff Processes. Retrieved from http://portal.chmi.cz/files/portal/docs/poboc/CB/runoff_cz/print.htm

Stieglitz T. (2011) Submarine Groundwater Discharge. In: Hopley D. (eds) Encyclopedia of Modern Coral Reefs. Encyclopedia of Earth Sciences Series. Springer, Dordrecht

Stuckey, M.H., 2006, Low-flow, base-flow, and mean-flow regression equations for Pennsylvania streams: U.S. Geological Survey Scientific Investigations Report 2006-5130, 84 p.

Shane Cherry Consulting. (2015). DESCHUTES RIVER COHO SALMON Biological Recovery Plan Prepared for: Squaxin Island Tribe Natural Resources Department. Retrieved from http://blogs.nwifc.org/psp/files/2017/12/Deschutes-Coho-Recovery-Plan.pdf

Tallaksen, A review of baseflow recession analysis, Journal of Hydrology, Volume 165, Issues 1–4, 1995, Pages 349-370, ISSN 0022-1694, https://doi.org/10.1016/0022-1694(94)02540-R.

Thomas, B. F., Vogel, R. M., Kroll, C. N., and Famiglietti, J. S. (2013), Estimation of the baseflow recession constant under human interference, *Water Resource. Res.*, 49, 7366– 7379, doi:10.1002/wrcr.20532.

Thurston County Community Planning & Economic Development (TCCP). (2018). State Mandated Well Form. Retrieved from https://www.thurstoncountywa.gov/planning/planningdocuments/water-State-Mandated=Well-Form-02.13.18.pdf

Thomas, B. F., Vogel, R. M., & Famiglietti, J. S. (2015). Objective hydrograph baseflow recession analysis. *Journal of Hydrology*, *525*, 102–112. doi: 10.1016/j.jhydrol.2015.03.028

Thurston Regional Planning Council [TRPC]. (2015). Deschutes Watershed Land Use Analysis: Current Conditions Report. Retrieved from https://www.co.thurston.wa.us/planning/watershed/docs/deschutes-project-materials/deschutes-current-conditions-report.pdf

Thurston County. (2017). 2017 Water Year Report. April 2018. Retrieved from https://www.thurstoncountywa.gov/sw/swmonitoringdocuments/Water%20Year%202017%20Final%20Report.pdf

Thurston County. (2017). Wellhead Protection Program. Retrieved from https://www.co.thurston.wa.us/health/ehhw/wellhead_prot.html

Thurston Regional Planning Council [TRPC]. (2019). *Population Forecast Allocations*. *June*.

Population, Housing & Employment Data Tables: Thurston Regional Planning Council, WA (TRPC). (n.d.). Retrieved March 4, 2020, from https://www.trpc.org/480/Population-Housing-Employment-Data

Thurston County Community Planning & Economic Development [Thurston County]. (2018). *State mandated well form*. *360*, 1–3.

Thurston Regional Planning Council (TRPC). (June 2019). Population Forecast Allocations for Thurston County. Retrieved from https://www.trpc.org/DocumentCenter/View/6931/2018-Population-Forecast-Allocations?bidId=

U.S. Census Bureau. (2014). Census of Population and Housing. Retrieved March 9th, 2020 from https://www.census.gov/prod/www/decennial.html

USGS. (n.d.). Base flow in rivers. Retrieved February 21, 2020, from https://www.usgs.gov/special-topic/water-science-school/science/base-flow-rivers?qt-science_center_objects=0#qt-science_center_objects

USGS (n.d.), Retrieved January 26, 2020, from https://waterdata.usgs.gov/nwis.

USGS. (2018). USGS Water Use Data for the Nation. Retrieved February 26, 2020, from https://waterdata.usgs.gov/nwis/wu

Veldkamp, T., Wada, Y., Aerts, J. *et al.* Water scarcity hotspots travel downstream due to human interventions in the 20th and 21st century. *Nat Commun* 8, 15697 (2017). https://doi.org/10.1038/ncomms15697

Wada, Y. et al. Modeling global water use for the 21st century: Water Futures and Solutions (WFaS) initiative and its approaches. Geosci. Model Dev. 9, 175–222 (2016).

Wagner, L., and Bilhimer, D. (2015). Deschutes River, Percival Creek, and Budd Inlet Tributaries Temperature, Fecal Coliform Bacteria, Dissolved Oxygen, pH, and Fine Sediment TMDL: Water Quality Improvement Report and Implementation Plan. *Department of Ecology.* 15-10-012. Retrieved from https://fortress.wa.gov/ecy/publications/SummaryPages/1510012.html

Wang, D., and X. Cai (2009), Detecting human interferences to low flows through baseflow recession analysis, *Water Resour. Res.,* 45, W07426, doi:10.1029/2009WR007819.

Washington State Department of Transportation (WSDOT). (2012). County Boundaries of Washington State. [ESRI ArcGIS Map Layer]. WSDOT Online Map Center. https://data.wsdot.wa.gov/arcgis/rest/services/Shared/CountyBoundaries/MapServer

Water footprint calculator (2018). Water Use, Withdrawal and Consumption. *What is a water footprint.* Retrieved from https://www.watercalculator.org/footprint/water-use-withdrawal-consumption/

Washington State Department of Ecology. (January 2017). An Introduction to: Instream Flows and Instream Flow Rules. Publication # 17-11-001. Retrieved from https://fortress.wa.gov/ecy/publications/documents/1711002.pdf

Washington State Department of Ecology, W. S. D. (2001). Setting instream flows in Washington State. Publication #98-1813-WR., November.

Washington State Department of Ecology. (2012). Deschutes River, Capitol Lake, and Budd Inlet Temperature, Fecal Coliform Bacteria, Dissolved Oxygen, pH, and Fine Sediment Total Maximum Daily Load Technical Report - Water Quality Study Findings (Issue 12).

Washington State Department of Ecology. (n.d.). Protecting stream flows. Retrieved February 20, 2020, from https://ecology.wa.gov/Water-Shorelines/Water-supply/Protecting-stream-flows

Whatcom Cty. v. Hirst, 186 Wash. 2d 648, 662, n. 4, 381 P.3d 1 (2016)

Winter, T. C., Harvey, J. W., Franke, O. L., Alley, W. M. (1998). Groundwater and Surface Water: A Single Resource. *U. S. Geological Survey*. Circular 1139. Retrieved from https://pubs.usgs.gov/circ/circ1139/#pdf

Wittenberg, Hartmut. (1994). Nonlinear Analysis of Flow Recession Curves. *IAHS Publ*.. 221.

WRIA 13 Salmon Habitat Recovery Committee [WRIA 13]. (2019). Salmon Habitat Recovery Process Guide FINAL. Retrieved from https://www.trpc.org/DocumentCenter/View/6779/01_FINAL-2019-WRIA-13-Process-Guide-5-6-2019

Yang, Z., Zhang, Q., & Hao, X. (2016). Evapotranspiration Trend and Its Relationship with Precipitation over the Loess Plateau during the Last Three Decades. *Advances in Meteorology*, *2016*, 1–10. doi: 10.1155/2016/6809749

Yang, H., Choi, H. T., Lim, H. (2018). Applicability Assessment of Estimation Methods for Baseflow Recession Constants in Small Forest Catchments. *Water.*1(8), 1074. Retrieved from https://doi.org/10.3390/w10081074

Zimmerman, M. (2010). 2010 Wild Coho Forecasts for Puget Sound, Washington Coast, and Lower Columbia. Olympia, WA: Washington Department of Fish and Wildlife, Science Division.

Chapter 7: Appendices

Appendix A. Baseflow Composition in the Deschutes River and Washington State. Sinclair & Pitz, 1999.

Location	USGS gauge station	years	Base flow composition of total annual streamflow (%)				
			Jun	July	Aug	Sep	Oct
Lower Deschutes	12080010 E Street in Tumwater	22	92	96	97	92	74
Upper Deschutes	12079000 near Rainier	37	81	92	91	81	57
Washington State	Average of 582 gauging stations		-	86	86	77	69

Appendix B. Population Projection Compared to 2012. TRPC, 2019.

		Total Population							Percent of Population						
Jurisdiction		2017	2020	2025	2030	2035	2040	2045	2017	2020	2025	2030	2035	2040	2045
Bucoda & UGA	New	580	590	630	680	720	760	800	0.2%	0.2%	0.2%	0.2%	0.2%	0.2%	0.2%
	Old		580	670	890	1,060	1,220			0.2%	0.2%	0.3%	0.3%	0.3%	
Lacey & UGA	New	83,810	91,480	98,040	102,320	105,970	109,680	113,370	30.3%	31.1%	31.0%	30.5%	29.9%	29.6%	29.6%
	Old		88,610	95,000	101,510	107,720	114,200			29.9%	29.5%	29.1%	29.1%	29.0%	
Olympia & UGA	New	64,450	67,580	72,110	76,390	80,720	84,400	87,680	23.3%	23.0%	22.8%	22.7%	22.8%	22.8%	22.9%
	Old		67,850	74,030	79,940	84,400	88,610			22.9%	23.0%	22.9%	22.8%	22.5%	
Rainier & UGA	New	2,040	2,250	2,470	2,690	2,850	3,210	3,330	0.7%	0.8%	0.8%	0.8%	0.8%	0.9%	0.9%
	Old		2,150	2,310	2,840	3,150	3,450			0.7%	0.7%	0.8%	0.8%	0.9%	
Tenino & UGA	New	1,800	1,880	2,070	2,330	2,580	2,770	2,840	0.7%	0.6%	0.7%	0.7%	0.7%	0.7%	0.7%
	Old		1,760	2,030	2,750	3,190	3,780			0.6%	0.6%	0.8%	0.9%	1.0%	
Tumwater & UGA	New	26,550	29,770	34,520	38,710	42,340	44,950	46,080	9.6%	10.1%	10.9%	11.5%	11.9%	12.1%	12.0%
	Old		30,840	35,620	40,160	42,880	46,300			10.4%	11.1%	11.5%	11.6%	11.8%	
Yelm & UGA	New	10,060	11,420	14,920	18,770	22,310	25,330	27,560	3.6%	3.9%	4.7%	5.6%	6.3%	6.8%	7.2%
	Old		14,050	18,600	22,460	26,280	30,770			4.7%	5.8%	6.4%	7.1%	7.8%	
Grand Mound UGA	New	1,340	1,550	1,870	2,270	2,500	2,670	2,740	0.5%	0.5%	0.6%	0.7%	0.7%	0.7%	0.7%
	Old		1,470	1,630	1,770	1,880	1,990			0.5%	0.5%	0.5%	0.5%	0.5%	
Chehalis Reservation	New	70	70	70	70	60	60	60	0.0%	0.0%	0.0%	0.0%	0.0%	0.0%	0.0%
	Old		90	110	130	160	190			0.0%	0.0%	0.0%	0.0%	0.0%	
Nisqually Reservation	New	710	820	860	870	890	910	930	0.3%	0.3%	0.3%	0.3%	0.3%	0.2%	0.2%
	Old		980	1,040	1,070	1,120	1,230			0.3%	0.3%	0.3%	0.3%	0.3%	
County	New	85,480	86,880	88,950	90,890	93,440	95,960	98,110	30.9%	29.5%	28.1%	27.1%	26.4%	25.9%	25.6%
	Old		87,500	91,130	95,030	98,740	101,930			29.6%	28.3%	27.3%	26.6%	25.9%	
Total	**New**	**276,900**	**294,300**	**316,500**	**336,000**	**354,400**	**370,700**	**383,500**	**100.0%**	**100.0%**	**100.0%**	**100.0%**	**100.0%**	**100.0%**	**100.0%**
	Old		**295,870**	**322,170**	**348,550**	**370,590**	**393,670**			**100.0%**	**100.0%**	**100.0%**	**100.0%**	**100.0%**	

Note. "Old" is the 2012 Forecast.

Appendix C. Total Dwelling Unit Projection in Thurston County. *TRPC, 2019.*

Jurisdiction		2017	2020	2025	2030	2035	2040	2045
Bucoda	Total	250	250	280	310	330	360	380
Lacey	City	20,930	22,340	23,660	24,470	25,190	25,800	26,340
	UGA	13,940	16,270	18,760	20,490	21,760	23,070	24,390
	Total	34,870	38,610	42,420	44,960	46,950	48,870	50,730
Olympia	City	24,650	26,340	29,210	32,120	34,630	36,580	38,280
	UGA	4,890	5,140	5,510	5,690	5,890	6,290	6,740
	Total	29,540	31,480	34,720	37,810	40,520	42,870	45,020
Rainier	City	800	900	1,010	1,130	1,210	1,380	1,420
	UGA	50	50	50	60	60	60	80
	Total	850	950	1,060	1,190	1,270	1,440	1,500
Tenino	City	770	820	920	1,060	1,180	1,270	1,300
	UGA	10	10	10	10	10	10	10
	Total	780	830	930	1,070	1,190	1,280	1,310
Tumwater	City	10,200	11,510	13,200	14,620	15,870	16,820	17,390
	UGA	1,400	1,620	2,360	3,110	3,650	4,000	4,070
	Total	11,600	13,130	15,560	17,730	19,520	20,820	21,460
Yelm	City	3,170	3,730	5,300	7,090	8,690	10,070	10,950
	UGA	530	540	550	560	570	570	670
	Total	3,700	4,270	5,850	7,650	9,260	10,640	11,620
Grand Mound UGA		420	460	510	600	670	720	730
Chehalis Reservation		20	20	20	20	20	20	20
Nisqually Reservation		230	290	310	320	320	330	330
Total Cities		60,770	65,890	73,580	80,800	87,100	92,280	96,060
Total UGAs (1)		21,240	24,090	27,750	30,520	32,610	34,720	36,690
Total Reservations (2)		250	310	330	340	340	350	350
Rural Unincorporated (3)		34,550	35,560	37,360	39,050	40,480	41,710	42,680
Thurston County Total		**116,800**	**125,800**	**139,000**	**150,700**	**160,500**	**169,000**	**175,800**

2017-20	2020-25	2025-30	2030-35	2035-40	2040-45	2017-45
0.8%	1.9%	2.3%	1.3%	1.4%	1.0%	1.5%
2.2%	1.2%	0.7%	0.6%	0.5%	0.4%	0.8%
5.3%	2.9%	1.8%	1.2%	1.2%	1.1%	2.0%
3.5%	1.9%	1.2%	0.9%	0.8%	0.8%	1.3%
2.2%	2.1%	1.9%	1.5%	1.1%	0.9%	1.6%
1.7%	1.4%	0.6%	0.7%	1.3%	1.4%	1.2%
2.1%	2.0%	1.7%	1.4%	1.1%	1.0%	1.5%
3.8%	2.4%	2.3%	1.4%	2.6%	0.6%	2.1%
0.7%	1.2%	1.3%	1.1%	1.1%	3.6%	1.6%
3.7%	2.3%	2.2%	1.4%	2.6%	0.8%	2.0%
1.9%	2.4%	2.8%	2.2%	1.5%	0.4%	1.9%
0.0%	0.0%	0.0%	0.0%	2.6%	20.4%	3.8%
1.9%	2.4%	2.8%	2.2%	1.5%	0.5%	1.9%
4.1%	2.8%	2.1%	1.6%	1.2%	0.7%	1.9%
5.1%	7.7%	5.7%	3.3%	1.8%	0.4%	3.9%
4.2%	3.4%	2.7%	1.9%	1.3%	0.6%	2.2%
5.6%	7.3%	6.0%	4.2%	3.0%	1.7%	4.5%
0.4%	0.4%	0.4%	0.3%	0.3%	3.1%	0.8%
4.9%	6.5%	5.5%	3.9%	2.8%	1.8%	4.2%
2.8%	2.3%	3.2%	2.4%	1.3%	0.4%	2.0%
0.0%	0.0%	0.0%	0.0%	0.0%	0.0%	0.0%
8.1%	1.6%	0.3%	0.3%	0.2%	0.2%	1.3%
2.7%	2.2%	1.9%	1.5%	1.2%	0.8%	1.6%
4.3%	2.9%	1.9%	1.3%	1.3%	1.1%	2.0%
7.4%	1.5%	0.2%	0.2%	0.2%	0.2%	1.2%
1.0%	1.0%	0.9%	0.7%	0.6%	0.5%	0.8%
2.5%	**2.0%**	**1.6%**	**1.3%**	**1.0%**	**0.8%**	**1.5%**

Notes.

(top) Total dwelling unit projections in numbers. (bottom) Total dwelling unit projections in percentages.

1. Urban Growth Area (UGA): Unincorporated area designated to the annexed into city limits over 20 years to accommodate urban growth.

2. Reservations: Estimate is for Thurston County portion of reservation only.

2. Rural Unincorporated County is the portion of the unincorporated county that lies outside UGA and Reservation boundaries.

Appendix D. Linear baseflow recession constant (K)

Appendix D-1: Linear case

As described in Sec. 2.7.1, the general differential equation for changes of baseflow $Q(t)$ with time is

$$\frac{dQ}{dt} = -aQ^b \quad (4)$$

In the "linear case", with $b = 1$, this reduces to simple exponential decay of the baseflow:

$$\frac{dQ}{dt} = -aQ$$

In general, the solution[66] takes the form $Q(t) = Q_0 e^{-at} + constant$ where a has units of (1/time).

If $Q(t) = Q_0 e^{-at} + constant$, then

$$\frac{dQ}{dt} = Q_0 \frac{d}{dt} e^{-at} + \frac{d}{dt}(constant) = -aQ_0 e^{-a} + 0 = -a\, Q(t)$$

Substitution of $a = \frac{1}{c}$ yields the linear baseflow recession equation:

$$Q(t) = Q_0 e^{-t/c} \quad (5\text{-}1)$$

where c is one form of the recession constant (with units of 1/time).

A nondimensional recession constant, $K = e^{-1/c}$, is often used in baseflow analysis:

$$Q(t) = Q_0 e^{-t/c} = Q_0 K^t$$

In summary, the "linear" baseflow recession equation describes exponential decay of groundwater discharge (dQ) in a recession period (dt).

[66] Source: E.J. Zita, 2020; Thomas et al., 2013

Appendix D-2: Nonlinear case

In the nonlinear case (b≠1), the differential equation for the baseflow does not have a simple exponential decay. The general solution for $Q_t = Q_0(1 + \frac{(1-b){Q_0}^{1-b}}{ab} t)^{1/b-1}$ (5-2) is shown by Dupuit-Boussinesq (1904), where a and b indicate constants.

Appendix D-3: Nonlinear case with $\boldsymbol{b = 1/2}$

In the special case of $b = \frac{1}{2}$ (Wittenberg, 1999), the nonlinear baseflow equation simplifies:

$$Q_t = Q_0(1 + \frac{(1-b){Q_0}^{1-b}}{ab} t)^{1/b-1} \qquad (5\text{-}2)$$

The constant b is unitless, and the constant a has units.

The exponent becomes:

$$\frac{1}{b-1} = \frac{1}{1/2 - 1} = \frac{1}{-1/2} = -2$$

The multiplier in the second term on the right becomes:

$$\frac{(1-b)}{ab} = \frac{(1 - 1/2)}{a/2} = \frac{1/2}{a/2} = \frac{1}{a}$$

Therefore, the solution to the nonlinear differential equation for Q_t takes the form

$$\frac{Q_t}{Q_0} = \left(1 + \frac{(1-b)Q_0^{1-b}}{a\,b} t\right)^{1/b-1} = \left(1 + \frac{Q_0^{1/2}}{a} t\right)^{-2}$$

This is written in equations (10) and (11-1) as

$$\frac{Q_t}{Q_0} = \left(1 + \frac{Q_0^{0.5}}{a} t\right)^{-2}$$

This can be rewritten using the natural logarithm, for easier graphical analysis of recession constants:

$$ln\left(\frac{Q_t}{Q_0}\right) = ln\left(1 + \frac{t}{a} Q_0^{0.5}\right)^{-2} = -2\, ln\left(1 + \frac{t}{a} Q_0^{0.5}\right)$$

$$ln\left(\frac{Q_t}{Q_0}\right) = -2\, ln\left(\frac{a + tQ_0^{0.5}}{a}\right)$$

Appendix E. Selection of Baseflow Recession period (t)

Date (month_date_year)	Base flow (cfs)	Three-day moving average (cfs)	Decreasing Three-day moving average (included: Y, excluded: N)
6_1_2004	141.46	138.82	N
6_2_2004	148.07	140.18	N
6_3_2004	151.62	147.05	N
6_4_2004	152.99	150.89	N
6_5_2004	153.19	152.60	N
6_6_2004	153.38	153.19	N
6_7_2004	154.43	153.67	N
6_8_2004	154.95	154.25	N
6_9_2004	154.53	154.64	N
6_10_2004	154.22	154.57	Y
6_11_2004	153.57	154.11	Y
6_12_2004	152.46	153.42	Y
6_13_2004	151.75	152.59	Y
6_14_2004	152.59	152.27	Y
6_15_2004	152.68	152.34	Y
6_16_2004	151.73	152.33	Y
6_17_2004	150.35	151.59	Y
6_18_2004	148.35	150.14	Y
6_19_2004	145.88	148.19	Y
6_20_2004	143.26	145.83	Y
6_21_2004	140	143.05	Y
6_22_2004	134	139.09	Y
6_23_2004	130	134.67	Y
6_24_2004	127	130.33	Y
6_25_2004	124.72	127.24	Y
6_26_2004	122.43	124.72	Y
6_27_2004	119.99	122.38	Y
6_28_2004	117	119.81	Y
6_29_2004	114	117.00	Y
6_30_2004	111.74	114.25	Y

Notes

1. Exemplary data of selecting baseflow recession period between June and October of 2004.

2. cfs=cubic feet per second

3. Red-shaded dates are excluded while non-shaded dates are selected recession periods. Baseflow Derived from the NWIS and Separated from the WHAT program.

Appendix F. Yearly Withdrawal Amount. Data from the Thurston County Water Planning.

Year	Withdrawals (cfs)
1945	7.0
1946	7.1
1947	7.3
1948	7.8
1949	8.1
1950	8.6
1951	9.2
1952	9.9
1953	10.2
1954	10.6
1955	10.8
1956	10.9
1957	11.1
1958	11.7
1959	11.9
1960	12.0
1961	12.2
1962	13.2
1963	13.3
1964	13.6
1965	13.8
1966	14.0
1967	14.4
1968	14.8
1969	15.3
1970	15.9
1971	35.4
1972	36.1
1973	37.4
1974	41.1
1975	42.0
1976	42.1
1977	46.4
1978	48.7
1979	50.1
1980	51.4
1981	52.0
1982	52.4
1983	52.5
1984	52.6

1985	52.8
1986	53.2
1987	53.5
1988	55.6
1989	56.0
1990	56.7
1991	56.9
1992	57.2
1993	58.1
1994	58.4
1995	58.8
1996	59.6
1997	74.8
1998	73.3
1999	73.7
2000	74.2
2001	74.4
2002	74.6
2003	74.8
2004	75.4
2005	75.8
2006	76.2
2007	76.6
2008	77.6
2009	77.8
2010	77.9
2010	77.9
2011	78.0
2012	78.1
2013	78.2
2014	78.2
2015	78.3
2016	78.4
2017	78.5
2018	78.6
2019	78.7

Note. Unit of withdrawal amount: cfs (=cubic feet per second)

Appendix G. Estimated Maximum Baseflow (Q0) and Recession Period (t) with Three Methods

Year	Q0 Averaged	Recession Period t Averaged	Q0 Forecasted	Recession Period t Forecasted	Q0 from Trendline	Recession Period t Trendline
2020	151.08	64.07	188.03	64.76	166.55	61.75
2021	151.08	64.07	158.09	64.75	191.75	64.68
2022	151.08	64.07	173.75	64.73	191.75	64.68
2023	151.08	64.07	207.15	64.71	191.75	64.68
2024	151.08	64.07	201.65	64.68	191.75	64.68
2025	151.08	64.07	202.37	64.18	191.75	64.68
2026	151.08	64.07	236.42	64.29	191.75	64.68
2027	151.08	64.07	168.02	64.58	191.75	64.68
2028	151.08	64.07	166.79	64.55	191.75	64.68
2029	151.08	64.07	154.06	64.51	191.75	64.68
2030	151.08	64.07	149.42	64.48	191.75	64.68
2031	151.08	64.07	162.66	64.45	191.75	64.68
2032	151.08	64.07	168.26	64.42	191.75	64.68
2033	151.08	64.07	161.51	64.40	191.75	64.68
2034	151.08	64.07	168.03	64.37	191.75	64.68
2035	151.08	64.07	164.84	64.34	191.75	64.68
2036	151.08	64.07	198.17	64.32	191.75	64.68
2037	151.08	64.07	162.17	64.30	191.75	64.68
2038	151.08	64.07	153.46	64.28	191.75	64.68
2039	151.08	64.07	163.37	64.26	191.75	64.68
2040	151.08	64.07	161.81	64.24	191.75	64.68
2041	151.08	64.07	163.65	64.22	191.75	64.68
2042	151.08	64.07	166.09	64.20	191.75	64.68
2043	151.08	64.07	180.91	64.19	191.75	64.68
2044	151.08	64.07	162.68	64.17	191.75	64.68
2045	151.08	64.07	157.44	64.16	191.75	64.68
2046	151.08	64.07	141.97	64.15	191.75	64.68
2047	151.08	64.07	153.65	64.13	191.75	64.68
2048	151.08	64.07	151.78	64.10	191.75	64.68
2049	151.08	64.07	144.61	64.09	191.75	64.68
2050	151.08	64.07	160.04	64.09	191.75	64.68
2051	151.08	64.07	163.31	64.09	191.75	64.68
2052	151.08	64.07	159.17	64.08	191.75	64.68
2053	151.08	64.07	169.81	64.08	191.75	64.68
2054	151.08	64.07	152.08	64.08	191.75	64.68
2055	151.08	64.07	156.94	64.07	191.75	64.68
2056	151.08	64.07	162.39	64.07	191.75	64.68
2057	151.08	64.07	158.23	64.07	191.75	64.68

2058	151.08	64.07	150.39	64.06	191.75	64.68
2059	151.08	64.07	141.62	64.06	191.75	64.68
2060	151.08	64.07	152.11	64.06	191.75	64.68
2061	151.08	64.07	150.68	64.06	191.75	64.68
2062	151.08	64.07	143.68	64.06	191.75	64.68
2063	151.08	64.07	158.37	64.05	191.75	64.68
2064	151.08	64.07	162.91	64.05	191.75	64.68
2065	151.08	64.07	160.30	64.05	191.75	64.68
2066	151.08	64.07	171.79	64.05	191.75	64.68
2067	151.08	64.07	155.09	64.05	191.75	64.68
2068	151.08	64.07	161.43	64.05	191.75	64.68
2069	151.08	64.07	157.72	63.99	191.75	64.68

Appendix H. Linear and Nonlinear Baseflow Recession Constants

Year	Linear Recession Constant (K)	Nonlinear Recession Constant (a)
1945	0.9928	2558.9955
1945	0.9930	2351.8220
1946	0.9892	1971.0938
1946	0.9959	4290.7265
1947	0.9922	2553.9656
1947	0.9923	2215.0582
1948	0.9895	2334.5024
1949	0.9935	3035.7791
1949	0.9944	3089.1486
1950	0.9931	3156.4849
1951	0.9910	2458.2793
1952	0.9904	2172.2599
1952	0.9963	4484.2434
1953	0.9724	763.7303
1953	0.9860	1474.4337
1953	0.9763	993.7024
1954	0.9896	2218.4145
1954	0.9908	2074.7958
1955	0.9898	1975.8590
1956	0.9887	1876.6910
1957	0.9904	2313.0591
1957	0.9945	3362.4928
1958	0.9931	3237.1552
1958	0.9931	2691.9016
1958	0.9961	4240.2148
1959	0.9905	2279.8239
1959	0.9937	3241.2719
1960	0.9908	2536.6494
1960	0.9960	4937.3030
1961	0.9913	2608.7381
1961	0.9953	4074.8594
1962	0.9911	2327.7524
1962	0.9769	1049.9607
1963	0.9939	3544.4930
1963	0.9967	5955.8823
1964	0.9956	4471.3682
1965	0.9951	4061.7204
1966	0.9947	3760.3718
1967	0.9944	3530.4167

1968	0.9940	3349.9668
1969	0.9937	3205.2186
1970	0.9935	3087.0363
1971	0.9932	2989.1330
1972	0.9930	2907.0406
1973	0.9928	2837.4965
1974	0.9927	2778.0630
1975	0.9925	2726.8820
1976	0.9924	2682.5126
1977	0.9922	2643.8201
1978	0.9921	2609.8989
1979	0.9920	2580.0175
1980	0.9919	2553.5785
1981	0.9918	2530.0894
1982	0.9917	2509.1403
1983	0.9917	2490.3874
1984	0.9916	2473.5402
1985	0.9915	2458.3514
1986	0.9915	2444.6096
1987	0.9914	2432.1322
1988	0.9914	2420.7615
1989	0.9913	2410.3600
1990	0.9913	2400.8074
1991	0.9912	2391.9980
1992	0.9945	2989.5108
1992	0.9893	1439.6610
1993	0.9890	1886.4665
1994	0.9925	2536.9415
1994	0.9779	744.0308
1995	0.9882	1706.4452
1995	0.9868	1141.9587
1996	0.9921	2843.7103
1996	0.9951	3846.5794
1997	0.9895	2536.7088
1997	0.9896	2025.7319
1997	0.9467	564.2662
1998	0.9895	2025.3650
1999	0.9921	2652.6749
2000	0.9902	2259.6359
2001	0.9927	2427.5159
2002	0.9929	2613.7319
2002	0.9968	4826.2589
2003	0.9914	1856.5984

2004	0.9851	1315.0212
2004	0.9619	472.0873
2004	0.9620	543.0450
2005	0.9897	1760.8839
2006	0.9864	1272.5680
2007	0.9934	2868.9909
2008	0.9839	1404.9047
2008	0.9915	2090.3379
2008	0.9970	6170.0066
2009	0.9934	2915.3080
2009	0.9938	2771.6966
2010	0.9831	1583.5799
2010	0.9913	2568.5644
2010	0.9844	1363.5509
2011	0.9877	2186.9412
2011	0.9923	2733.4669
2012	0.9906	2422.4603
2013	0.9872	1799.7205
2013	0.9526	701.3387
2014	0.9893	1983.5954
2015	0.9909	2243.8879
2015	0.9934	2589.4065
2016	0.9934	3237.7681
2016	0.9948	3705.5930
2017	0.9879	1929.3518
2018	0.9917	2532.9231
2018	0.9964	4971.2368
2019	0.9954	4478.6727
2019	0.9847	1131.6141
2020	0.9925	2463.8251
2021	0.9925	2459.3790
2022	0.9920	2454.9940
2023	0.9916	2583.7397
2024	0.9922	2502.0069
2025	0.9921	2600.2817
2026	0.9921	2543.2892
2027	0.9919	2498.5893
2028	0.9918	2523.6186
2029	0.9917	2518.8230
2030	0.9917	2514.1397
2031	0.9917	2509.5624
2032	0.9917	2486.3633
2033	0.9917	2483.4566

2034	0.9916	2488.4642
2035	0.9916	2484.1907
2036	0.9916	2479.9944
2037	0.9916	2475.8712
2038	0.9916	2471.8173
2039	0.9915	2467.8290
2040	0.9915	2463.9031
2041	0.9915	2460.0363
2042	0.9915	2456.2258
2043	0.9914	2452.4688
2044	0.9914	2448.7627
2045	0.9914	2445.1051
2046	0.9914	2441.4936
2047	0.9913	2437.9262
2048	0.9913	2434.4007
2049	0.9913	2430.9154
2050	0.9913	2427.4683
2051	0.9913	2424.0579
2052	0.9912	2420.6825
2053	0.9912	2417.3405
2054	0.9912	2414.0306
2055	0.9912	2410.7515
2056	0.9911	2407.5018
2057	0.9911	2404.2803
2058	0.9911	2401.0859
2059	0.9911	2397.9175
2060	0.9910	2394.7741
2061	0.9910	2391.6548
2062	0.9910	2388.5585
2063	0.9910	2385.4844
2064	0.9909	2382.4317
2065	0.9909	2379.3995
2066	0.9909	2376.3872
2067	0.9908	2373.3940
2068	0.9908	2370.4193
2069	0.9908	2367.4623

Appendix I. Estimation of the Future Minimum Baseflow (Q_t)

Year	Forecasted Future Q_t (cfs)	Q_t estimated from the Averaged Q_0 & t		Q_t estimated from the Forecasted Q_0 & t		Q_t estimated from the Trendline Q_0 & t	
		Linear	Nonlinear	Linear	Nonlinear	Linear	Nonlinear
2020	78.3	93.5	118.0	115.8	143.3	104.9	129.8
2021	78.3	93.4	118.0	97.3	122.6	118.1	145.9
2022	78.1	90.2	117.9	103.2	133.5	113.9	145.8
2023	78.0	87.7	119.1	119.7	157.9	110.8	147.4
2024	77.9	91.2	118.3	121.2	153.1	115.3	146.4
2025	77.8	91.1	119.2	122.0	155.1	115.1	147.5
2026	77.7	91.0	118.7	142.2	177.3	115.0	146.9
2027	77.6	90.0	118.3	99.6	130.0	113.6	146.3
2028	77.5	89.0	118.5	97.8	129.4	112.4	146.6
2029	77.7	88.9	118.5	90.3	120.5	112.2	146.6
2030	77.7	88.7	118.5	87.5	117.1	112.0	146.5
2031	77.7	88.6	118.4	95.1	126.4	111.9	146.5
2032	77.6	88.5	118.2	98.3	130.1	111.7	146.2
2033	77.5	88.4	118.2	94.2	125.4	111.6	146.2
2034	77.5	88.2	118.2	97.9	130.0	111.4	146.2
2035	77.4	88.1	118.2	95.9	127.7	111.3	146.2
2036	77.4	88.0	118.1	115.2	150.7	111.1	146.1
2037	77.3	87.9	118.1	94.1	125.8	110.9	146.1
2038	77.3	87.7	118.1	89.0	119.7	110.8	146.0
2039	77.2	87.6	118.0	94.6	126.6	110.6	146.0
2040	77.2	87.5	118.0	93.6	125.5	110.4	145.9
2041	77.1	87.3	118.0	94.5	126.7	110.3	145.9
2042	77.1	87.2	117.9	95.8	128.4	110.1	145.8
2043	77.1	87.1	117.9	104.2	138.6	110.0	145.8
2044	77.0	87.0	117.9	93.6	125.9	109.8	145.7
2045	77.0	86.8	117.8	90.4	122.3	109.6	145.7
2046	77.0	86.7	117.8	81.4	111.3	109.5	145.6
2047	76.9	86.6	117.8	88.0	119.5	109.3	145.6
2048	76.9	86.4	117.7	86.8	118.2	109.1	145.5
2049	76.9	86.3	117.7	82.6	113.1	109.0	145.5
2050	76.8	86.2	117.7	91.3	123.9	108.8	145.4
2051	76.8	86.0	117.6	93.0	126.2	108.6	145.4
2052	76.8	85.9	117.6	90.5	123.2	108.4	145.4
2053	76.8	85.8	117.6	96.4	130.6	108.3	145.3
2054	76.7	85.6	117.5	86.2	118.2	108.1	145.3
2055	76.7	85.5	117.5	88.8	121.6	107.9	145.2
2056	76.7	85.4	117.5	91.7	125.3	107.8	145.2

2057	76.7	85.2	117.4	89.3	122.4	107.6	145.2
2058	76.6	85.1	117.4	84.7	116.9	107.4	145.1
2059	76.6	84.9	117.4	79.6	110.7	107.2	145.1
2060	76.6	84.8	117.3	85.4	118.1	107.1	145.0
2061	76.6	84.7	117.3	84.5	117.0	106.9	145.0
2062	76.6	84.5	117.3	80.4	112.1	106.7	144.9
2063	76.5	84.4	117.2	88.5	122.3	106.5	144.9
2064	76.5	84.2	117.2	90.9	125.5	106.3	144.9
2065	76.5	84.1	117.2	89.3	123.6	106.2	144.8
2066	76.5	84.0	117.2	95.5	131.5	106.0	144.8
2067	76.5	83.8	117.1	86.1	119.9	105.8	144.8
2068	76.5	83.7	117.1	89.4	124.3	105.6	144.7
2069	76.4	83.5	117.1	87.3	121.7	105.4	144.7

Note. The unit of estimated Q_t: cubic feet per second (cfs), Q_0: cfs, t: days.

Appendix J. Estimated Minimum Baseflow (*Qt*) under Impacted and Natural Scenarios.

	Impact (W)		W = 0 (impacted)		$W \neq 0$ (increasing)		$W \neq 0$ (2015's)	
Year	yearly withdrawals (W)	Population Change	Constant K	Estimated Q_t	Constant K	Estimated Q_t	Constant K	Estimated Q_t
1945*	7.0		1.0	64.0	1.0	71.1		71.1
1945	7.0		1.0	59.6	1.0	66.6		66.6
1946*	7.1		1.0	79.8	1.0	86.9		86.9
1946	7.1		1.0	72.8	1.0	79.9		79.9
1947*	7.3		1.0	68.7	1.0	76.1		76.1
1947	7.3		1.0	68.5	1.0	75.8		75.8
1948	7.8		1.0	89.8	1.0	97.6		97.6
1949*	8.1		1.0	73.2	1.0	81.4		81.4
1949	8.1		1.0	72.2	1.0	80.4		80.4
1950	8.6		1.0	88.7	1.0	97.3		97.3
1951	9.2		1.0	81.1	1.0	90.3		90.3
1952*	9.9		1.0	75.1	1.0	85.0		85.0
1952	9.9		1.0	60.9	1.0	70.8		70.8
1953*	10.2		1.0	81.1	1.0	91.4		91.4
1953	10.2		1.0	88.3	1.0	98.6		98.6
1953	10.2		1.0	125.9	1.0	136.2		136.2
1954*	10.6		1.0	88.8	1.0	99.3		99.3
1954	10.6		1.0	83.5	1.0	94.1		94.1
1955	10.8		1.0	88.2	1.0	99.0		99.0
1956	10.9		1.0	93.0	1.0	103.9		103.9
1957*	11.1		1.0	97.7	1.0	108.8		108.8
1957	11.1		1.0	75.3	1.0	86.4		86.4
1958*	11.7		1.0	118.4	1.0	130.1		130.1
1958	11.7		1.0	66.4	1.0	78.1		78.1
1958	11.7		1.0	66.3	1.0	78.0		78.0
1959*	11.9		1.0	84.3	1.0	96.2		96.2
1959	11.9		1.0	101.0	1.0	112.9		112.9
1960*	12.0		1.0	96.8	1.0	108.7		108.7
1960	12.0		1.0	86.8	1.0	98.7		98.7
1961*	12.2		1.0	92.0	1.0	104.1		104.1
1961	12.2		1.0	87.5	1.0	99.6		99.6
1962*	13.2		1.0	72.1	1.0	85.3		85.3
1962	13.2		1.0	124.0	1.0	137.2		137.2
1963*	13.3		1.0	95.3	1.0	108.6		108.6
1963	13.3		1.0	88.7	1.0	102.0		102.0
1964	13.6		1.0	87.3	1.0	100.9		100.9
1965	13.8		1.0	86.6	1.0	100.4		100.4
1966	14.0		1.0	85.9	1.0	99.9		99.9
1967	14.4		1.0	85.3	1.0	99.7		99.7
1968	14.8		1.0	84.6	1.0	99.4		99.4
1969	15.3		1.0	83.9	1.0	99.2		99.2
1970	15.9		1.0	83.2	1.0	99.1		99.1
1971	35.4		1.0	82.5	1.0	118.0		118.0
1972	36.1		1.0	81.9	1.0	118.0		118.0
1973	37.4		1.0	81.2	1.0	118.5		118.5
1974	41.1		1.0	80.5	1.0	121.6		121.6

1975	42.0		1.0	79.8	1.0	121.8		121.8
1976	42.1		1.0	79.2	1.0	121.3		121.3
1977	46.4		1.0	78.5	1.0	124.9		124.9
1978	48.7		1.0	77.8	1.0	126.5		126.5
1979	50.1		1.0	77.1	1.0	127.2		127.2
1980	51.4		1.0	76.4	1.0	127.9		127.9
1981	52.0		1.0	75.8	1.0	127.7		127.7
1982	52.4		1.0	75.1	1.0	127.4		127.4
1983	52.5		1.0	74.4	1.0	126.9		126.9
1984	52.6		1.0	73.7	1.0	126.4		126.4
1985	52.8		1.0	73.0	1.0	125.8		125.8
1986	53.2		1.0	72.4	1.0	125.6		125.6
1987	53.5		1.0	71.7	1.0	125.2		125.2
1988	55.6		1.0	71.0	1.0	126.7		126.7
1989	56.0		1.0	70.3	1.0	126.3		126.3
1990	56.7		1.0	69.7	1.0	126.3		126.3
1991	56.9		1.0	69.0	1.0	125.9		125.9
1992*	57.2		1.0	52.5	1.0	109.6		109.6
1992	57.2		1.0	54.2	1.0	111.4		111.4
1993	58.1		1.0	60.5	1.0	118.6		118.6
1994*	58.4		1.0	73.1	1.0	131.5		131.5
1994	58.4		1.0	50.8	1.0	109.2		109.2
1995*	58.8		1.0	70.2	1.0	129.0		129.0
1995	58.8		1.0	45.3	1.0	104.1		104.1
1996*	59.6		1.0	89.1	1.0	148.7		148.7
1996	59.6		1.0	84.9	1.0	144.5		144.5
1997*	72.9		1.0	120.2	1.0	193.1		193.1
1997	72.9		1.0	102.4	1.0	175.4		175.4
1997	74.8		0.9	156.5	1.0	231.3		231.3
1998	73.3		1.0	61.9	1.0	135.2		135.2
1999	73.7		1.0	74.8	1.0	148.5		148.5
2000	74.2		1.0	75.7	1.0	149.9		149.9
2001	74.4		1.0	52.4	1.0	126.9		126.9
2002*	74.6		1.0	59.0	1.0	133.6		133.6
2002	74.6		1.0	58.6	1.0	133.2		133.2
2003	74.8		1.0	41.6	1.0	116.4		116.4
2004*	75.4		1.0	64.4	1.0	139.8		139.8
2004	75.4		1.0	67.0	1.0	142.4		142.4
2004	75.4		1.0	83.2	1.0	158.6		158.6
2005	75.8		1.0	47.9	1.0	123.7		123.7
2006	76.2		1.0	40.4	1.0	116.7		116.7
2007	76.6		1.0	65.2	1.0	141.7		141.7
2008*	77.6		1.0	79.0	1.0	156.6		156.6
2008	77.6		1.0	69.1	1.0	146.7		146.7
2008	77.6		1.0	81.6	1.0	159.2		159.2
2009*	77.8		1.0	70.6	1.0	148.5		148.5
2009	77.8		1.0	67.2	1.0	145.0		145.0
2010*	77.9		1.0	98.3	1.0	176.3		176.3
2010	77.9		1.0	118.0	1.0	195.9		195.9
2010	77.9		1.0	106.5	1.0	184.5		184.5
2011*	78.0		1.0	123.6	1.0	201.6		201.6
2011	78.0		1.0	96.4	1.0	174.4		174.4

2012	78.1		1.0	75.5	1.0	153.6		153.6
2013	78.2		1.0	84.9	1.0	163.1		163.1
2013	78.2		1.0	155.9	1.0	234.1		234.1
2014	78.2		1.0	68.5	1.0	146.7		146.7
2015*	78.3		1.0	70.4	1.0	148.8		148.8
2015	78.3		1.0	65.8	1.0	144.2		144.2
2016*	78.4		1.0	99.4	1.0	177.8		177.8
2016	78.4		1.0	81.6	1.0	160.1		160.1
2017	78.5		1.0	73.6	1.0	152.1		152.1
2018*	78.6		1.0	78.1	1.0	156.7		156.7
2018	78.6		1.0	79.9	1.0	158.5		158.5
2019*	78.7		1.0	91.4	1.0	170.1		170.1
2019	78.7		1.0	62.7	1.0	141.4		141.4
2020	86.2	1.1	1.0	78.3	1.0	173.2	1.0	107.2
2021	86.2	1.1	1.0	78.3	1.0	173.2	1.0	107.2
2022	86.2	1.1	1.0	78.1	1.0	173.0	1.0	107.0
2023	86.2	1.1	1.0	78.0	1.0	172.9	1.0	106.8
2024	86.2	1.1	1.0	77.9	1.0	172.8	1.0	106.6
2025	92.7	1.2	1.0	77.8	1.0	187.5	1.0	106.5
2026	92.7	1.2	1.0	77.7	1.0	187.4	1.0	106.4
2027	92.7	1.2	1.0	77.6	1.0	187.4	1.0	106.3
2028	92.7	1.2	1.0	77.5	1.0	187.3	1.0	106.2
2029	92.7	1.2	1.0	77.7	1.0	187.5	1.0	106.5
2030	98.4	1.3	1.0	77.7	1.0	201.4	1.0	106.4
2031	98.4	1.3	1.0	77.7	1.0	201.4	1.0	106.4
2032	98.4	1.3	1.0	77.6	1.0	201.3	1.0	106.3
2033	98.4	1.3	1.0	77.5	1.0	201.2	1.0	106.2
2034	98.4	1.3	1.0	77.5	1.0	201.2	1.0	106.1
2035	103.8	1.3	1.0	77.4	1.0	215.0	1.0	106.0
2036	103.8	1.3	1.0	77.4	1.0	215.0	1.0	105.9
2037	103.8	1.3	1.0	77.3	1.0	214.9	1.0	105.9
2038	103.8	1.3	1.0	77.3	1.0	214.9	1.0	105.8
2039	103.8	1.3	1.0	77.2	1.0	214.8	1.0	105.8
2040	108.6	1.4	1.0	77.2	1.0	227.7	1.0	105.7
2041	108.6	1.4	1.0	77.1	1.0	227.7	1.0	105.6
2042	108.6	1.4	1.0	77.1	1.0	227.7	1.0	105.6
2043	108.6	1.4	1.0	77.1	1.0	227.6	1.0	105.5
2044	108.6	1.4	1.0	77.0	1.0	227.6	1.0	105.5
2045	112.4	1.4	1.0	77.0	1.0	238.1	1.0	105.4
2046	112.4	1.4	1.0	77.0	1.0	238.1	1.0	105.4
2047	112.4	1.4	1.0	76.9	1.0	238.1	1.0	105.4
2048	112.4	1.4	1.0	76.9	1.0	238.0	1.0	105.3
2049	112.4	1.4	1.0	76.9	1.0	238.0	1.0	105.3
2050	119.9	1.5	1.0	76.8	1.0	260.3	1.0	105.2
2051	119.9	1.5	1.0	76.8	1.0	260.3	1.0	105.2
2052	119.9	1.5	1.0	76.8	1.0	260.2	1.0	105.2
2053	119.9	1.5	1.0	76.8	1.0	260.2	1.0	105.1
2054	119.9	1.5	1.0	76.7	1.0	260.2	1.0	105.1
2055	127.9	1.6	1.0	76.7	1.0	285.6	1.0	105.1
2056	127.9	1.6	1.0	76.7	1.0	285.5	1.0	105.0
2057	127.9	1.6	1.0	76.7	1.0	285.5	1.0	105.0

2058	127.9	1.6	1.0	76.6	1.0	285.5	1.0	105.0
2059	127.9	1.6	1.0	76.6	1.0	285.5	1.0	104.9
2060	136.5	1.7	1.0	76.6	1.0	314.4	1.0	104.9
2061	136.5	1.7	1.0	76.6	1.0	314.4	1.0	104.9
2062	136.5	1.7	1.0	76.6	1.0	314.3	1.0	104.9
2063	136.5	1.7	1.0	76.5	1.0	314.3	1.0	104.8
2064	136.5	1.7	1.0	76.5	1.0	314.3	1.0	104.8
2065	145.6	1.9	1.0	76.5	1.0	347.2	1.0	104.8
2066	145.6	1.9	1.0	76.5	1.0	347.2	1.0	104.8
2067	145.6	1.9	1.0	76.5	1.0	347.2	1.0	104.7
2068	145.6	1.9	1.0	76.5	1.0	347.2	1.0	104.7
2069	145.6	1.9	1.0	76.4	1.0	347.2	1.0	104.7

Notes.

1. Duplicating years (*) indicate there were multiple recession periods within the year.

2. Population change indicates the portion of increased population of a year compared with the population of 2012.

Appendix K. The Ratio of Groundwater Withdrawals to the Minimum Baseflow (Q_t)

Year	Yearly Withdrawals (W, cfs)	Population Change (against 2015)	W(=increase) / Q_t (%)	W(=2015) / Q_t (%)
1945*	7.0		9.9	
1945	7.0		10.5	
1946*	7.1		8.2	
1946	7.1		8.9	
1947*	7.3		10.7	
1947	7.3		10.7	
1948	7.8		8.7	
1949*	8.1		11.1	
1949	8.1		11.3	
1950	8.6		9.7	
1951	9.2		11.4	
1952*	9.9		13.2	
1952	9.9		16.3	
1953*	10.2		12.6	
1953	10.2		11.6	
1953	10.2		8.1	
1954*	10.6		11.9	
1954	10.6		12.6	
1955	10.8		12.2	
1956	10.9		11.7	
1957*	11.1		11.3	
1957	11.1		14.7	
1958*	11.7		9.9	
1958	11.7		17.6	
1958	11.7		17.6	
1959*	11.9		14.1	
1959	11.9		11.8	
1960*	12.0		12.4	
1960	12.0		13.8	
1961*	12.2		13.2	
1961	12.2		13.9	
1962*	13.2		18.2	
1962	13.2		10.6	
1963*	13.3		14.0	
1963	13.3		15.0	
1964	13.6		15.5	
1965	13.8		15.9	
1966	14.0		16.3	
1967	14.4		16.9	
1968	14.8		17.5	

1969	15.3		18.3	
1970	15.9		19.1	
1971	35.4		42.9	
1972	36.1		44.1	
1973	37.4		46.0	
1974	41.1		51.0	
1975	42.0		52.6	
1976	42.1		53.2	
1977	46.4		59.2	
1978	48.7		62.6	
1979	50.1		64.9	
1980	51.4		67.3	
1981	52.0		68.6	
1982	52.4		69.7	
1983	52.5		70.5	
1984	52.6		71.4	
1985	52.8		72.3	
1986	53.2		73.5	
1987	53.5		74.6	
1988	55.6		78.4	
1989	56.0		79.6	
1990	56.7		81.3	
1991	56.9		82.6	
1992*	57.2		108.9	
1992	57.2		105.4	
1993	58.1		96.0	
1994*	58.4		80.0	
1994	58.4		115.1	
1995*	58.8		83.7	
1995	58.8		129.8	
1996*	59.6		66.8	
1996	59.6		70.2	
1997*	72.9		60.7	
1997	72.9		71.2	
1997	74.8		47.8	
1998	73.3		118.3	
1999	73.7		98.5	
2000	74.2		98.0	
2001	74.4		141.9	
2002*	74.6		126.5	
2002	74.6		127.2	
2003	74.8		179.7	
2004*	75.4		117.2	
2004	75.4		112.6	

2004	75.4		90.7	
2005	75.8		158.2	
2006	76.2		188.5	
2007	76.6		117.5	
2008*	77.6		98.3	
2008	77.6		112.3	
2008	77.6		95.0	
2009*	77.8		110.2	
2009	77.8		115.8	
2010*	77.9		79.3	
2010	77.9		66.1	
2010	77.9		73.2	
2011*	78.0		63.1	
2011	78.0		80.9	
2012	78.1		103.5	
2013*	78.2		92.1	
2013	78.2		50.2	
2014	78.2		114.3	
2015*	78.3		111.3	
2015	78.3		119.0	
2016*	78.4		78.9	
2016	78.4		96.1	
2017	78.5		106.7	
2018*	78.6		100.6	
2018	78.6		98.4	
2019*	78.7		86.0	
2019	78.7		125.4	
2020	86.2	1.1	110.2	100.5
2021	86.2	1.1	110.1	100.5
2022	86.2	1.1	110.3	100.6
2023	86.2	1.1	110.5	100.8
2024	86.2	1.1	110.7	101.0
2025	92.7	1.2	119.2	101.1
2026	92.7	1.2	119.4	101.3
2027	92.7	1.2	119.5	101.3
2028	92.7	1.2	119.6	101.4
2029	92.7	1.2	119.3	101.2
2030	98.4	1.3	126.7	101.2
2031	98.4	1.3	126.7	101.2
2032	98.4	1.3	126.9	101.4
2033	98.4	1.3	127.0	101.5
2034	98.4	1.3	127.1	101.5
2035	103.8	1.3	134.1	101.6
2036	103.8	1.3	134.2	101.7

2037	103.8	1.3	134.3	101.7
2038	103.8	1.3	134.4	101.8
2039	103.8	1.3	134.5	101.9
2040	108.6	1.4	140.7	101.9
2041	108.6	1.4	140.8	102.0
2042	108.6	1.4	140.9	102.0
2043	108.6	1.4	140.9	102.1
2044	108.6	1.4	141.0	102.1
2045	112.4	1.4	145.9	102.2
2046	112.4	1.4	146.0	102.2
2047	112.4	1.4	146.1	102.2
2048	112.4	1.4	146.1	102.3
2049	112.4	1.4	146.2	102.3
2050	119.9	1.5	156.0	102.4
2051	119.9	1.5	156.1	102.4
2052	119.9	1.5	156.1	102.4
2053	119.9	1.5	156.2	102.5
2054	119.9	1.5	156.3	102.5
2055	127.9	1.6	166.8	102.5
2056	127.9	1.6	166.8	102.6
2057	127.9	1.6	166.9	102.6
2058	127.9	1.6	166.9	102.6
2059	127.9	1.6	167.0	102.7
2060	136.5	1.7	178.2	102.7
2061	136.5	1.7	178.2	102.7
2062	136.5	1.7	178.3	102.7
2063	136.5	1.7	178.3	102.8
2064	136.5	1.7	178.4	102.8
2065	145.6	1.9	190.4	102.8
2066	145.6	1.9	190.4	102.8
2067	145.6	1.9	190.4	102.8
2068	145.6	1.9	190.5	102.9
2069	145.6	1.9	190.5	102.9

Notes.

1. Duplicating years (*) indicate there were multiple recession periods within the year.

2. Population change indicates the rate of increased population of a year compared with the population of 2012.